

**Manual**

---

**Rietveld Analysis  
Program**

**BGMN<sup>®</sup>**

Jörg Bergmann, Dresden, Germany

The authors wish to express their sincere gratitude to Dr. R. Kleeberg of the Institute of Mineralogy of the Freiberg University of Mining and Technology / Germany for providing the measurement data and the analysis results as well as many constructive discussions.

4<sup>th</sup>, revised edition, Dec 2005

Copyright ©1996, 1998, 1999, 2005 by J. Bergmann (program author)

BGMN is a German registered trademark of Dr. Jörg Bergmann, Dresden / Germany.

J. Bergmann, T. Taut (manual authors)

Printed in Germany

The references and data being part of this manual are subject to change without prior notice. No part of this publication may be reproduced, stored in a retrieval system or transmitted for any purpose in any form or by any means, electronic, mechanical, photocopying, recording or otherwise, without the prior written consent from Dr. J. Bergmann / Germany.

The authors welcome suggestions for improvement of this manual.

E-Mail: [support@bgmn.de](mailto:support@bgmn.de)

# Preface

The **BGMN** program is the result of developments that started in 1980 when I was awarded my Ph.D. degree. In the beginnings I worked at the profile model, the mathematical core and the GOAL concept (experimental design). The development was carried out on IBM-similar mainframes of the Robotron company in the PL/1 programming language.

As personal computers of higher speed became available, I started to encode the software into ANSI-C on PC in 1989. The **BGMN** Rietveld program system has been developed since the end of 1993.

The staff of SEIFERT-FPM made excellent connections with Beta testers who promoted the program improvement. My special thanks are said to Dr. Kleeberg from the Institute of Mineralogy of the Freiberg University of Mining and Technology. Many applications of the phase analysis program result from his inspirations. Dr. Jehnichen and Dr. Friedel of the Institute of Polymer Research in Dresden influenced my works significantly, too. A lot of variants to handle molecule crystals were inserted on their request. Thanks to Th. Monecke from the Freiberg institute, I was able to clarify the unique PO model used in **BGMN** beginning with the 4<sup>th</sup> edition of this manual.

I am very grateful to the first user of the **BGMN** program who has also written this manual. From my point of view, the manual becomes more expressive and to be handled easier, when it is written by an experienced user instead of the developer himself.

## Preface to the 2005 revision

Having passed 6 years of **BGMN** development, I have totally revised the **BGMN** manual. For example, now there is a GUI named **BGMNwin**, which will be distributed with **BGMN**. The installation instruction was rewritten from scratch, and some functions of the old package are no longer needed. Thanks again to Dr. Kleeberg for his helpful discussion.

Jörg Bergmann — Dresden, June 30, 2009

## How to get support

If you have any questions, please have a look at the **BGMN** site at

<http://www.bgm.de>

If this does not help: The firm Rich. Seifert & Co., Ahrensburg, Germany, is responsible for every question, in first line. You may directly contact the program author at

[support@bgmn.de](mailto:support@bgmn.de)



# Contents

<b>1</b>	<b>Introduction</b>	<b>1</b>
1.1	The Rietveld method in X-ray powder diffractometry . . . . .	1
1.2	Practical problems . . . . .	1
1.3	Using this manual . . . . .	1
<b>2</b>	<b>Advantages of BGMN</b>	<b>3</b>
2.1	New profile model . . . . .	3
2.2	New refinement algorithm for ensuring convergence . . . . .	3
2.3	Special functions . . . . .	3
<b>3</b>	<b>Installation</b>	<b>5</b>
3.1	Hardware and software requirements . . . . .	5
3.2	Installation of BGMN . . . . .	5
3.3	Installation of RasMol . . . . .	5
3.4	Installation of ORTEP-3 for Windows . . . . .	6
3.5	Installation of <b>PowderCell</b> . . . . .	6
<b>4</b>	<b>User's Guide</b>	<b>7</b>
4.1	Modelling of goniometer function by raytracing . . . . .	7
	Step 1: Geometric profile estimation . . . . .	8
	Step 2: Interpolation of goniometer function by the program MAKEGEQ . . . . .	9
	Display of calculated profiles . . . . .	10
4.2	Input of sample structure data . . . . .	10
	First part: Define lattice and phase-specific parameters . . . . .	11
	Ongoing lines: Define atoms inside the asymmetric unit of the unit cell . . . . .	12
4.3	Refinement procedure . . . . .	13
	Control file . . . . .	13
	Start and execution of calculation . . . . .	15
4.4	Output of results . . . . .	15
	List of results . . . . .	15
	Result representation . . . . .	18
	Peak list . . . . .	18
4.5	Improvement of results . . . . .	20
	Preferred orientation . . . . .	20

Anisotropic peak width . . . . .	20
Anisotropic temperature factor (Debye-Waller-factor) . . . . .	20
4.6 Calculation example . . . . .	21
<b>5 Theory</b>	<b>23</b>
5.1 Optimization method . . . . .	23
5.2 Counting rate on the $i^{th}$ measuring point . . . . .	24
5.3 Determination of background . . . . .	24
5.4 Scale and preferred orientation . . . . .	25
Automatic reduction of PO/anisotropy models . . . . .	28
5.5 Profile function . . . . .	28
Wavelength distribution . . . . .	29
Geometry function . . . . .	29
Sample function . . . . .	31
5.6 Mean crystallite size . . . . .	32
Comparison with microscopic measurements of grain size . . . . .	34
5.7 Microabsorption . . . . .	34
5.8 Structure factor . . . . .	35
5.9 Temperature factors (Debye-Waller-factors) . . . . .	36
5.10 Neutron powder diffraction . . . . .	37
5.11 Quality parameters . . . . .	38
Global $R$ values . . . . .	38
Phase-specific $R$ values . . . . .	39
Quality parameter $1 - \rho$ . . . . .	40
<b>6 Sample preparation</b>	<b>41</b>
6.1 Sample statistics . . . . .	41
Reduce grain size by grinding . . . . .	41
Enhance divergence of the primary beam . . . . .	41
Sample spinning . . . . .	43
Automatic divergence slit . . . . .	43
6.2 Preferred orientation . . . . .	43
Sample spinning and transmission geometry . . . . .	43
6.3 Microabsorption . . . . .	44
6.4 Sample roughness . . . . .	44
6.5 Sample holder (measurement in reflection) . . . . .	44
<b>7 Measuring strategy</b>	<b>47</b>
7.1 Diffractometer control . . . . .	47
Variable counting time . . . . .	47
Variable (automatic) divergence slits . . . . .	48
7.2 Sample illumination . . . . .	51
7.3 Measurement geometry . . . . .	51

Reflection . . . . .	51
Transmission . . . . .	51
Capillary . . . . .	51
<b>8 General restrictions</b>	<b>55</b>
8.1 Physical and mathematical restrictions . . . . .	55
Obtainable precision of intensities and phase contents . . . . .	55
Preferred orientation at grazing incidence . . . . .	55
Primary monochromator . . . . .	55
Neutrons (constant wavelength and time of flight) . . . . .	56
8.2 Restrictions due to software . . . . .	56
<b>9 Phase analysis</b>	<b>57</b>
9.1 Mixture of goethite and quartz . . . . .	57
9.2 Determination of amorphous content . . . . .	62
9.3 Metashale Böhlscheiben . . . . .	66
9.4 Rules for phase analysis . . . . .	69
<b>10 Size/strain analysis</b>	<b>71</b>
10.1 Analysis of a virgilite sample . . . . .	71
10.2 Tube tails correction . . . . .	76
10.3 Learnt device functions . . . . .	79
10.4 Rules for profile analysis (size/strain analysis) . . . . .	80
<b>A Short reference</b>	<b>83</b>
A.1 GEOMET . . . . .	83
A.2 VERZERR . . . . .	85
A.3 MAKEGEQ . . . . .	85
A.4 BGMN . . . . .	86
Control file . . . . .	86
Structure file . . . . .	91
Format of the *.lst result file . . . . .	101
Automatic refinement strategy . . . . .	101
A.5 Output . . . . .	101
A.6 Formula interpreter . . . . .	102
<b>B Examples</b>	<b>107</b>
B.1 Files for the example in chapter “User’s Guide” . . . . .	107
Control file <i>Ringverz.sav</i> . . . . .	107
Result file <i>ringverz.ger</i> . . . . .	108
Structure file <i>pbso4ani.str</i> . . . . .	109
Control file <i>pbso4ani.sav</i> . . . . .	109
PowderCell result graph . . . . .	110
RasMol result graph . . . . .	110

---

ShelX result graph . . . . .	111
B.2 Files for the example “Metashale Böhlscheiben” . . . . .	112
Control file <i>Tran0205.sav</i> . . . . .	112
Quartz structure file <i>quarz.str</i> . . . . .	112
Chlorite structure file <i>aphro1.str</i> . . . . .	112
Muscovite structure file <i>mus2m1n.str</i> . . . . .	113
Albite structure file <i>albtief1.str</i> . . . . .	113
Microcline structure file <i>micmax.str</i> . . . . .	113
Control file for refinement by BGMN . . . . .	114
B.3 Files or learnt peak profiles . . . . .	114
<b>C Additional data files</b>	<b>115</b>
C.1 Format of the <i>spacegrp.dat</i> spacegroup file . . . . .	115
C.2 Atomic form amplitudes . . . . .	115

# Chapter 1

## Introduction

### 1.1 The Use of the Rietveld method in X-ray powder diffractometry

The standard application of X-ray powder diffraction is qualitative and quantitative phase analysis. Starting from the pioneering work of H. Rietveld [23], [24], powder diffraction methods are also used for structure refinement and structure solution when single crystals are not available. During the last twenty years, a lot of efforts were undertaken to combine the Rietveld method with microstructural analysis in sophisticated whole-pattern fitting methods. Thus, an ongoing development of programs for the analysis of powder diffraction patterns can be observed.

### 1.2 Practical problems

Rietveld analysis can be executed in a lot of programs. Many functions were added since the first publication of H. Rietveld in 1967 [23].

Most of the developers paid special attention to extend the profile model enabling the user to describe the peak shape within a wide angular range as exact as possible. Despite of all efforts, it was not possible to introduce a universal, precise profile model easy to be used until now. Up to twelve parameters are required to represent the profile shape over the entire angular range. These parameters must be fitted in conjunction with the crystallographic model parameters, resulting in parameter correlation present. This is a main source of divergence of the optimization algorithm, incorrect minima and program crashes.

In addition, the wide-spread Rietveld programs like **DBWS** [29] need a lot of intuition for operation: Having declared an unfavorable set of parameters, the Rietveld programs react very sensibly. As a rule, they breakdown with an error inside the numerical library. In that case, the calculation which had been terminated compulsorily must be restarted from the beginning. This termination results from the use of simple optimization algorithms which cannot consider the physically reasonable ranges of parameters.

BGMN was developed to overcome these problems.

### 1.3 Using this manual

This manual is written for support and guidance to study the BGMN program system. A structure refinement of anglesite ( $\text{PbSO}_4$ ) is described as a first application and for fast learning (in the chapter

“Guide through the program”). The mathematical fundamentals of the Rietveld analysis are explained in the chapter “Theory”. Correct data acquiring is an important precondition for evaluation. For that reason, a chapter on sample preparation and the measuring strategy is inserted. Further chapters deal with preferred fields of application known as “phase analysis” and “size/strain analysis”. Special features of **BGMN** are described in the chapters “learnt peak profiles” and “*hkl* intensity extracting/LeBail fitting”.

A comprehensive table of references explaining program parameters and integrated files completes the manual.

For better visualisation, some phrases are formatted as mentioned below:

- File names are written in *italics*,
- Program names are printed in **bold letters**,
- Environment variables and parameter names are printed in **sans serif font**,
- Output texts of the programs as well as inputs to the program are printed in `Courier font`.

All periods for running the program refer to a computer with a Pentium 4 processor, clock frequency 2.4 GHz, 1 GB RAM.

# Chapter 2

## Advantages of BGMN

### 2.1 New profile model

As the obviously most important advantage of the **BGMN** program system, a completely innovative peak profile model was introduced into the Rietveld analysis for the very first time. We succeeded to completely separate the influences of the experimental set-up (device function) on the measured diffraction pattern from the sample's contribution. The device function is computed by ray-tracing method or extracted from a standard measurement as a preceding operation. When running the optimisation algorithm, all profile parameters depending on the device are kept constant. Following this strategy, correlation between profile and structure parameters — as found in other Rietveld programs — is completely eliminated.

If the device function is calculated by raytracing from fundamental device parameters it is easy to enhance the angular range of the Rietveld analysis down to a  $2\Theta$  angle of  $6^\circ$  despite of the asymmetry of the lines in this region without significant lost of precision. Thus, larger divergencies can be accepted in order to enhance the intensity for better results in structure refinement and phase analysis.

### 2.2 New refinement algorithm for ensuring convergence

As a second benefit being of the same importance for practice as the first one, a totally new mathematical refinement algorithm was developed. In this algorithm, optional boundaries can be introduced for each parameter. As already mentioned above, the influences on peak shape arising from device and sample are separated from each other. For that reason and as a result of optional boundaries for all parameters, it is guaranteed that the **BGMN** program system does converge in *every case*! This effect stands for an essential practical improvement of the Rietveld analysis.

In that sense,

*The BGMN program system is the first software enabling totally automatic Rietveld analysis for routine operation at all.*

### 2.3 Special functions

Some special functions are available for improving the functionality of the program:

**Statistical error analysis** We inserted a reliable statistical error analysis related to the new refinement algorithm. The software performs a statistical error estimation for each parameter cal-

culated. These error values are much more reliable for qualitatively correct results than the  $R$ -values often given.

**Description and correction of preferred orientation** In traditional Rietveld programs, the preferred orientation of the crystals in the sample was modelled by the March function [12]. In this function, exactly one preferred orientation can be calculated, e.g. for the crystallite orientation on a cleavage face. The March function is not suitable to describe orientation distributions.

To overcome the limitations of the March function, the model of spherical harmonics which can also be applied for samples of sophisticated orientation distributions was introduced. Parameter correlation and incorrect results can be avoided by defining the suitable order of the spherical harmonics and by automatic reduction of the chosen model depending on the errors of previous refinement steps.

**Real structure functions** The new profile model also includes possibilities to describe microstructural models. Having isolated the device's influence, one receives the pure diffraction pattern of the sample. From here, a physically based microstructural model to describe individual broadening of lines may be used. One can apply this model for each phase separately and even for anisotropic behaviour. The program is able to calculate crystallite size and microstrain separately. Some tools exist to formulate models for bimodal size distribution or for different types of stacking faults.

**Molecular crystals (rigid bodies)** Functions describing lattice positions, which are placed by molecules instead of atoms were introduced. In cases of molecules, rotational parameters and translational ones are available. Based on the functions for molecules, modifications of valency angles, torsion around bondings as well as stretching/compressing within molecules may be defined.

**Free programmability** If the functions integrated are not sufficient to solve the special problem, new parameters and dependencies may be defined by means of the formula interpreter as integrated in the program. This way, it is easy to describe parameter constraints which are not part of the standard program capacity (e.g. between different atomic positions). It is also possible to formulate dependencies for individual line broadening and shifting. Doing so, much more complicated disorder than only size/strain may be described.

# Chapter 3

## Installation

### 3.1 Hardware and software requirements

Due to the system-independent software development, **BGMN** and its GUI **BGMNwin** runs on many Windows and Linux systems. **BGMN/BGMNwin** demand for only 10 MByte hard disk space (plus user data space) and typical 20 MByte RAM (plus system space) for typical laboratory data. Processor speed should be as good as possible, multicore/multiprocessor PC's are welcome (and may speed up **BGMN** in multithreaded mode).

### 3.2 Installation of BGMN

Here, the installation of **BGMN/BGMNwin** for Windows will be explained. For other operating systems, read the installation instructions on the distributed CD.

At first, you must have a copy of an up-to-date JAVA runtime available. Attention: Nowadays, Windows systems come with a Java plugin for the Internet Explorer (and, maybe, for Netscape/Mozilla/Firefox or other browsers). This is *not* sufficient. You may check this by opening a (black) DOS-window on your Windows system and typing

```
java -version
```

If a version number is printed, all is OK. At least, you need a Java runtime 1.3.0. Java runtimes are available from <http://java.sun.com>.

Having Java installed properly, start `bgmninstall`. This will set up the **BGMN/BGMNwin** program. All programs and data as necessary for running **BGMNwin** will be installed. `bgmninstall` checks for the Java version and terminates if no Java is installed (or is not accessible).

### 3.3 Installation of RasMol

**RasMol** [26] is a program for graphic representation of molecules. It was developed at the Edinburgh university and can be downloaded at <http://www.umass.edu/microbio/RasMol> (free of charge). The program is installed by calling the self-unpacking file. The full manual text is available either in postscript or HTML format at <http://www.umass.edu/microbio/RasMol/distrib/rasman.htm>.

**RasMol** processes molecule files in the format of the Brookhaven protein data base (*\*.pdb*), an optional output format of **BGMN**. The molecules can be displayed and rotated in different modes and colours. Results can be printed. File output in PostScript format or bitmap output (*\*.gif*, *\*.bmp* etc.)

is possible.

To get the unit cell represented correctly, **RasMol** for Windows 2.6 Beta 2 is supposed. This version has a bug when processing the  $y$  screen coordinates. As a result of this error, the unit cell is mirrored whereby the sense of screwing of the molecules could be inverted.

### 3.4 Installation of ORTEP-3 for Windows

**ORTEP-III** [8] stands for a program generated at the Oak Ridge National Laboratory. **ORTEP-III** was developed to represent the thermal vibration ellipsoids. The software is available as FORTRAN source code for different computer levels and operating systems. It has a specific input format tailored for the crystal structures. To be used with **BGMN**, this structure file must be created manually. For the program and installation instructions see the **ORTEP-III** homepage <http://www.ornl.gov/ortep/>.

Since the beginning of 1997, a beta version of **ORTEP-3** for Windows (<http://www.chem.gla.ac.uk/~Louis/ortep3>) is available. This version includes interactive graphic representation and is able to read the ShelX output files of **BGMN** (extension *\*.res*). That means you don't have to program in the typical **ORTEP-III** data format. The program only runs under Windows 3.1 and Windows 95, but not under Windows NT.

Load the program as packed file *ortep3.zip* from the homepage listed above. Installation instructions are given in this file.

### 3.5 Installation of PowderCell

**PowderCell** [18] is a free program for displaying crystal structures and calculation of powder patterns. Furthermore, the program reads different types of structure files and can write them into **BGMN** *\*.str* structure description file. **PowderCell** also enables the transformation of spacegroup settings and cell choices as well as the recalculation of anisotropic into isotropic temperature factors. The program can be obtained from <http://www.ccp14.ac.uk/tutorial/powdcell>.

# Chapter 4

## User's Guide

Here, we describe the general functionality of the **BGMNwin** package. As an introduction, see figure 4.1:

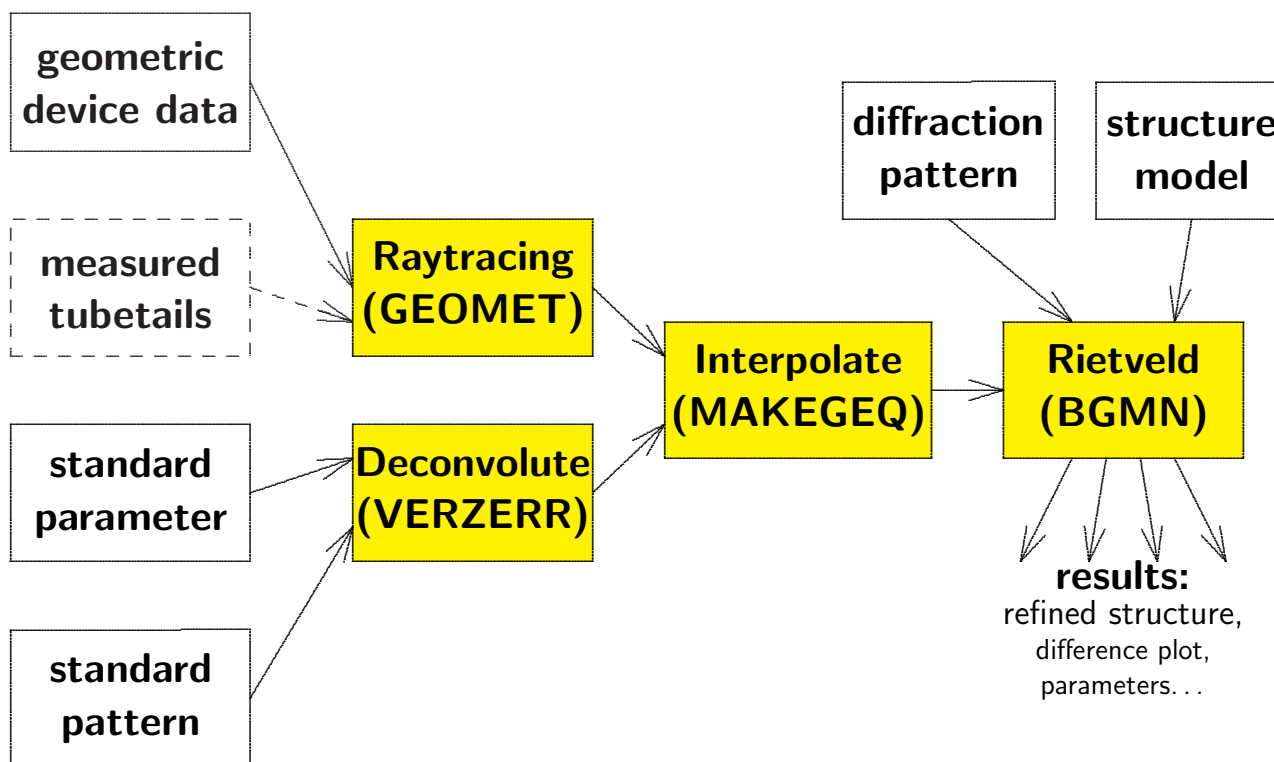


Figure 4.1: Overview of the BGMNwin functionality

Let's have a look at an example<sup>1</sup> to explain functionality and use of the **BGMN** program system. The example describes a refinement of a single phase, measured in conventional Bragg-Brentano geometry.

### 4.1 Modelling of goniometer function by raytracing

The goniometer function is modelled in two steps to avoid time-consuming calculations of one and the same function.

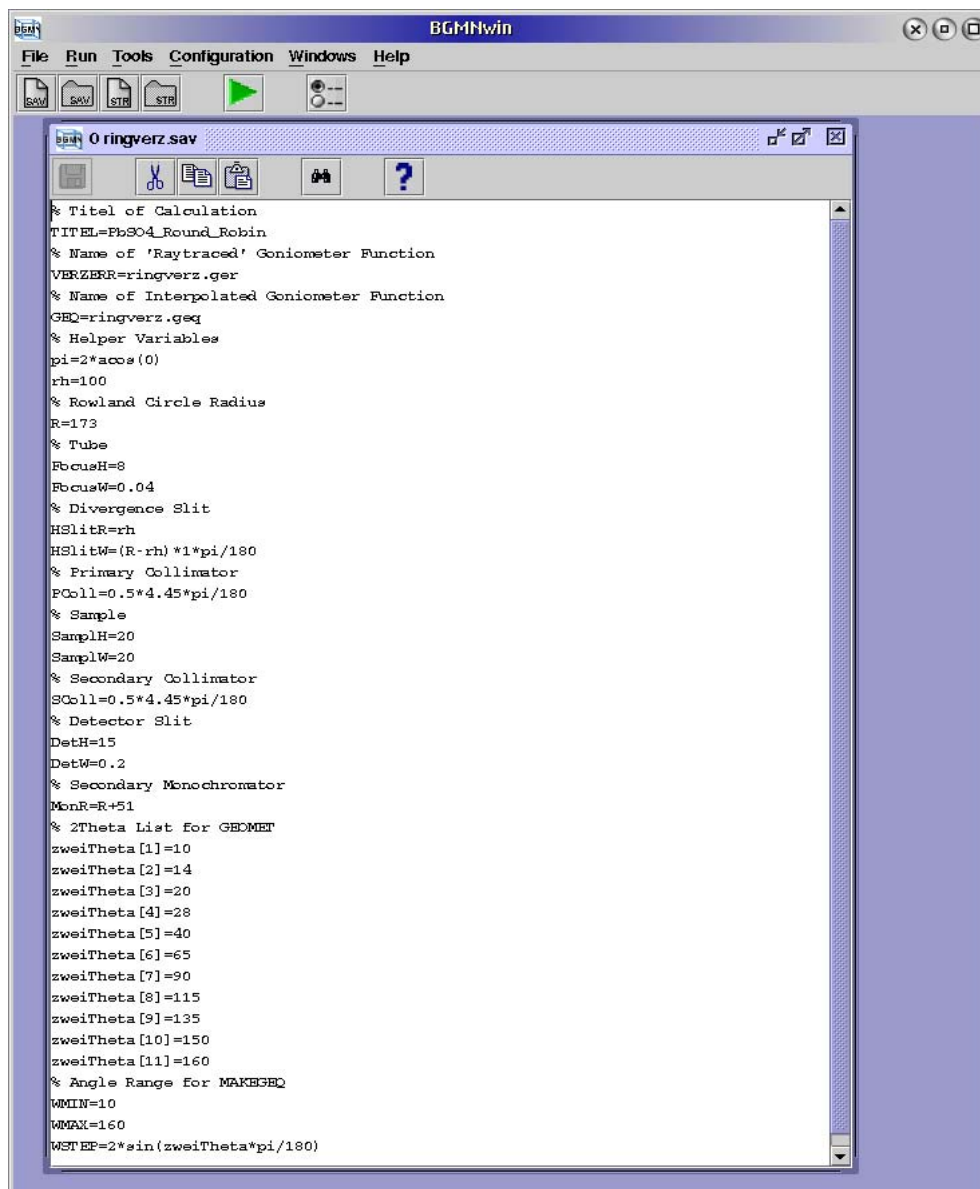
<sup>1</sup>Anglesite (PbSO<sub>4</sub>), measurement data of the Rietveld Round Robin [13]

## Step 1: Geometric profile estimation at discrete angular positions

Open **BGMNwin** and chose

File→Open Control File

Browse to the *PBSO4\ringverz.sav* file. Open it:



```

% Titel of Calculation
TTITEL=PbSO4_RoundRobin
% Name of 'Raytraced' Goniometer Function
VERZERR=ringverz.ger
% Name of Interpolated Goniometer Function
GEQ=ringverz.geq
% Helper Variables
pi=2*acos(0)
rh=100
% Rowland Circle Radius
R=173
% Tube
Fbush=8
FbushW=0.04
% Divergence Slit
HSlitR=rh
HSlitW=(R-rh)*1*pi/180
% Primary Collimator
PColl=0.5*4.45*pi/180
% Sample
SamplH=20
SamplW=20
% Secondary Collimator
SColl=0.5*4.45*pi/180
% Detector Slit
DetH=15
DetW=0.2
% Secondary Monochromator
MonR=R+51
% 2Theta List for GEOMET
zweiTheta [1]=10
zweiTheta [2]=14
zweiTheta [3]=20
zweiTheta [4]=28
zweiTheta [5]=40
zweiTheta [6]=65
zweiTheta [7]=90
zweiTheta [8]=115
zweiTheta [9]=135
zweiTheta [10]=150
zweiTheta [11]=160
% Angle Range for MAKEGEQ
WMIN=10
WMAX=160
WSTEP=2*sin(zweiTheta*pi/180)

```

See also Appendix B.1.

The theory of this step is explained in detail in chapter 5.5.

For this example, we are using the common Bragg-Brentano geometry. Therefore, we determine the geometric profile function by raytracing.

The profile function of an ideal, thin sample at discrete angular positions is calculated from geometric data of the X-ray tube, the goniometer and the detector. In the first stage the profile functions are determined by means of a raytracing algorithm.

Exemplary goniometer fundamental parameters:

- Measuring circle radius 173 mm

- Fine focus X-ray tube with optical focus  $8 \text{ mm} \times 0.04 \text{ mm}$
- Primary collimator  $0.5 \times 4.45^\circ$  axial divergence angle
- Divergence slit  $1^\circ$
- Sample dimensions of  $10 \text{ mm} \times 20 \text{ mm}$
- Secondary collimator  $0.5 \times 4.45^\circ$
- Detector slit  $0.2 \text{ mm} \times 15 \text{ mm}$
- Graphite secondary monochromator (distance to the measuring circle  $51 \text{ mm}$ )

For detailed description of geometry parameters see Appendix A.1, B.1.

The anti-scatter slit does not limit the beam path. For that reason the slit is not required for calculation. The profile function is computed at the following angle positions  $2\Theta$ :

- $10^\circ, 14^\circ, 20^\circ, 28^\circ, 40^\circ, 65^\circ, 90^\circ, 120^\circ, 135^\circ, 150^\circ, 160^\circ$

For carrying out the calculation, the control file *ringverz.sav* (see example in appendix) was written. Start the calculation by selecting

Run→Geomet

browse to the *PBSO4\ringverz.sav* file and press OK. The calculation needs some minutes depending from the CPU frequency. On screen, you can follow the angular positions of calculated profile functions. As a result, the file *ringverz.ger* containing the calculated profile parameters is generated. *ringverz.ger* is a text file which is needed for the second step.

## Step 2: Interpolation of goniometer function by the program MAKEGEQ

Again, edit the *ringverz.sav* file. See Appendix B.1. In this second step additional profiles are interpolated between the individual profiles computed in step 1 in a procedure demanding for a lot of time. In the example the interpolation was executed between  $10$  and  $160^\circ$  at variable increments. At a  $2\Theta$  angle of  $90^\circ$ , the step size as given by the variable *WSTEP* is  $2^\circ$ . This is the meaning of the following lines in the *ringverz.sav* file:

```
WMIN=10
WMAX=160
WSTEP=2*sin(zweiTheta*pi/180)
```

Thus, the program automatically generates variable increments for interpolation of the profiles. Such a procedure is more suitable than constant increments of e.g.  $0.5^\circ$ .

If you know the approximate value of the sample's attenuation coefficient, you can also consider the profile deformation as a result of the X-rays penetrating the sample. Transmission effects in the case of thin samples can also be considered here. In the actual example, the penetration effect can be ignored because of the height absorption of  $\text{PbSO}_4$ .

The calculation can be done by using the control file *ringverz.sav* of the first step, extended by the parameters for angular range and penetration depth/sample thickness. Please select

Run→MakeGEQ

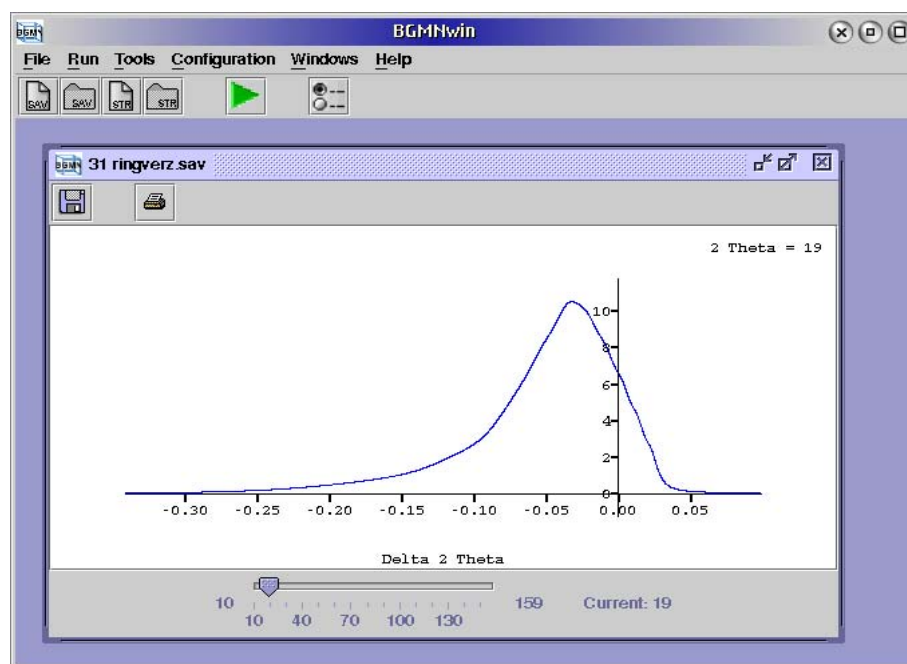
browse to the *ringverz.ger* file and press OK. As a result we obtain the binary file *ringverz.geq* including the interpolated profiles. This file contains all geometric profile information as necessary for the Rietveld refinement.

## Display of calculated profiles

The device profile is displayed by

Tools→Show Device Function

Browse to the *ringverz.ger* file, press OK and wait some seconds. You may select different  $2\Theta$  angles by moving the slide on the bottom of the device window. You may zoom in/out using the left/right mouse button:



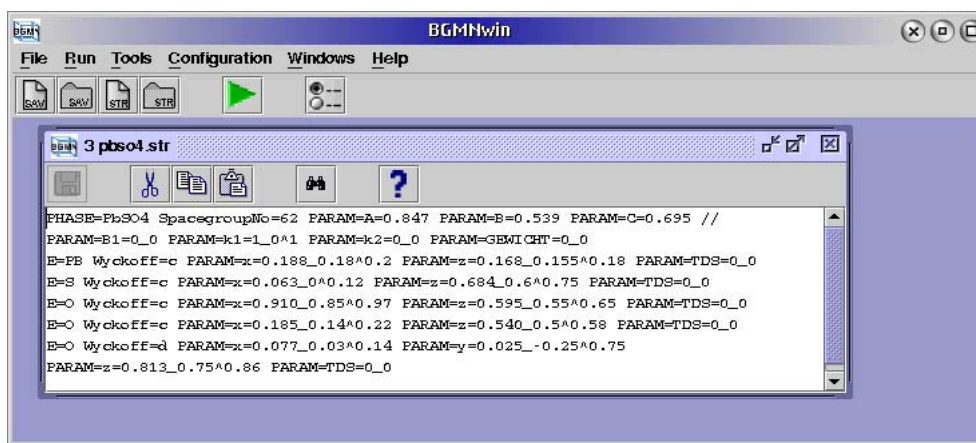
The geometric profile is shown purely, not taking into account the wavelength distribution. The intensity distribution around the ideal angle is represented. Asymmetric tails and the shift of the maximum to a lower angle can be seen clearly.

## 4.2 Input of sample structure data

For Rietveld analysis, the crystal structure models of the individual phases being part of the sample must be known. For example, the crystal structure of anglesite ( $\text{PbSO}_4$ ) is described as follows: Select

File→Open Structure File ,

browse to the *PBSO4\pbs04.str* file and open it:



Structure data must be prepared in ASCII text files with the extension *\*.sav*.

### First part: Define lattice and all phase-specific parameters

Phase name, lattice constants, real structure parameters (B1, k1 and k2), isotropic or anisotropic scale (in the case of available preferred orientations) and maybe further global parameters are specified in the first part of the *pbs04.str* file. Comments may be inserted at the end of every line beginning with *//*.

The **PHASE** parameter stands for the name of this compound. This name appears during program output. When missing, the name of the structure file will be used.

Specify the spacegroup number or the Hermann-Mauguin symbol:

```
SpacegroupNo=62
```

Note that different settings or choices of origin may exist for the same Hermann-Mauguin symbol. For details see A.4, section “structure file”. All parameters to be refined are added by **PARAM=**. The name of the parameter is followed by the start value for refinement calculation, e.g.

```
PARAM=A=0.85
```

For default, the SI unit nm is used for program calculations. If you want to use Å instead of nm, change the unit by **UNIT**:

```
UNIT=ANGSTROEM
```

Subsequently lattice constants, widths and Debye-Waller-factors are computed in Å.

To increase the robustness of calculation and to avoid incorrect minima it is often useful to set parameter restraints. Insert limits by the character “\_” followed by a lower limit value or by “^” followed by an upper limit value. For notation see the following example of a lattice constant:

```
PARAM=A=0.85_0.8^0.9
```

The identifiers **A**, **B**, **C**, **ALPHA**, **BETA** and **GAMMA** denominate the lattice constants in the predefined manner. You may ignore input of these parameters if **B** or **C** are equal to **A** or if the angles are 90° or 120° caused by the spacegroup symmetry. Maybe additional lattice constants will be ignored in the case that the spacegroup involves some special constraints for the lattice constants. Supposing e.g. a cubic lattice, the input **PARAM=B=...** would not give any effect.

The **GEWICHT** parameter (scale factor) must also be specified. **GEWICHT** quantifies the phase's weight fraction in the sample<sup>2</sup>. Starting value may be zero:

```
PARAM=GEWICHT=0_0
```

The lower boundary results from physical reasons to avoid a negative parameter.

In practice the phases are characterized by line broadening as a function of crystallite size and of microstrain. The width parameters **B1** and **k1** are introduced for those ratios of crystallite size broadening appearing in each case:

```
PARAM=B1=0_0
```

**B1** cannot be negative. In the case of very large crystallites **B1** converges to zero.

```
PARAM=k1=0_0^1
```

The **k1** boundaries are founded mathematically. Small **k1** values correspond to a wide distribution of crystallite sizes and high **k1** values a narrow one.

Microstrain broadening is considered by **k2**:

```
PARAM=k2=0_0
```

**k2** is the square of the value for microstrain "rms".

The definition of the lattice and the phase-specific parameters is finished now. But we still need some information about the atoms or ions inside the unit cell.

## Ongoing lines: Define atoms inside the asymmetric unit

Beginning with the first occurrence of

```
E=
```

the atoms<sup>3</sup> inside the unit cell are characterized. The number of atoms is not limited.

As a necessary input identify the element in capital letters. Write for instance:

```
E=PB
```

Furthermore specify its position in the unit cell. Define the Wyckoff position:

```
Wyckoff=c
```

Determine the free **x**, **y** and **z** coordinates as demanded by the Wyckoff position in lower case letters. If necessary, refine these coordinate positions as parameters, e.g.

```
PARAM=x=0.19_0.16^0.22
```

As learnt from experience, it is useful to specify lower and upper boundaries.

You can also introduce the parameter **TDS** for the Debye-Waller-factor, whereas **TDS** stands for "thermal-diffuse scattering". Introduce **TDS** depending of the atom:

```
PARAM=TDS=0_0
```

default unit is nm<sup>2</sup>, exceptional if **UNIT=ANGSTROEM** is set.

Structure description is finished after having edited all atoms.

---

<sup>2</sup>The parameter **GEWICHT** is designated as a scale factor like in other Rietveld programs, but related to the molar mass of the structure. It also may contain information for the correction of the preferred orientation.

<sup>3</sup>"Atoms": always also stands synonymously for ions.

## 4.3 Refinement procedure

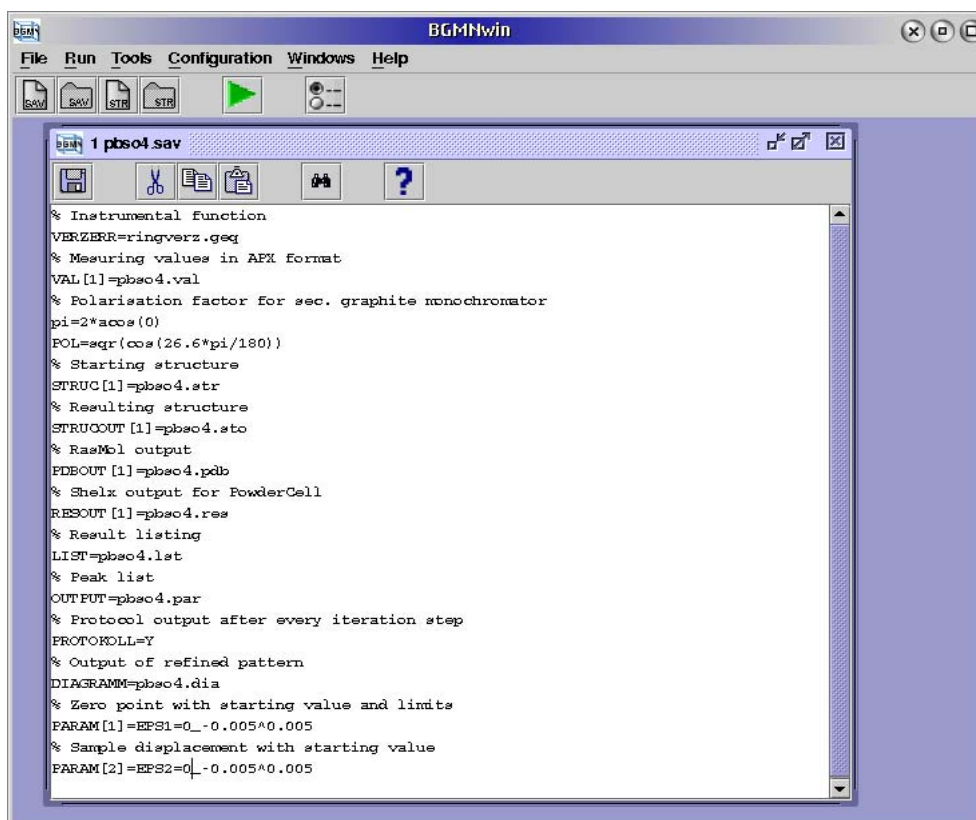
### Control file

The refinement calculation is controlled by a *\*.sav* file which contains information on the device, measurement data, involved phases and global parameters. In cases of missing entries, the program generates reasonable default values.

In **BGMNwin**, select

File→Open Control File

browse to the *pbs04.sav* file and open it:



The following items are necessary:

Specify the device function calculated before:

```
VERZERR=ringverz.geq
```

Specify the file of measuring values in the APX-63 ASCII (*\*.val*):

```
VAL[1]=pbs04.val
```

BGMN also accepts old versions of both the DiffracAT (*\*.raw*) or the APD (*\*.rd*) binary format, or two versions of the GSAS *\*.gsa* format: the STD and the ESD variants. In the case of GSAS files, the wavelength must be set either by

```
LAMBDA=
```

or by

SYNCHROTRON=

in the \*.sav file. In case of other file formats the wavelength information is taken from the data file itself.

Please pay attention that the preselected time must be transferred correctly when converting other formats into the APX-63 format. These data are absolutely necessary for calculation of the weights for optimization and determination of errors (computation procedures).

Set the polarisation factor when applying a graphite secondary monochromator:

```
pi=2*acos(0)
POL=sqr(cos(26.6*pi/180))
```

The pi constant is required to convert the  $2\Theta$  monochromator angle of 26.6 degs into a radian scale. Specify the Structure to be refined:

```
STRUC[1]=pbs04.str
```

Define the output of the result structure in structure file format (optional):

```
STRUCOUT[1]=pbs04.sto
```

Result structure in atomic co-ordinates in the PDB file format (optional):

```
PDBOUT[1]=pbs04.pdb
```

Result structure in Cartesian co-ordinates in the RES file format (optional):

```
RESOUT[1]=pbs04.res
```

Output list including all global parameters and structure parameters, text output:

```
LIST=pbs04.lst
```

Output file of all peak and background parameters for further processing as table:

```
OUTPUT=pbs04.par
```

Output of a diagram for observing the pattern fitting during and after refinement:

```
DIAGRAMM=pbs04.dia
```

Global parameters for zero offset (EPS1) and correction of the sample displacement (EPS2) using initial values:

```
PARAM[1]=EPS1=0_-0.002^0.002
PARAM[2]=EPS2=0_-0.002^0.002
```

Protocol line corresponding to each step of iteration:

```
PROTOKOLL=Y
```

Now the refinement calculation can be started.

## Start and execution of calculation

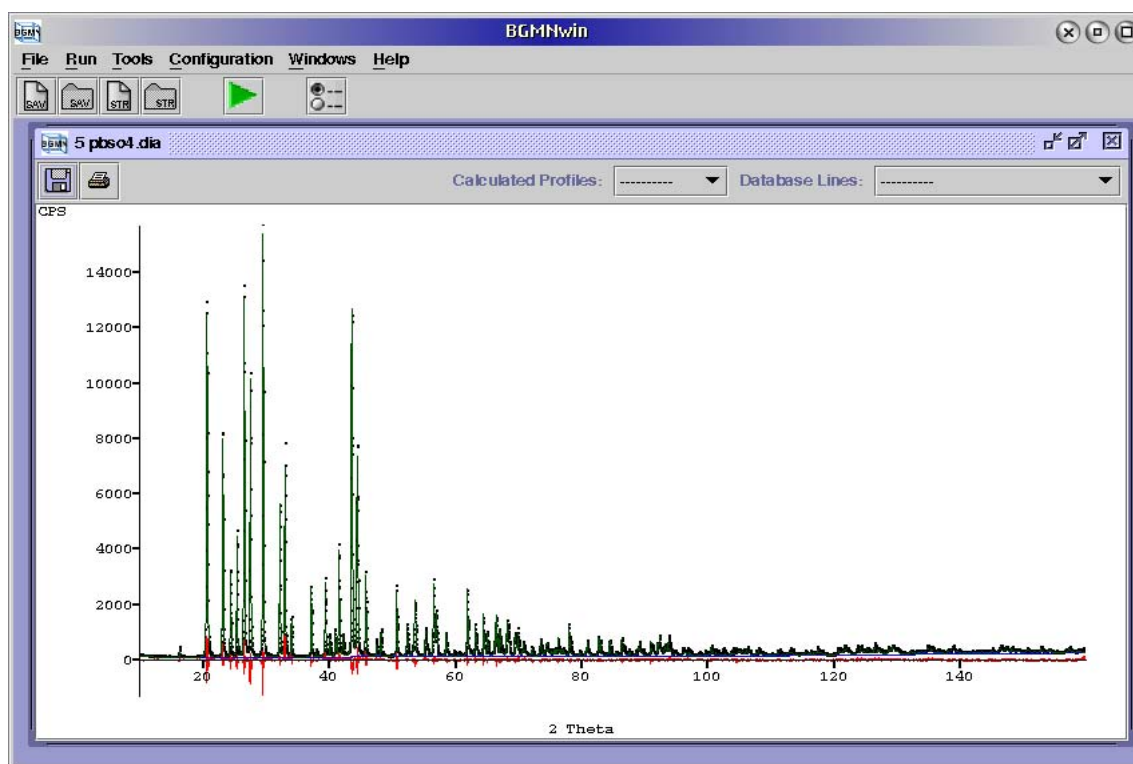
Starting the refinement calculation is possible after having performed the calculation of the device function and having input the structures and the control file. It is recommended to put all files which refer to a specific problem into a separate subdirectory. Start the calculation in this subdirectory by selecting

Run→BGMN

browse to the *pbs04.sav* file, select the item “Show diagram during calculation” and press OK.

The calculation has started and some information is displayed in a text a window. If an output protocol was demanded by `PROTOKOLL=Y`, then the iteration protocol is visible in this window. In the protocol line the first column is the number of the iteration step. The second column stands for the weighted least squares sum. For a good iteration the 3rd value will regularly slow down until there will be no change on the second value, the 4th value will be a small positive number deeply below 1.0 (regularization) and the 5th value will be instantly 1.0 (generalization).

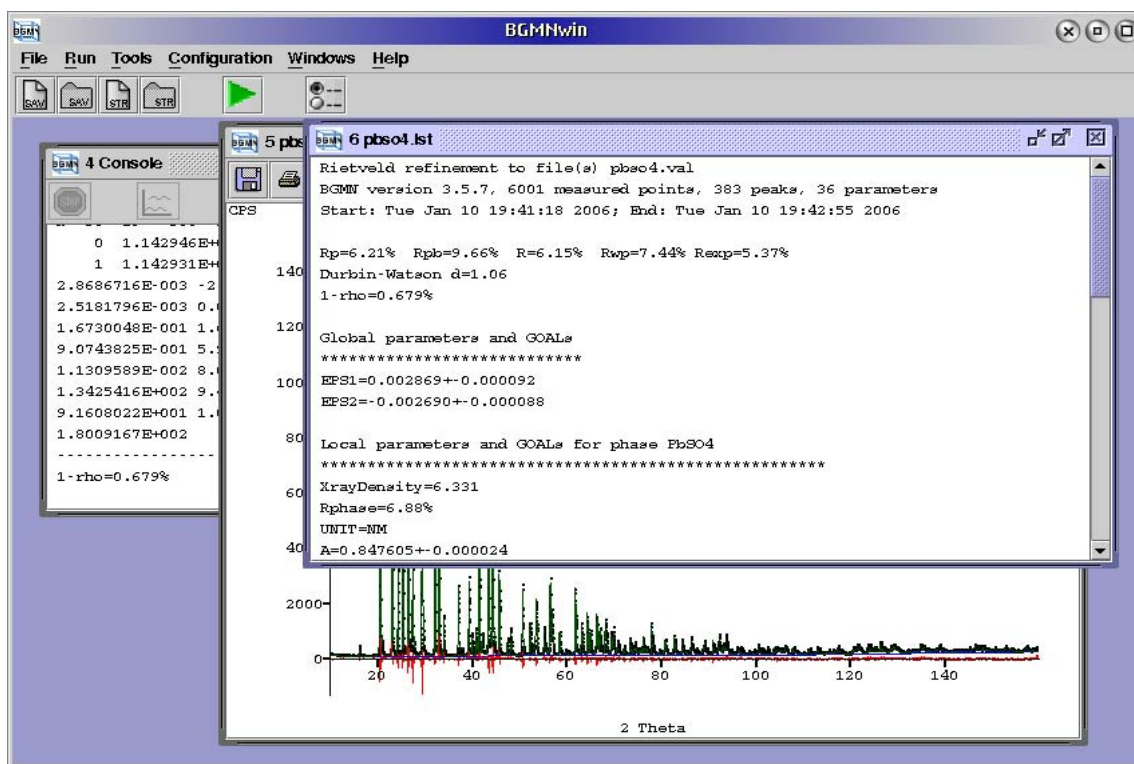
If a diagram was demanded by `DIAGRAMM= . . .` then a graphic window opens. It shows the pattern data, the refined curves and background. You may zoom into the window and select some other features. The “Calculated Profiles” menu can be used display individual phase patterns. With the “Database Lines” menu, the line positions all structure files stored in the *structures* subdirectory of the **BGMN** installation directory can be displayed. This tool is foreseen for checking the completeness of phase identification.



## 4.4 Output of results

### List of results

After successful iteration, the result list (*pbs04.lst* file) is created and immediately shown in a result window:



```
Rietveld refinement to file(s) pbs04.val
BGMN version 4.0.15, 6001 measured points, 384 peaks, 36 parameters
Start: Sun Sep 21 19:09:03 2008; End: Sun Sep 21 19:09:40 2008
31 iteration steps
```

The  $R$  values obtained as a result of fitting:

```
Rp=6.12% Rpb=9.49% R=6.11% Rwp=7.21% Rexp=5.37%
Durbin-Watson d=1.13
1-rho=0.639%
```

Determined global parameters and associated stochastic errors:

```
Global parameters and GOALS
*****
EPS1=0.002796+-0.000088
EPS2=-0.002620+-0.000084
```

Determined parameters and their statistical errors for the refined structures:

```
Local parameters and GOALS for phase PbSO4
*****
```

Space group:

```
SpacegroupNo=62
HermannMauguin=P2_1/n2_1/m2_1/a
```

X-ray density in  $\text{g/cm}^3$ :

```
XrayDensity=6.330
```

Phase specific  $R$ -value:

Rphase=6.87%

Unit used for all data inside this structure description (e.g. lattice parameters, distances, size broadening and temperature factors):

UNIT=NM

Lattice constants in nm:

A=0.847625+-0.000023

B=0.539600+-0.000014

C=0.695664+-0.000019

Physical peak width parameters ( $B1$  in 1/nm,  $k1$  non-dimensional,  $k2$  in 1/(nm<sup>2</sup>)):

B1=0.002520+-0.000037

k1=0

k2=0.0000000655+-0.0000000075

Scale parameter:

GEWICHT=0.11191+-0.00038

Determined parameters and associated stochastic errors for refined atomic positions:

Atomic positions for phase PbSO4

-----

Short data for atomic position:

4 c 0.1880 0.2500 0.1673 E=(PB(1.0000))

Results for atomic position parameters each with random error:

x=0.187995+-0.000063

z=0.167293+-0.000091

TDS=0.01624+-0.00013

Results of further atomic positions:

4 c 0.0643 0.2500 0.6847 E=(S(1.0000))

x=0.06428+-0.00036

z=0.68471+-0.00047

TDS=0.00991+-0.00061

4 c 0.9074 0.2500 0.5959 E=(O(1.0000))

x=0.90737+-0.00086

z=0.59587+-0.00097

TDS=0.0137+-0.0018

4 c 0.1884 0.2500 0.5401 E=(O(1.0000))

x=0.18836+-0.00094

z=0.5401+-0.0012

```

TDS=0.0128+-0.0016

      8 d      0.0803  0.0293  0.8110      E=(O(1.0000))
x=0.08027+-0.00058
y=0.02928+-0.00079
z=0.81096+-0.00082
TDS=0.0127+-0.0011

```

The output may vary somewhat depending on the computed parameters and the number of phases.

## Result representation

If you have used the *pbso4.str* entry

```
STRUCOUT [1] =pbso4.sto
```

to store the refinement results of the  $\text{PbSO}_4$  structure in the specified file *pbso4.sto*, then a copy of the *pbso4.str* structure file is created. In this new file, the initial parameter start values are replaced by the results of the refinement. If necessary further calculation can be done without changing the initial structure file.

If the entry

```
PDBOUT [1] =pbso4.pdb
```

exists in the control file, the refined structure is written into a file in the “Brookhaven Protein Database” (PDB) format in Cartesian co-ordinates. **RasMol** is an efficient tool for graphic representation and printing in this file format. You may find useful a line containing `PACK=Y` in the structure file for correct representation of the unit cell in **RasMol**.

The structure file format of the widely used program **ShelX** is also available for display. Create a structure file in the **ShelX** format by the entry

```
RESOUT [1] =pbso4.res
```

in the *pbso4.sav* file. Such structure files may be read by **PowderCell** and other programs for display.

## Peak list

If information on individual peaks is required, simply select

```
Tools→Show Peak List
```

, browse to the *PBSO4\ringverz.sav* file and press OK. This creates a table of all peaks fitted in the measuring range:

0 Peak List

E:\BGMNWIN\output.exe "pbso4.sav" "CHDIR=E:\VAL\www.bgm.de\pbso4" NICE=31  
 BGMN and related programs Copyright (C) J. Bergmann Dresden 1991-2005  
 BGMN is a registered trademark of J. Bergmann  
 Version 3.5.7  
 Developers version for internal use only  
 changing working directory to E:\VAL\www.bgm.de\pbso4

2 Theta	Int	%	d	sk=1/d	b1	b2^2	Phase	H	h	k	l	TEKTUR	F
degree	degree*cps		nm	1/nm	1/nm	nm** -2							
16.486	6.2812E+001	2.19	0.537732	1.859662	0.0025182	2.26130E-007	PbSO4	4	1	0	1		22.45
20.836	2.0626E+003	71.91	0.426362	2.345425	0.0025182	3.59700E-007	PbSO4	4	0	1	1		163.51
20.963	7.7874E+002	27.15	0.423803	2.359589	0.0025182	3.64060E-007	PbSO4	2	2	0	0		142.98
23.356	1.4443E+003	50.35	0.380889	2.625440	0.0025182	4.50710E-007	PbSO4	8	1	1	1		108.86
24.599	5.5749E+002	19.44	0.361927	2.762985	0.0025182	4.99180E-007	PbSO4	4	2	0	1		100.93
25.613	7.9643E+002	27.77	0.347824	2.875014	0.0025182	5.40480E-007	PbSO4	2	0	0	2		177.93
26.750	2.3811E+003	83.01	0.333292	3.000375	0.0025182	5.88640E-007	PbSO4	4	2	1	0		227.64
27.725	1.8547E+003	64.66	0.321784	3.107671	0.0025182	6.31490E-007	PbSO4	4	1	0	2		208.58
29.725	2.8683E+003	100.00	0.300574	3.326962	0.0025182	7.23760E-007	PbSO4	8	2	1	1		197.36
32.397	1.0606E+003	36.98	0.276372	3.618316	0.0025182	8.56070E-007	PbSO4	8	1	1	2		131.45
33.209	1.3245E+003	46.18	0.269794	3.706530	0.0025182	8.98320E-007	PbSO4	2	0	2	0		301.64
33.327	5.0632E+001	1.77	0.268866	3.719323	0.0025182	9.04530E-007	PbSO4	4	2	0	2		41.86
34.258	2.5641E+002	8.94	0.261769	3.820165	0.0025182	9.54250E-007	PbSO4	4	3	0	1		97.01
37.292	2.3771E+000	0.08	0.241144	4.146892	0.0025182	1.12450E-006	PbSO4	8	1	2	1		7.23

The columns of the table are:

2 Theta

angle of the peak in  $^{\circ}$  (weighted average of  $K\alpha_1$  and  $K\alpha_2$ )

Int

intensity in  $\text{cps} \times ^{\circ}$

%

normalized intensity (the strongest peak corresponds to 100%)

d

lattice plane distance of the reflection in nm

1/d

inverse lattice plane distance in  $\text{nm}^{-1}$

b1

Cauchy width of the sample function (Lorentzian)

b2^2

Cauchy square width of the sample function (squared Lorentzian) in  $\text{nm}^{-2}$ . The sample function is a convolution product of a Lorentzian- and a squared Lorentzian function (see section 5.5).

PHASE

phase identifier, corresponds with PHASE= . . . in the \*.str structure file

H

multiplicity of the lattice plane

h, k, l

Miller's indices of the peak, each a representative for peaks equivalent according to symmetry

- TEXTUR preferred orientation correction factor which describes the intensity difference from the isotropic distribution. Specified for anisotropic scales only. This factor corresponds to the inverse pole figure at the reflection position.
- F absolute value of the structure amplitude  $|F|$

## 4.5 Improvement of results

Edit *pbso4.str* again. You may change the file for creating a more complex starting model. Typical examples of more complex parameters are:

### Preferred orientation

In the case of preferred orientation the scale parameter has to be specified in different way, e.g.

```
GEWICHT=SPHAR2
```

Note that the specific keyword **SPHARx** is introduced to define a positive definite function holding the crystal's symmetry.

Regarding the  $\text{PbSO}_4$  example, the result is influenced insignificantly by introducing a simple description of preferred orientation by **SPHAR2**. The  $R_{wp}$  value goes down from 7.44% to 7.28%. Obviously, the sample has been prepared almost without texture.

### Anisotropic peak width

Anisotropic crystallite size and/or anisotropic microstrain may occur. The program is able to cope with both cases via integrated functions.

To calculate anisotropic crystallite sizes the following input is sufficient:

```
B1=ANISO or B1=ANISOLIN
```

Subsequently the program automatically generates a set of parameters for the determination of the Lorentzian peak widths depending on the lattice direction.

Supposing anisotropic microstrain as additional impacts, write in *pbso4.str*

```
k2=ANISO or k2=ANISOSQR
```

In this case an anisotropic parameter set for squared Lorentzian peak widths is created. This calculation demands for sufficiently precise measurement data. For further description of the anisotropic micro strain modelling by a tensor of rank 4 see Chapter 10.

Having introduced anisotropic widths **B1**, the  $R_{wp}$  value goes down from 7.44% to 7.37%. Anisotropic microstrain cannot be evidenced. Note that the isotropic broadening resulting from microstrain is very small anyway.

### Anisotropic temperature factor (Debye-Waller-factor)

The program also provides an option to consider anisotropic temperature factors by

```
TDS=ANISO
```

instead of

```
PARAM=TDS=0_0
```

for each atom in the \*.str file.

Thus a suitable parameter set is created automatically in a way similar to anisotropic peak widths. But the calculation of anisotropic temperature factors demands for a data set of sufficient accuracy and an angular range being as large as possible. Such data set is necessary to reduce correlation, e.g. with the parameters of the preferred orientation.

Introduce an upper boundary for the isotropic initial iteration to avoid parameters *for anisotropic temperature factors* whose large values make no sense, for example:

```
TDS=ANISO^2.5
```

This boundary is an isotropic Debye-Waller-factor. The relationship between the TDS parameters and the common inputs for **B** and/or **U** is described in chapter “Theory”, section “Temperature factors”.

## 4.6 Calculation example

The following calculation includes all the improvements mentioned above (weak preferred orientations are considered by SPHAR2, anisotropic width **B1** and anisotropic temperature factors TDS for all atoms). The new output results are obtained for PbSO<sub>4</sub>:

```
Rietveld refinement to file(s) pbso4.val
BGMN version 4.0.15, 6001 measured points, 384 peaks, 71 parameters
Start: Sun Sep 21 19:22:53 2008; End: Sun Sep 21 19:24:31 2008
73 iteration steps

Rp=5.63% Rpb=8.69% R=5.43% Rwp=6.53% Rexp=5.36%
Durbin-Watson d=1.34
1-rho=0.523%

Global parameters and GOALS
*****
EPS1=0.002794+-0.000076
EPS2=-0.002621+-0.000072

Local parameters and GOALS for phase PbSO4
*****
SpacegroupNo=62
HermannMauguin=P2_1/n2_1/m2_1/a
XrayDensity=6.330
Rphase=5.97%
UNIT=NM
A=0.847627+-0.000019
B=0.539602+-0.000013
C=0.695668+-0.000016
k1=0
k2=0.0000000761+-0.0000000070
GEWICHT=SPHAR2, MeanValue(GEWICHT)=0.111878
B1=ANISOLIN, MeanValue(B1)=0.00247611, sqrt3(det(B1))=0.00236677
Atomic positions for phase PbSO4
-----
  4 c    0.1879  0.2500  0.1671    E=(PB(1.0000))
x=0.187883+-0.000059
z=0.167078+-0.000090
TDS=ANISO, vibrational matrice for 1st atomic position:
(beta dimensionless, U in nm**2)
beta[i,j]=(0.00403, 0.00000, 0.00033 U[i,j]=(0.0001467, 0.0000000, 0.0000099
          0.00000, 0.01856, 0.00000          0.0000000, 0.0002738, 0.0000000
          0.00033, 0.00000, 0.00781)          0.0000099, 0.0000000, 0.0001915)

  4 c    0.0636  0.2500  0.6847    E=(S(1.0000))
```

```

x=0.06362+-0.00035
z=0.68466+-0.00048
TDS=ANISO, vibrational matrice for 1st atomic position:
(beta dimensionless, U in nm**2)
beta[i,j]=(0.00274, 0.00000, 0.00063 U[i,j]=(0.0000996, 0.0000000, 0.0000187
          0.00000, 0.00774, 0.00000          0.0000000, 0.0001142, 0.0000000
          0.00063, 0.00000, 0.00471)          0.0000187, 0.0000000, 0.0001155)

  4 c    0.9079  0.2500  0.5967      E=(O(1.0000))
x=0.90794+-0.00083
z=0.59675+-0.00097
TDS=ANISO, vibrational matrice for 1st atomic position:
(beta dimensionless, U in nm**2)
beta[i,j]=(0.00429, 0.00000,-0.00455 U[i,j]=(0.0001560, 0.0000000,-0.0001359
          0.00000, 0.02074, 0.00000          0.0000000, 0.0003059, 0.0000000
          -0.00455, 0.00000, 0.00902)          -0.0001359, 0.0000000, 0.0002212)

  4 c    0.1920  0.2500  0.5442      E=(O(1.0000))
x=0.19196+-0.00092
z=0.5442+-0.0013
TDS=ANISO, vibrational matrice for 1st atomic position:
(beta dimensionless, U in nm**2)
beta[i,j]=(0.00328, 0.00000, 0.00693 U[i,j]=(0.0001195, 0.0000000, 0.0002072
          0.00000, 0.01349, 0.00000          0.0000000, 0.0001990, 0.0000000
          0.00693, 0.00000, 0.01519)          0.0002072, 0.0000000, 0.0003724)

  8 d    0.0792  0.0289  0.8075      E=(O(1.0000))
x=0.07917+-0.00057
y=0.02894+-0.00075
z=0.80752+-0.00078
TDS=ANISO, vibrational matrice for 1st atomic position:
(beta dimensionless, U in nm**2)
beta[i,j]=(0.00265,-0.00072,-0.00059 U[i,j]=(0.0000963,-0.0000167,-0.0000178
          -0.00072, 0.01145,-0.00252          -0.0000167, 0.0001689,-0.0000480
          -0.00059,-0.00252, 0.00446)          -0.0000178,-0.0000480, 0.0001094)

```

Pay attention to the low error values of the individual parameters (lattice constants, atomic coordinates) evidencing the high model quality with respect to the crystal structure. Compared with the results of the Round Robin Test for  $\text{PbSO}_4$  [13] the calculation could be confirmed as correct.

# Chapter 5

## Theory

This chapter explains the fundamental background of the Rietveld method as used to implement the Rietveld method by the **BGMN** program.

Cross-references are inserted to illustrate the relationships of the formula parameters to those parameters being mentioned in the chapters before or in the references. As a rule, if there is no explanation, the corresponding parameter is determined automatically in the program.

### 5.1 Optimization method

The Rietveld method is an optimization procedure to fit a model of the examined sample to a measured diffraction pattern. A parameter set is used for fitting. Hereby the least squares sum is minimized as follows:

$$\sum_{i=1}^M w_i (y_i - y_{ic})^2 \quad (5.1)$$

with

- $M$  Pattern length (number of data points).
- $y_i$  Measured intensity at pattern data point  $i$ .
- $y_{ic}$  Computed intensity at pattern data point  $i$ .
- $w_i$  Weight at pattern data point  $i$ , commonly  $T_i \cdot y_i^{-1}$
- $T_i$  Counting time as preselected for pattern data point  $i$

As to be seen from the following explanations, the parameters of the crystallographic model are mostly non-linear. For physical reasons, their parameter ranges are limited. Consequently, the program has to solve a non-linear optimization problem with constraints and restraints

The non-linear optimization algorithm of **BGMN** was developed carefully. The routine is based on an algorithm given by Schwetlick [27]. All first derivatives demanding for extremely high CPU time (these are the derivatives of the diagram intensity according to the peak and background parameters) are determined analytically. Derivatives from peak- to structure parameters are approximated by difference quotients using a formula interpreter which is integrated into **BGMN**. In contrast to Schwetlick [27], the following special features are implemented:

1. During calculation the generalization and regularization are kept variable. The regularization parameter for the  $n + 1^{th}$  step is pre-estimated from the deviation of the descent point of step  $n$

against the ideal parabola according to the approximated Hesse matrix. Consequently, the full increment  $\gamma = 1$  can be taken for calculation in most cases.

2. In the central, linear part of the algorithm the RG-CD algorithm described by Sadowski in [25] replaces the simple method to solve a set of equations through the approximated Hesse matrix. In its entire version this algorithm allows to integrate as many inequation constraints for linear parameter combinations as desired. In reality we implemented a simplified version of the type parameter  $\geq$  lower boundary and/or parameter  $\leq$  upper boundary.

This simplified form allows us to define parameter specific lower and upper boundaries. The algorithm, which may be applied optionally, rather reduces execution time than it makes the calculation longer. It is an iteration following  $n$  steps where  $n$  is the number of parameters. The iteration ends exactly in the minimum. The program terminates the calculation if a refinement step is sufficiently small. Thus, CPU time is reduced when using a lot of parameters.

## 5.2 Counting rate on the $i^{th}$ measuring point

The counting rate on the  $i^{th}$  measuring point is the sum of the corresponding contributions provided by all Bragg reflections  $k$  from the phases  $j$  being part of the sample:

$$y'_i = y_{bi} + \sum_{j=1}^M \sum_{k=1}^N S_j P_{jk} H_{jk} L |F_{jk}|^2 \quad (5.2)$$

with

$y_{bi}$  Background counting rate

$S_j$  Scale and/or scale factor; if preferred orientation is available, also depending on  $k$ ;  
Structure file parameter: GEWICHT

$P_{jk}$  Profile function

$H_{jk}$  Multiplicity of the reflection  $k$

$L$  Lorentzian plus polarisation factor  $L = \frac{1 + \text{POL} \cos^2 \Theta_{jk}}{\sin^2 \Theta_{jk} \cos \Theta_{jk}}$   
POL = 1 without secondary monochromator  
POL =  $\cos^2 2\Theta_{\text{Monochromator}}$  for secondary monochromator with mosaic structure  
POL is an entry in the \*.sav control file.

$F_{jk}$  Structure amplitude; the structure factor is the square of structure amplitude

$M$  Number of phases

$N$  Number of Bragg reflections of the phase  $j$

## 5.3 Determination of background

The background profile is fitted by a Lagrangian polynomial of the  $n^{th}$  order. The background parameters (the coefficients of the Lagrangian polynomial) are supposed to be positive. This condition is necessary but not sufficient for positive definite background. Using a Lagrangian polynomial with positive definite coefficients guarantees a stable background convergence in practical all cases.

The polynomial order is determined automatically depending on the angular range. Manual input of the order is required in very special cases only, (entry into the control file: RU).

Alternatively, you can apply an autonomous background diagram (available externally) for background fitting. This diagram uses a scale factor as parameter. The necessary entry into the control file is UNT. Arbitrary increments are permitted for UNT. Nevertheless, pay attention that the angular range to be fitted is covered.

## 5.4 Scale and preferred orientation

Supposing an ideal random sample without any preferred orientation (PO), the scale parameter is a scalar with its quantity proportional to the weight ratio of the phase.

As a rule, samples have almost one, but often a number of POs in each phase. In this case, the weight content must be estimated from the mean value of the scale parameter.

Advanced Rietveld programs describe POs with the help of spheric harmonic functions. Because they have to fulfil the symmetry conditions of the crystal structure given by the Laue class, symmetrised linear combinations of spherical harmonic functions are the basis for sophisticated PO models.

Supposing that the measurement of the polycrystal sample is made on a rotating sample in conventional Bragg-Brentano measuring geometry, the PO correction factor  $T(\vec{h})$ , also called average polar axis density in the literature, can be conveniently approximated by a finite series of spheric harmonic functions

$$T(\vec{h}) = T(\vartheta_{\vec{h}}, \varphi_{\vec{h}}) = \sum_{\ell=0,2,4,\dots}^n \sum_{m=-\ell}^{\ell} a_{\ell,m} Y_{\ell,m}(\vartheta_{\vec{h}}, \varphi_{\vec{h}}) \quad (5.3)$$

where the average polar and azimuthal angles  $\vartheta$  and  $\varphi$  describe the direction of the reciprocal lattice vector  $\vec{h}$  in a suitable spheric coordinate system.

The coefficients  $a_{\ell,m}$  in equation (5.3) are adjustable parameters. The first term  $a_{0,0}Y_{0,0}$  is angular independent and, therefore, describes a random orientation of crystallites whereas the other terms represent the deviation from this ideal case. In X-ray powder diffraction only symmetrised spherical functions of even order need to be considered because only these functions fulfil the symmetry  $\bar{1}$  that is common to all Laue classes (Friedel's law).

To derive an algorithm that is unique to all Laue classes and to all  $n$ , equation (5.3) can be expressed as

$$T(\vartheta, \varphi) = \frac{\sum_{i_1=1}^3 \sum_{i_2=1}^3 \cdots \sum_{i_n=1}^3 G_{i_1, i_2, \dots, i_n}^0 x_{i_1} x_{i_2} \cdots x_{i_n}}{r^n} \quad (5.4)$$

whereas  $x_i$  are three coordinates in arbitrary cartesian coordinates,  $r$  is the distance to the zero point  $\sqrt{x_1^2 + x_2^2 + x_3^2}$  and  $G^0$  is a fully symmetric tensor of order  $n$ .

There is some linear dependency between cartesian coordinates and the coordinates of the reciprocal lattice  $h_i$ . Therefore, after some linear transformation, we get the equation

$$T(\vec{h}) = \frac{\sum_{i_1=1}^3 \sum_{i_2=1}^3 \cdots \sum_{i_n=1}^3 G_{i_1, i_2, \dots, i_n} h_{i_1} h_{i_2} \cdots h_{i_n}}{|\vec{h}|^n} \quad (5.5)$$

for some other fully symmetric tensor  $G$  of order  $n$ .

The number of independent components of the tensor  $G$  can be greatly reduced by symmetry considerations. If the  $A_{ij}^k$  with  $i, j = 1 \dots 3$  are the transformation matrices of the point group, a tensor  $\hat{G}$

that is invariant to the transformation

$$\hat{G}_{i_1, i_2 \dots i_n} = \sum_{j_1=1}^3 \sum_{j_2=1}^3 \dots \sum_{j_n=1}^3 \hat{G}_{j_1, j_2 \dots j_n} A_{i_1 j_1}^k A_{i_2 j_2}^k \dots A_{i_n j_n}^k \quad (5.6)$$

for each  $k$  has to be found. This expression is written as

$$\hat{G} = \mathcal{A}^k \hat{G} \quad (5.7)$$

in a symbolic notation. An invariant tensor  $\hat{G}$  can easily be constructed applying the  $\Gamma_1$ -projection operator

$$\bar{\mathcal{A}} = \frac{1}{m} \sum_{k=1}^m \mathcal{A}^k \quad (5.8)$$

to a non-invariant tensor  $G$

$$\hat{G} = \bar{\mathcal{A}} G \quad (5.9)$$

Then, the average polar axis density is given by

$$T(\vec{h}) = \frac{\sum_{i_1=1}^3 \sum_{i_2=1}^3 \dots \sum_{i_n=1}^3 \hat{G}_{i_1 i_2 \dots i_n} h_{i_1} h_{i_2} \dots h_{i_n}}{|\vec{h}|^n} \quad (5.10)$$

The tensor  $\hat{G}$  can be easily derived using the general positions

$$X^k = (X_1^k, X_2^k, X_3^k) \quad (5.11)$$

as given by the International Tables and tabulated in the *spacegrp.dat* file for the **BGMN** program. The matrices  $A_{ij}^k$  are given by

$$A_{ij}^k = \frac{\partial X_i^k}{\partial x_j} \quad (5.12)$$

and  $T(\vec{h})$  is easily obtained by a simple numeric algorithm unique to all Laue classes and all orders  $n$  of correction. Thus, **BGMN** is calculating  $T(\vec{h})$  when demanded for every Laue-class and order, respectively. For a detailed discussion on this topic see [4]. In contrast, other Rietveld programs apply the different  $\Gamma_1$ -operators to all Laue classes in an analytic form and get a lot of formula, each for every Laue class and every order of correction  $n$ .

For demonstration, table 5.1 gives the number of independent elements of the tensor  $\hat{G}$  for every order  $n$  until 10 and every Laue class.

Table 5.1: Effective number of scale parameters of even spherical harmonics depending on harmonics' order and the Laue group; the order of the spherical harmonics is determined by the command GEWICHT=SPHARx. Cited from [20]

Crystal system	Laue group	Schönflies (types I/II)	SPHAR2	SPHAR4	SPHAR6	SPHAR8	SPHAR10
triclinic	-1	(C1/Ci)	1+5=6	1+5+9=15	1+5+9+13=28	1+5+9+13+17=45	1+5+9+13+17+21=66
monoclinic	2/m	(C 2/C2H)	1+3=4	1+3+5=9	1+3+5+7=16	1+3+5+7+9=25	1+3+5+7+9+11=36
orthorhombic	2/m 2/m 2/m	(D 2/D2H)	1+2=3	1+2+3=6	1+2+3+4=10	1+2+3+4+5=15	1+2+3+4+5+6=21
tetragonal	4/m	(C 4/C4H)	1+1=2	1+1+3=5	1+1+3+3=8	1+1+3+3+5=13	1+1+3+3+5+5=18
tetragonal	4/mmm	(D 4/D4H)	1+1=2	1+1+2=4	1+1+2+2=6	1+1+2+2+3=9	1+1+2+2+3+3=12
rhombohedral	-3	(C3/S6)	1+1=2	1+1+3=5	1+1+3+5=10	1+1+3+5+5=15	1+1+3+5+5+7=22
rhombohedral	-3m	(D3/D3d)	1+1=2	1+1+2=4	1+1+2+3=7	1+1+2+3+3=10	1+1+2+3+3+4=14
hexagonal	6/m	(C 6/C6H)	1+1=2	1+1+1=3	1+1+1+3=6	1+1+1+3+3=9	1+1+1+3+3+3=12
hexagonal	6/mmm	(D 6/D6H)	1+1=2	1+1+1=3	1+1+1+2=5	1+1+1+2+2=7	1+1+1+2+2+2=9
cubic	m3	(T/Th)	1+0=1	1+0+1=2	1+0+1+2=4	1+0+1+2+1=5	1+0+1+2+1+2=7
cubic	m3m	(Without/Oh)	1+0=1	1+0+1=2	1+0+1+1=3	1+0+1+1+1=4	1+0+1+1+1+1=5

The average polar axis density  $T(\vec{h})$  as given by equation (5.10) has still two shortcomings. First, it should be positive definite which is not guaranteed by equation (5.10). Therefore, a new average polar axis density is defined by the non-linear transformation

$$\tilde{T}(\vec{h}) = e^{T(\vec{h})} \quad (5.13)$$

conserving the symmetry properties.

Secondly, in cases without preferred orientation, the average polar axis density should be identical to one. This is not guaranteed, neither by  $T$  nor by  $\tilde{T}$ . Following the common formula for the Rietveld intensity

$$I(\vec{h}) = T(\vec{h}) LPS |F(\vec{h})|^2, \quad (5.14)$$

we combine  $T$  and the scale factor  $S$  and call the result **non-normalized average polar axis density**. Using  $\tilde{T}$  as non-normalized polar axis density, we get a modified formula for the Rietveld intensity. Of course, following this way, the scale factor  $S$  is not available directly as parameter during Rietveld refinement. Instead of, it must be calculated as the mean value over all directions of the non-normalized average polar axis density  $\tilde{T}$ .

In some circumstances, especially for phases of low symmetry and low concentration, too sharp preferred orientations can be computed by SPHAR2. To enable a fitting of the preferred orientation in these cases too, the assignment `GEWICHT=ANISO` can be used as an alternative. This statement introduces a symmetrical matrix which is positively definite. The associated coefficients of the matrix' preferred orientation are abstracted from its square form  $hkl$ . The program guarantees that the corresponding ellipsoid fulfils the crystal's symmetry in any case. Depending on the crystal system, six parameters are fitted maximally.

## Automatic reduction of PO/anisotropy models

Complicated PO models (large maximum numbers of spherical harmonics) may cause large errors of phase contents. Therefore, for small contents, the application of such complicated PO models makes no sense. The total error including the systematic one will be enlarged and CPU time increases. In dirty cases, even numerical crashes may occur. Therefore, BGMN switches down automatically the PO/Anisotropy by comparing the significance of the isotrope scaling factors to the number of free parameters (see table 5.1). Furthermore, the order of the PO model will be reduced if too few peaks are in the angular range investigated.

For a structure specific switch off model, please see `LIMITx` and `ANISOLIMIT` in Appendix A.

## 5.5 Profile function

Since the pioneering work of Wilson [30] it is widely accepted that the entire diffraction pattern is a folding of  $\Lambda$  — the wavelength distribution —, the geometry function  $G$  and the sample function  $P^1$ . During a Rietveld analysis the wavelength distribution and the geometry function are constant. The sample function includes all parameters significant for microstructure.

The special power of the **BGMN** program is mainly based on the fact that the mentioned components of the profile function are separated numerically. For that reason, the wavelength distribution  $\Lambda$  and the geometry function  $G$  can be determined before. The Rietveld calculation only deals with determining the profile parameters depending on the sample. Consequently the refinement procedure becomes more robust and provides good convergence.

<sup>1</sup>In the following, a folding between wavelength distribution and geometry function is also called a device function.

The following section explains the calculation approach of the profile function.  
 The figure 5.1 is inserted to illustrate the **BGMN** profile model.

### Wavelength distribution

The wavelength distribution can be modelled by a set of Lorentzian functions describing both the  $K\alpha_1$  and the  $K\alpha_2$  line. Until 1997 data were only available for Cu-anodes. E.g. data given by Berger [1] were in common use. In [14] data for Cr, Fe, Co and Cu are given. In our opinion (see section 10.2), those data are more accurate compared to [1]. Therefore we recommend to use data cited from [14]. Additionally our own measurement of the Mo- $K\alpha_{1,2}$  doublet is available. It was determined on a diffractometer with a special super-fine slit arrangement. These data are stored as files *cu.lam* and so on and chosen automatically according to the anode material as given in the pattern data file. In case of synchrotron data, an infinite narrow delta function is chosen by the assignment

SYNCHROTRON= . . .

Please give the synchrotron wavelength in nm.

### Geometry function

The geometric part of a profile is depending on  $2\theta$ . The geometry function is characterized by fundamental apparatus parameters such as distances, divergence slits, angles etc.

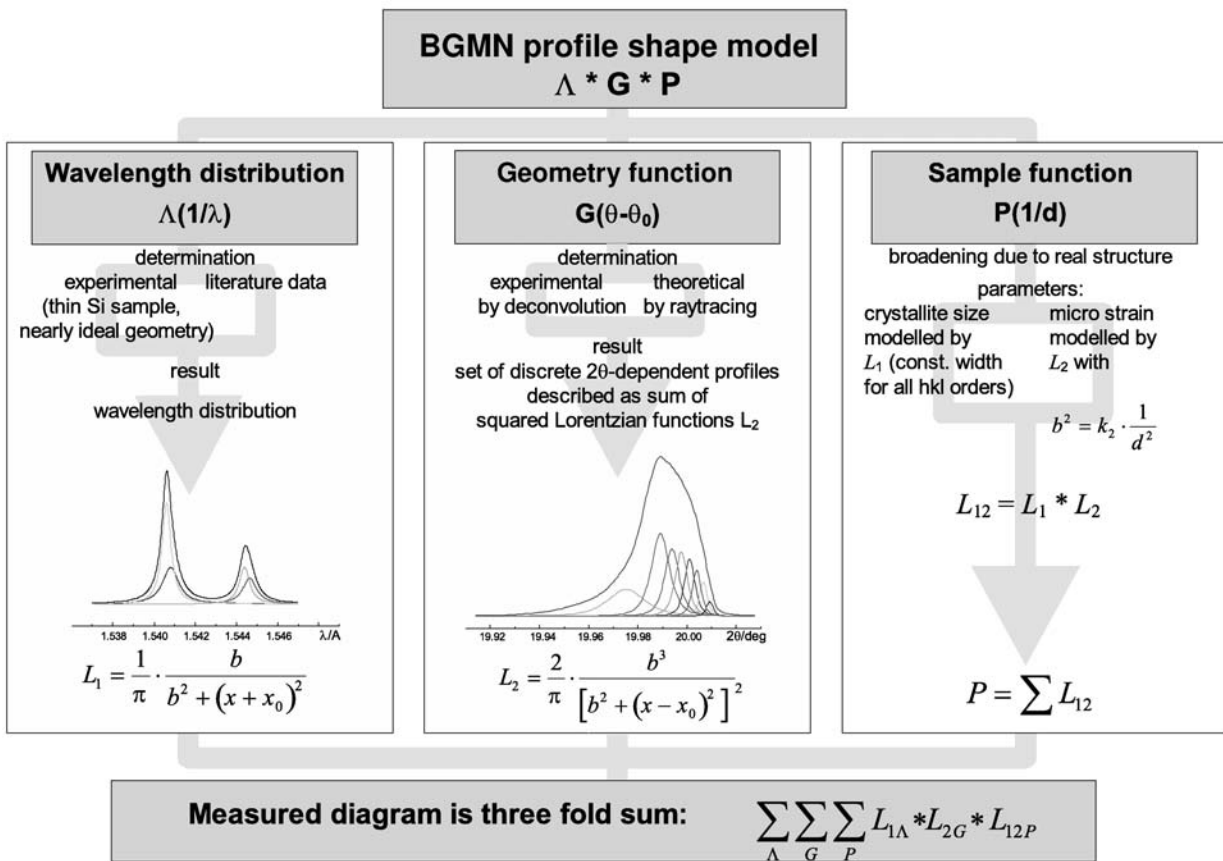


Figure 5.1: Determination of the profile function

There are two different ways for determination of the geometry function. We prefer, if possible anyway, the first way “raytracing” as done by **GEOMET**. The second method “learning profiles” as done by **VERZERR** will be described in detail in section 10.3.

### Calculation of the geometry function by raytracing

The geometry function is computed by a raytracing method within the program **GEOMET**. The procedure has to be carried out for some discrete angular positions covering the  $2\Theta$  range to be analysed. Inside the boundaries made up by the divergence slits, six degrees of freedom for a ray are randomly chosen in accordance with a commonly used Monte Carlo integration.

The degrees of freedom to be integrated over for calculation of the geometry function are:

- two degrees of freedom in the plane of the tube focus
- axial position in the vertical slit; in the case of a primary collimator, this degree of freedom is replaced by the inclination in the collimator
- equatorial position in the horizontal slit
- equatorial position in the receiving slit
- axial position in the receiving slit or on the crystal of the secondary monochromator; in case of a secondary collimator, this degree of freedom is replaced by inclination in the collimator

The scattering position on the sample as well as the position in additional slits are computed, thus considering further ray constraints. The program computes the angle  $\Theta$  appearing, if the event would be recorded. The goniometer axis is situated at the angle  $\Theta_0$  being different from  $\Theta$  as a rule. All successful experiments are classed into a very narrow grid in  $\Theta$ . Computation is terminated if the quantity of events in one grid channel is  $2/(\text{accuracy})^2$ . This quantity is around 40000 for default of 0.7% accuracy. For that reason, some million events must be computed per profile. The ratio of successful events to the total number of events is stored for further evaluation. Subsequently, a sum of squared Lorentzian functions is used for mathematical modelling of the geometry function at each angle  $\Theta$ . Thus, even strongly asymmetric profiles can be modelled as accurate as necessary. Squared Lorentzian functions are fitted to the peak computed by a Monte Carlo integration. At first an individual function is inserted. Subsequently further squared Lorentzian functions are added, until the fit has achieved the accuracy as demanded.

For more accurate profile description, we recommend correcting the raytraced profiles for tubetails. For details see section 10.2.

Many advanced geometric set-ups (position sensitive detectors, focusing X-ray mirrors etc) can not be described by raytracing. In such cases, one must use the learnt profiles method as described in section 10.3.

### Interpolation of geometry function

Because the geometric profile is needed for every angular position, the geometric function has to be interpolated between the angular positions as simulated by **GEOMET** or deconvoluted by **VERZERR**. This interpolation routine is carried out by the program **MAKEGEQ**. This step is necessary for any \*.ger file: Raytracing with or without tubetail correction or learnt profiles.

The profiles calculated by **GEOMET** are read by the program as input values. Now the interpolation is started at the preset angle values. For each angle the positions of both involving profiles are corrected towards “Maximum around 0”. The positions get scale values according to the situation

inside the interval of interpolation, the sum of all scales is 1. Following this procedure, the device function is constructed using point-by-point interpolation with >100 points which are not equidistant. The point number depends on the accuracy demanded. Following the same approach as **GEOMET**, a sum of squared Lorentzian functions is fitted to this asymmetric function until a certain accuracy is reached.

The profile shape is also influenced by the beam path in the sample. To consider the impact of the sample most accurately, some corrections of the geometry functions must already be carried out during interpolation by means of **MAKEGEQ**:

- penetration depth in the sample
- sample thickness and sample absorption for measurement in transmission
- capillary diameter and absorption for capillary geometry

The corresponding values must be given in the control file for starting **MAKEGEQ**. Except for the sample absorption for measurement in transmission, the above mentioned corrections cannot be done later.

For an incomplete correction of the penetration depth, the **EPS3** parameter, which is specified in the control file, can be fitted during the Rietveld analysis. This parameter stands for the peak shift due to radiation penetrating the sample but not for the change of the peak shape resulting from it. Note that **EPS3** correlates even with the other angle correcting parameters **EPS1** and **EPS2**. For that reason the application of **EPS3** is not recommended.

## Sample function

The sample function includes the contribution of the diffraction by the sample to the measured profile. Assuming an ideal crystalline sample whose crystallites have sufficient size and quantity, we would get a sum of Delta functions (each for each reflection) as sample function.

For real samples some line broadening due to crystallite size is to be considered. A Lorentzian function is taken for each peak of the sample function. This function is determined for each peak in the following way:

$$L_1 = \frac{1}{\pi} \frac{b_1}{b_1^2 + (x - x_0)^2} \quad (5.15)$$

with

$x_0$  Peak position  $\frac{1}{d}$

$b_1$  Peak width, described by crystallite size;  
Structure file parameter: **B1**

In isotropic cases the reflection width is one parameter for all peaks of a phase. In anisotropic cases, the reflection width parameter, being a function of the Miller indices of the reflection, is represented depending of the corresponding crystal system. It's description is performed by six parameters maximally.

In addition, the diffraction reflections can be widened due to microstrain and similar influences. The program considers this influence by folding the above introduced Lorentzian with a squared Lorentzian function:

$$L_{12} = L_1 * L_2 \quad (5.16)$$

where

$$L_2 = \frac{2}{\pi} \frac{b_2^3}{[b_2^2 + (x - x_0)^2]^2} \quad (5.17)$$

with

$b_2$  Width of the reflection, determined by microstrains and crystallite size distribution

and

$$b_2^2 = k_1 b_1^2 + k_2 \frac{1}{d^2} \quad (5.18)$$

Structure file parameters: k1 and k2

Note that the parameter  $k_2$  describing microstrain may also be anisotropic:

k2=ANISO

Taking for example the cubic crystal system, the ellipsoid is degenerated to a sphere. According to a generalized theory, the anisotropy of the microstrain parameter  $k_2$  must be described using a tensor of 4th stage. The key word ANISO4 was introduced for supporting this function:

k2=ANISO4

In following, the microstrain becomes anisotropic even in cubic crystal systems. The value of the parameter  $k_1$  depends on the width of the crystallite size distribution.

Depending on the crystal system, crystallite size and/or microstrains can also be anisotropic. In this case a positively definite symmetrical matrix is introduced. The corresponding width parameters are abstracted from the square of the above mentioned matrix by  $hkl$ . The program guarantees that the associated ellipsoid always has the symmetry of the crystal.

The relationship of the parameters  $b_1$  and  $k_1$  to the crystallite size is described in [21] as well as in the following section.

## 5.6 Mean crystallite size

The computation of the mean crystallite size starts from the distribution of the column length  $p_\nu(D)$ . This function was abstracted by Bertaut [5].

$$I(s) = \int_0^\infty \frac{\sin^2(\pi Ds)}{(\pi s)^2} \frac{p_\nu(D)}{D} dD \quad (5.19)$$

with

$D$  Length of a column orthogonally to the reflecting lattice plane

$p_\nu(D)$  Volume ratio of such a length fraction.

Let  $I(s)$  and  $p_\nu(D)$  be normalized to unitary. Using the approach

$$\frac{\partial^2 \chi(D)}{\partial D^2} = \frac{p_\nu(D)}{D}, \quad (5.20)$$

we get

$$I(s) = 2 \int_0^\infty \cos(2\pi sD) \chi(D) dD \quad (5.21)$$

as a result of double partial differentiation.

Equation 5.21 is the Fourier transform of an even function  $\chi(D)$ .

If we identify  $I(s)$  with the squared Lorentzain function  $L_{12}$  as used by **BGMN**, we get the Fourier transformed function

$$\chi(D) = (1 + 2\pi b_2 D) e^{-2\pi(b_1+b_2)D}. \quad (5.22)$$

After double differentiation, we get

$$p_\nu(D) = \left(4\pi^2 (b_1^2 - b_2^2) D + 8\pi^3 b_2 (b_1 + b_2)^2 D^2\right) e^{-2\pi(b_1+b_2)D} \quad (5.23)$$

For a pure crystallite size effect, there must be valid  $b_1 < b_2$ , otherwise the distribution of the column length of small  $D$  values would become negative. For that reason **BGMN** works with the constraint  $k_1 < 1$ . The last mentioned term is also normalized to unitary.

But we want to find out the distribution of crystallite size or the mean crystallite size rather than distribution of the column length or the mean column length. Consequently we have to assume a grain shape. In case of spheres with a diameter  $D_m$  the distribution of the column length is

$$p_{\nu,\text{sphere}} = \begin{cases} \frac{3D^2}{D_m^3} & \text{for } D \leq D_m \\ 0 & \text{otherwise} \end{cases} \quad (5.24)$$

$$\text{as normalized by } \int_0^{D_m} p_{\nu,\text{sphere}} = 1 \quad (5.25)$$

Assuming an arbitrary distribution function  $\omega(D_m)$  of the sphere diameter, the distribution of the column length is

$$p_\nu(D) = \int_D^\infty \omega(D_m) \frac{3D^2}{D_m^3} dD_m. \quad (5.26)$$

The lower limit  $D$  arises from the fact that spheres of small diameter values  $D_m$  do not influence  $p_\nu(D)$ . Having divided right and left part of equation by  $D^2$  and differentiated against the lower limit, we get

$$\omega(D_m) = \frac{2}{3} p_\nu(D) - \frac{D}{3} \frac{\partial p_\nu(D)}{\partial D}. \quad (5.27)$$

After differentiation, we obtain

$$\omega(D_m) = \left( \begin{array}{l} \frac{4\pi^2}{3} (b_1^2 - b_2^2) D \\ + \frac{8\pi^3}{3} (b_1 + b_2) (b_1^2 - b_2^2) D^2 \\ + \frac{16\pi^4}{3} b_2 (b_1 + b_2)^3 D^3 \end{array} \right) e^{-2\pi(b_1+b_2)D}. \quad (5.28)$$

This term is also normalized to unitary. Using  $b_2 = \sqrt{k_1} b_1$  as applied in **BGMN** we get

$$\overline{D} = \frac{4}{3\pi b_1} \frac{1 + 2\sqrt{k_1}}{(1 + \sqrt{k_1})^2}. \quad (5.29)$$

for the volume weighted mean sphere diameter.

**BGMN** introduces this term as the GrainSize function. In addition we want to determine the relative width of crystallite size distribution. We find out the relative width by dividing the standard deviation by the mean value:

$$\frac{\Delta D}{\overline{D}} = \frac{\sqrt{13 + 52\sqrt{k_1} + 7k_1}}{4\sqrt{2}(1 + 2\sqrt{k_1})}. \quad (5.30)$$

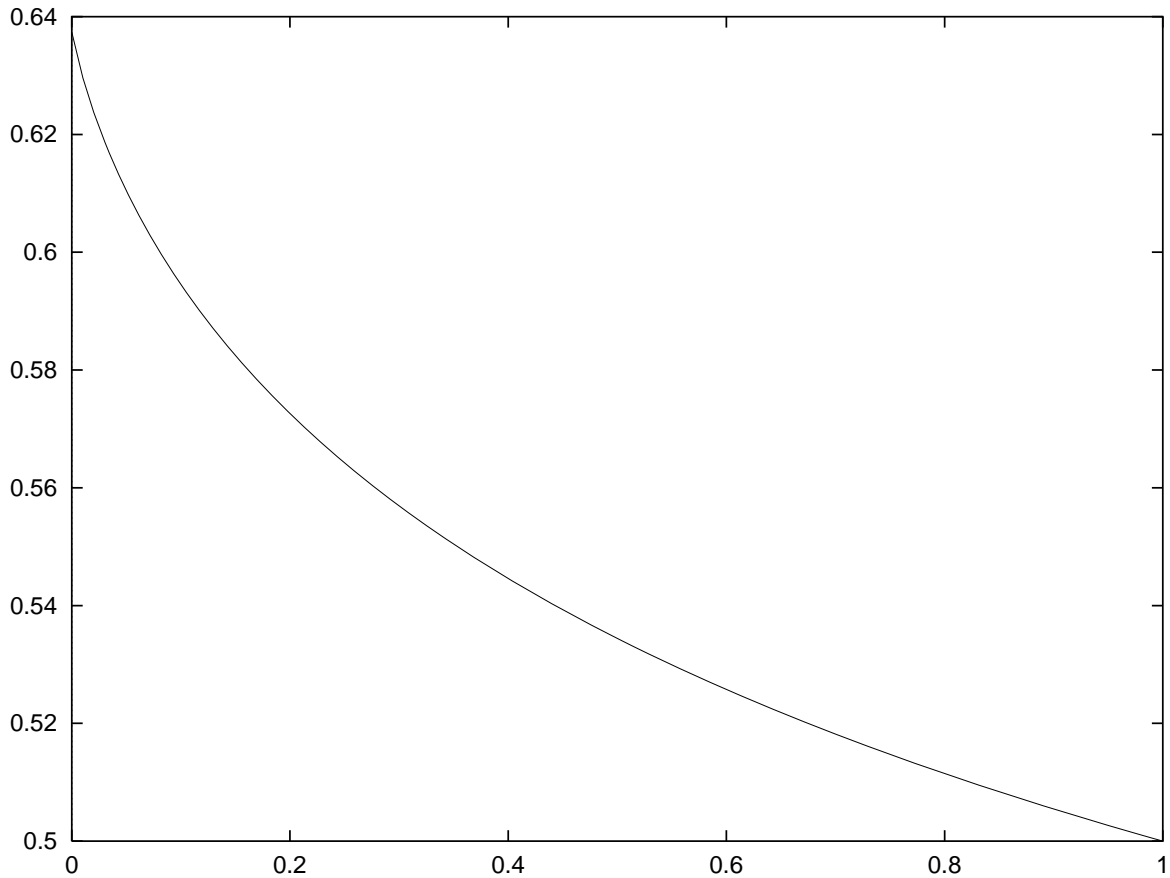


Figure 5.2: Relative width of the distribution of the crystallite size as a function of  $k_1$

The following figure represents the relative width of the distribution of the crystallite size depending on the program parameter  $k_1$ .

Obviously, the range of possible distribution is relatively small. For that reason the calculated parameter  $k_1$  is mostly situated on the interval boundaries, that is zero or one. As a consequence, this model is not useful for determination of wide crystallite size distribution functions.

### Comparison with microscopic measurements of grain size

For comparison with (electron) microscopic methods the mean sphere diameter as specified in (5.29) should be replaced by the mean column length

$$\overline{D}_s = \frac{1}{\pi b_1} \frac{1 + 2\sqrt{k_1}}{(1 + \sqrt{k_1})^2}, \quad (5.31)$$

that is  $\frac{3}{4}$  of the mean sphere diameter. Subgrains are often tilted against each other. Therefore the value obtained for the particles suitable for optical measurement depends on the corresponding measuring principle: For X-ray methods the determined crystallite sizes are significantly smaller than those obtained by optical techniques.

## 5.7 Microabsorption

For single phase samples the attenuation of X-radiation is only determined by the penetration depth of crystallites to be diffracted.

However, if the sample consists of more than one phase with different linear attenuation coefficients, analysis becomes more complicated by microabsorption. The phase with the higher linear attenuation coefficient attenuates X-radiation predominantly. The problem is even amplified by differing the grain sizes of the phases in addition to different linear attenuation coefficients. Consequently the content of that phase with the higher linear attenuation coefficient or the larger particle size will be determined too low.

If the mean particle sizes of all phases in the sample are known, it is possible in principle to correct for microabsorption by computation. This was done first by Brindley (1945) [7]. For the intensity correction he gives the formula

$$\frac{1}{V_a} \int_{V_a} e^{-(\mu_a - \bar{\mu})x} dV_a \quad , \quad (5.32)$$

where  $x$  is the length of the X-ray path inside the grain of a volume  $V_a$ . We approximate this equation:

$$\overline{e^{-(\mu_a - \bar{\mu})x}} \approx e^{-\overline{(\mu_a - \bar{\mu})x}} \quad (5.33)$$

Following our own investigations for spherical grains, this approximation is justified, because:

- The original Brindley formula (5.32) gives some angular dependence of the correction. E.g. for  $D(\mu_a - \bar{\mu}) = 1.0$  the exact formula gives a content correction of 2.08 ( $2\Theta = 20^\circ$ ) to 1.92 ( $2\Theta = 140^\circ$ ).
- Our approximation (5.33) gives a angular-independent value of 2.12.
- Conclusion: the error using the approximation is much smaller compared to that one using an angular-independent Brindley correction.

Therefore we suggest the following formula for the correction of the mass fractions:

$$e^{\frac{3}{4}\mu_a D_a} \quad , \quad (5.34)$$

where  $\mu_a$  and  $D_a$  are linear absorption coefficient, and mean diameter of the  $a$  phase, resp.

In common we suggest a GOAL formulation for correcting the scaling factor (mass fraction) of a phase as following:

```
GOAL:phasename=GEWICHT*ifthenelse(ifdef(d),exp(d*my*3/4),1)
```

where  $d$  is the mean grain diameter in  $\mu\text{m}$  of the ground sample, which may be supported in the main \*.sav file. **BGMN** presets the variable  $my$  (unit  $\mu\text{m}^{-1}$ ) which holds the linear attenuation coefficient of the (compact) phase. In cases of multiple subphases ( $\text{RefMult} > 1$ ), one must use  $my[1] \dots$

## 5.8 Structure factor

The structure factor  $|F_k|^2$  describes the scattering contribution of all  $O$  atoms of the unit cell to the reflection  $k$ .

$$F_k = \sum_{m=1}^O p_m f_m \left( \left| \vec{h} \right| \right) e^{(2\pi i \vec{h} \cdot \vec{r}_m)} \quad (5.35)$$

with

$O$             Number of atoms in the unit cell

$p_m$	Occupation probability
$f_m( \vec{h} )$	Atomic form amplitude
$\vec{h}$	Vector of Miller's indices
$\vec{r}_m$	Vector of atomic coordinates of atom $m$

The structure amplitude  $F_k$  represents the sum of scattering amplitudes  $f_m$  of all atoms considering the corresponding atom phases. The atomic form amplitudes of the atoms most of the ions are provided as nine-parameter approximations in the file *afaparm.dat*.

## 5.9 Temperature factors (Debye-Waller-factors)

Temperature factors are introduced to describe the attenuation of diffracted X-radiation by thermal motion of lattice elements. This dispersion named as thermal diffuse scattering reduces the diffraction intensity of the reflection  $k$  in comparison to the ideal crystal.

For a first approximation, the thermal diffuse scattering is described by the following modification of the structure amplitude:

$$F_k = \sum_{m=1}^O p_m f_m(|\vec{h}|) e^{(2\pi i \vec{h} \cdot \vec{r}_m)} e^{-B_m \left(\frac{\sin \Theta}{\lambda}\right)^2} \quad (5.36)$$

$B_m$  is the isotropic atomic temperature factor of the atom  $m$ . Excluding a factor of 100,  $B_m$  corresponds to the TDS entries as set in the the structure file, atomic description lines starting with E= . . . For a more accurate description, anisotropic temperature factors may be used. This demands for a thermal factor as described by positive definite matrices  $\beta_{ij}$ , each for each single atom in the unit cell. Accordingly, the second exponential function in equation (5.36) is replaced by:

$$e^{-h^2 \beta_{11} - k^2 \beta_{22} - l^2 \beta_{33} - 2hk \beta_{12} - 2hl \beta_{13} - 2kl \beta_{23}} \quad (5.37)$$

In general, the values of  $\beta_{ij}$  depend from the atomic number  $m$  in equations (5.35), (5.36). They have to follow the symmetry conditions of the spacegroup.

Anisotropic Debye-Waller-factors for atoms may be refined by entering TDS=ANISO to the structure file. The components calculated correspond to the values of  $\beta_{ij}$  given in literature, the  $\beta_{ij}$  values are dimensionless.

The program automatically considers the constraints of the space group symmetry. These constraints are described by Giacovazzo et al. (1992) on ps. 188 to 190. To increase the robustness of calculation, an isotropic upper limit  $B_0$  can be introduced for anisotropic temperature factors by TDS=ANISO^upperlimit.

An isotropic average may be abstracted from the components of the anisotropic matrix  $\beta_{ij}$  with  $a, b, c$  and  $\alpha, \beta, \gamma$  standing for the lattice constants:

$$B_0 = \frac{4}{3} \left[ \begin{array}{l} \beta_{11} a^2 + \beta_{22} b^2 + \beta_{33} c^2 + 2\beta_{12} ab \cos \gamma \\ + 2\beta_{13} ac \cos \beta + 2\beta_{23} bc \cos \alpha \end{array} \right] \quad (5.38)$$

For the  $U_{ij}$  matrix elements, which are also available in literature, the following approximation is valid:

$$B_0 = \frac{8\pi^2}{3} \left[ \frac{U_{11} \sin^2 \alpha + U_{22} \sin^2 \beta + U_{33} \sin^2 \gamma + 2U_{12} \sin \alpha \sin \beta \cos \gamma}{1 + 2 \cos \alpha \cos \beta \cos \gamma - \cos^2 \alpha - \cos^2 \beta - \cos^2 \gamma} \right] \quad (5.39)$$

Transformation for isotropic temperature factors is

$$B = 8\pi^2U. \quad (5.40)$$

*Attention:*

Since the values  $B$ ,  $U$  and  $U_{ij}$  given in literature have the dimension  $\text{\AA}^2$ , these values must be divided by 100 before being applied as TDS whose unit is  $\text{nm}^2$ . Exception:  $\beta_{ij}$  values are without dimension!

## 5.10 Neutron powder diffraction

Neutron powder diffraction is quite similar to X-Ray powder diffraction, but there are some specific features [16]:

- Neutrons as used for diffraction are, in general, thermic neutrons, they must be slowed down using a “moderator” as involved in a nuclear reactor. There may be other sources than nuclear reactors, but a moderator is mandatory.
- X-Rays are scattered by atomic shell electrons, neutrons by the nucleus.
- The atomic form factors will be replaced by the coherent bound neutron scattering lengths  $b$ , which (in most cases) simply are angle-independent constants.
- In distinction to atomic form factors, scattering lengths  $b$  change non-monotonic depending from atomic number. They may become negative, and they are different for different isotopes of a given atomic number.
- Neutrons own a magnetic moment, X-Rays not. Therefrom, Neutrons may interact with electronic magnetic dipoles of magnetic structures.
- In general, the linear absorption of neutrons is much weaker compared to X-Rays: much larger samples may be observed.

In principle, there are two different types of neutron powder diffraction facilities: CW (Constant Wavelength) and TOF (Time Of Flight). BGMN is able to handle CW patterns, only.

For some elements/isotopes, there is strong absorption of thermic neutrons: Cd, Sm, Gd, Eu. Some isotopes of Cd, Sm, Gd, Eu show neutron resonances [22] at thermic neutron energies. As well known from X-rays, there will be an imaginary part of  $b$ , and  $b$  will become strongly energy-dependent. These neutron resonances are part of the file *bcoh.dat*. Data in *bcoh.dat* are valid down to neutron wavelengths of 0.04nm (0.4 $\text{\AA}$ ). Below that limit, dozens of additional neutron resonances for elements with atomic number  $Z \geq 35$  will occur, and the content of *bcoh.dat* will become insufficient.

Magnetic scattering on shell electrons will not be handled automatically by BGMN. You may describe that by using user calculated structure amplitudes, which will be switched on by setting `FMULT` to a positive integer. Thus, you must provide a formula for the structure amplitude  $F$  including magnetic scattering.

The thermic motion of the nucleus may differ from the thermic motion of the shell electrons. In most cases, neutron diffraction will give different temperature factors compared to the X-Ray ones.

## 5.11 Quality parameters

### Global $R$ values

The Rietveld method is an optimization algorithm. The difference between measured and calculated diagrams is taken as optimization criterion. The weighted residual square sum  $R_{wp}$  is introduced to evaluate the fitting quality:

$$R_{wp} = \left[ \frac{\sum_{i=1}^M w_i (y_i - y_{ic})^2}{\sum_{i=1}^M w_i y_i^2} \right]^{\frac{1}{2}}, \quad (5.41)$$

with

- $M$  Pattern length (number of data points).
- $y_i$  Measured intensity at pattern data point  $i$ .
- $y_{ic}$  Computed intensity at pattern data point  $i$ .
- $w_i$  Weight at pattern data point  $i$ , commonly  $T_i \cdot y_i^{-1}$
- $T_i$  Counting time as preselected for pattern data point  $i$

Smaller  $R$  values stand for better fitting. But note that the  $R$  value is only a mathematical criterion. Assume that the diagram has a continuously high background rate. In that case a small  $R$  value may also be achieved although the fitting of the crystallographic model is relatively bad. This effect results from the fact, that the background fitting is also part of the calculation. For that reason  $R$  values can only be compared with each other, if they refer to the same diagram.

$R_{exp}$  is the possible minimum value for  $R_{wp}$  (supposing ideal fitting):

$$R_{exp} = \left( \frac{M - P}{\sum_{i=1}^M w_i y_i^2} \right)^{\frac{1}{2}} \quad (5.42)$$

with

- $P$  Number of independent refined parameters

$R_{exp}$  is used for comparison with  $R_{wp}$ , but it is also a criterion for measurement quality. Too high values may result from insufficient counting statistics.

*Attention: Having too much parameters refined,  $R_{exp}$  decreases. Hence, the gap between  $R_{wp}$  and  $R_{exp}$  may rise.*

For easy comparison with the results found by other Rietveld programs, the following  $R$  values are calculated in **BGMN**:

- Profile- $R$   $R_p$ :

$$R_p = \frac{\sum_{i=1}^M |y_i - y_{ic}|}{\sum_{i=1}^M y_i} \quad (5.43)$$

Resulting from the missing weighting factor, the  $R_p$  value is less expressive than  $R_{wp}$ .

- Profile- $R$   $R_{pb}$ , corrected background:

$$R_{pb} = \frac{\sum_{i=1}^M |y_i - y_{ic}|}{\sum_{i=1}^M |y_i - u_i|} \quad (5.44)$$

with

$u_i$  Computed background value  $i$ .

## Phase-specific $R$ values

The Bragg  $R$  value  $R_B$  is especially interesting under the aspects of crystallography. This value is also desirable for comparison with the results of structural analysis by single crystal methods.

$R_B$  is based on the integral intensity values concerning all reflections of a phase according to:

$$R_B = \frac{\sum_{j=1}^M |I_j - I_{jc}|}{\sum_{j=1}^M I_j} \quad (5.45)$$

with

$I_j$  Measured intensity of diffraction reflection  $j$

$I_{jc}$  Computed intensity of diffraction reflection  $j$

In Rietveld analysis only the computed intensity values are available. In fitting the measured reflection intensity values are not important at all. They cannot be determined accurately, e.g. by defolding. For that reason these values must be estimated according to the phase ratios.

The methods implemented in various programs to estimate the measured intensity values are not comparable. Sometimes these methods are evidently incorrect ([15]). Even the assumption of Rietveld, that the calculated phase rates are related to the measured intensity on each measuring point in the same way as the real rates, is only valid for sufficiently separated reflections but not for those ones being strongly overlapped.  $R_B$  would be found best by defolding the entire diffraction diagram without structural information. Nevertheless all the other parameters found as a result of refinement such as lattice constants should be included. Reflection intensity values would be the only free parameters. For less symmetric phases the parameter quantity could range from hundreds to thousand linear parameters. Note that the CPU time for determination of  $R_B$  may easily be doubled by considering the constraint “Parameter  $\geq 0$ ” which is an essential rule founded by physics!

For that reason **BGMN** determines a new phase-specific parameter named as  $R_{\text{phase}}$ . This parameter is similar to  $R_{wp}$ .

$$R_{\text{phase}} = \left[ \frac{\sum_{i=1}^M w_i (y_i - y_{ic})^2 \frac{y_{\text{phase},i}}{y_i}}{\sum_{i=1}^M w_i y_i^2 \frac{y_{\text{phase},i}}{y_i}} \right]^{\frac{1}{2}} = \left[ \frac{\sum_{i=1}^M w_i (y_i - y_{ic})^2 \frac{y_{\text{phase},i}}{y_i}}{\sum_{i=1}^M w_i y_i y_{\text{phase},i}} \right]^{\frac{1}{2}} \quad (5.46)$$

with

$y_{\text{phase},i}$  Component of intensity of the phase at measuring point  $i$ .

Consequently  $R_{\text{phase}}$  scales the deviations on each measuring point against the phase ratio related to this point. A high  $R_{\text{phase}}$  value stands for bad fitting of the associated phase. This information is especially useful for quantitative phase analysis.

## Quality parameter $1 - \rho$

To overcome the limits of common global  $R$  values, we introduced the quality parameter  $1 - \rho$ . This parameter does not depend on the effect-background-ratio that much. It is abstracted from the coefficient of correlation between the diagrams measured and fitted. To exclude background influences, a polynomial of the same order is put through both diagrams. This is the order of the background polynomial in the Rietveld fitting lying above the background polynomial itself. This polynomial is crossing the diagram in a way enabling that the average of all intensity values adapted by this polynomial is around zero. Subsequently the coefficient of correlation  $\rho$  between both diagrams is calculated. If both curves coincide, this value is 1. In reality, it is less than 1. We get the difference  $1 - \rho$  as output. For sufficient fitting, this value should be around 1%. In contrast to the  $R$  values, this new quality parameter also allows *a comparison of the fitting results of different diffraction patterns*.

Last not least, we recommend not to evaluate the results by means of the  $R$  values, only. As a rule, check the plausibility of parameters by investigating the individual parameter errors. For example this plausibility check can be advantageous to localise phase-dependent errors easily.

# Chapter 6

## Sample preparation

Sample preparation causes the highest systematic error in X-ray powder diffractometry (see [17]). These errors result from influences such as insufficient sample statistics, preferred orientation, microabsorption and sample roughness. The Rietveld method is only partly suitable to correct their impact on the diffraction diagram.

For that reason, it is very important to minimize the mentioned error influences by careful sample preparation.

### 6.1 Sample statistics

X-ray powder diffractometry is based on the assumption that the X-rays are diffracted on a sufficiently great quantity ( $> 10^4$ ) of crystallites. Note that the assumptions concerning the profile shape and the intensity of the diffraction reflections are valid under these circumstances only. To increase the number crystallites involved in the diffraction process, use the following possibilities:

#### Reduce grain size by grinding

If the sample material has a coarse graininess, grain sizes of 2 to 10  $\mu\text{m}$  should be achieved at all by milling. Alterations inside the real structure of the crystallites or phase changes must be avoided, as far as possible.

It is not recommended to mill grain sizes until values below 1  $\mu\text{m}$ , because peaks will be widened due to crystallite size and maybe even due to real structure. Low energy mills with a high active milling surface like the McCrone micronising mill are favourable, as well as wet milling.

#### Enhance divergence of the primary beam

Rietveld analysis with **BGMN** does not demand for any extremely high resolution of the diffractometer. Use primary beam divergence values as high as possible depending on the sample dimensions. For multi-phase samples we must find a compromise between peak overlapping and best grain statistics.

We recommend not to use narrow axial divergence collimators. When removing the second collimator, which is often in use for standard device settings, the measured intensity will be increased around 200%. Grain statistics can also be improved by an enlarged axial angular divergence of the diffracted beam. As a result, we get a strongly asymmetric profile shape which can be modelled excellently in the program causing no further errors. This behaviour is illustrated in the following figures. For measurement of the SRM660 ( $\text{LaB}_6$ ) sample, an URD6 diffractometer with/without secondary collimator

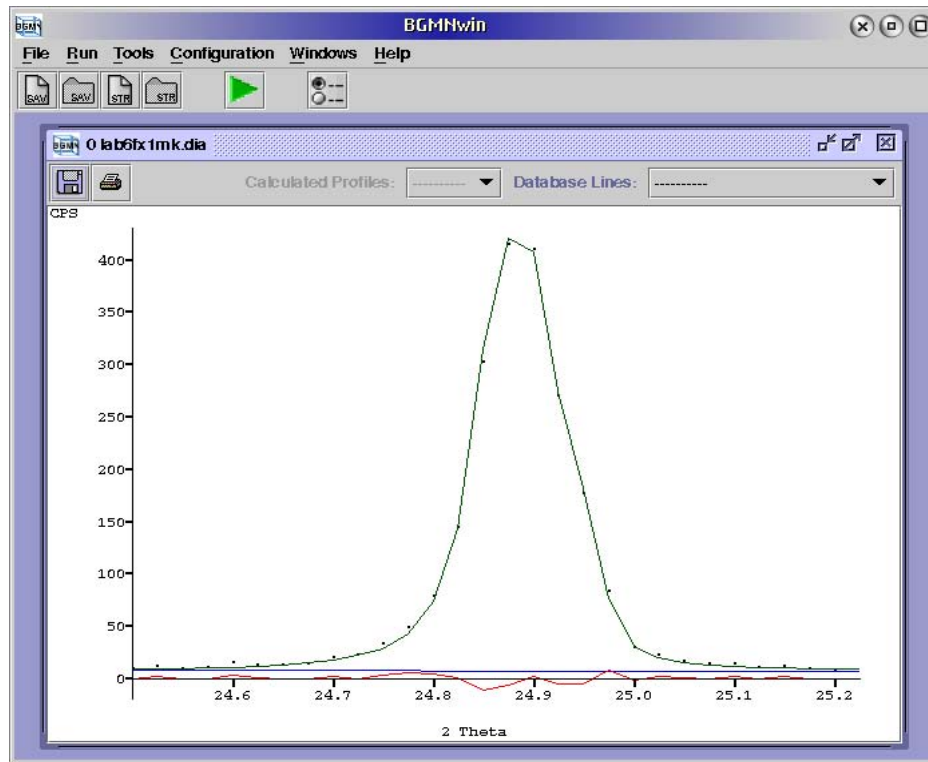


Figure 6.1: 100 reflection of a  $\text{LaB}_6$  sample (SRM660), measured with secondary collimator;  $R_{wp} = 13.81\%$

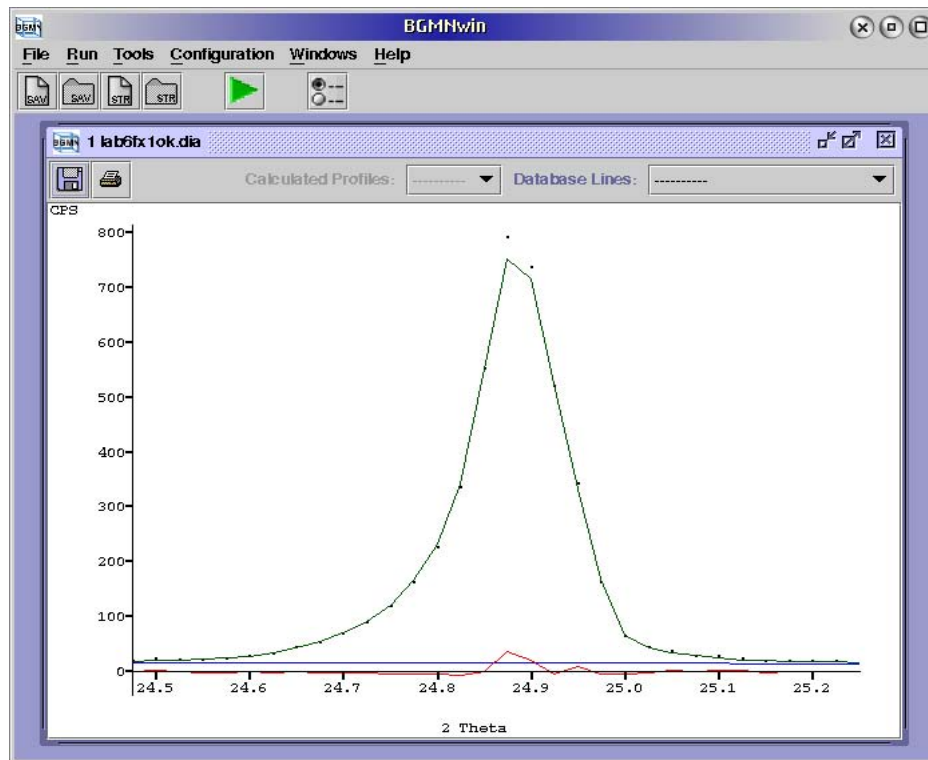


Figure 6.2: 100 reflection of a  $\text{LaB}_6$  sample (SRM660), measured without secondary collimator;  $R_{wp} = 10.43\%$

was used.

As to be learnt from the figures, the measured intensity is almost twice when removing the secondary collimator. Even the  $R_{wp}$  value is a little bit better. Thus it is proven that we do not lose any accuracy for the computed peak model.

## Sample spinning

Grain statistics can also be improved by spinning the sample during measurement. In addition the problem of preferred orientation can be reduced to certain degree, depending on the axial divergence.

## Automatic divergence slit

Grain statistics at high angles can be improved using an automatic (variable) divergence slit. See section 7.1.

## 6.2 Preferred orientation

As a basic supposition for Rietveld analysis and many other procedures of X-ray diffractometry, the crystallites should be situated in the sample in random orientation. But the crystallites often tend to get their orientation along specific crystallographic directions, for example during filling the sample holder. In that case, one direction can be favoured, e.g. by a preferred cleavage face or growth directions of small crystallites. Commonly we even have to cope with a number of preferred directions.

To tackle this problem, sample preparation must first of all try to avoid preferred orientations. It is true that the described program can correct a certain level of preferred orientation. Unfortunately, these corrections may result in correlation with parameters being significant for crystallography parameters however. For that reason the correction of preferred orientations within the program is the last thing you should do. The parameters used to correct preferred orientations are described in chapter “Theory”, section “Scale and preferred orientation”.

## Sample spinning and transmission geometry

As already mentioned, preferred orientations can be compensated to a certain degree by spinning the sample.

Let the crystallites be preferentially 001-oriented in direction of the sample normal. In reflection geometry, only crystallites with small tilts against the sample normal get into the reflection position. This behaviour is caused by the beam divergence due to rotation. In transmission geometry, the spinning axis of the sample is oriented orthogonal to the diffraction vector. For that reason, the number of the scattering crystallites is essentially higher than in reflection geometry.

Provided that it is possible under the aspects of instrument sample transparency and preparation, it is recommended to measure with spinning sample and in transmission geometry. Grain statistics are improved in comparison to reflection geometry. Simultaneously, the problems resulting from preferred orientation are reduced.

### 6.3 Microabsorption

As we demonstrated in section 5.7, the influence of microabsorption may be corrected in principle. But an exact correction demands for the knowledge of the values of all grain-size distributions of all phases. The correction introduced in section 5.7 is a kind of approximation, but still needs the knowledge of the exact mean grain size of all phases. For ideal attenuation behaviour of the sample, the grains should be so small that each grain absorbs no more than one per cent of X-radiation immission. The best way to tackle with the problems mentioned above is to make samples as homogeneous as possible, with fine grains for all phases.

In some cases it could also be useful to use a different anode material to avoid any problems resulting from microabsorption. This recommendation is especially valid for minerals containing large amounts of iron. Use Co-K<sub>α</sub> radiation instead of Cu-K<sub>α</sub> radiation. For Cu-K<sub>α</sub> radiation, the mass attenuation coefficients of Al<sub>2</sub>O<sub>3</sub> and Fe<sub>2</sub>O<sub>3</sub> differ by around 700%. In the case of Co-K<sub>α</sub> radiation there will be no practical difference anymore.

### 6.4 Sample roughness

Surface roughness of powder samples ranges from several micrometers to tens of micrometers due to their physical state. In the case of low incidence angles X-radiation is completely absorbed by protruding grains. As a result a reduced number of crystallites is involved in diffraction. This can be learnt from a background decrease for small diffraction angles. The error acts in the same way even on the background and the diffraction intensity. Consequently, reflections acting under small angles have insufficient intensity. Because there is no effective way to correct for these effects, it is recommended to prepare a sample with minimum sample roughness and to exclude very low angles from the Rietveld refinement.

### 6.5 Sample holder (measurement in reflection)

If it is possible to prepare sufficiently large samples, there are almost no constraints for the material of the sample holder. In this case we can collimate the primary X-ray in such a way that the radiation arrives on the area of the sample holder. In the case of sufficient sample thickness the sample holder cannot produce any diffraction background or even any reflections at all.

However, if we have only few sample material, it could be useful to apply a sample holder with a Si- or quartz- monocrystal bottom.

Be especially careful when mounting the sample onto the sample holder/diffractometer. Place the sample surface exactly at the rotation axis of the goniometer. A value of  $\Delta d$  for the deviation of the sample surface from the rotation axis results in a deviation in  $2\Theta$  following the relationship mentioned below:

$$\Delta 2\Theta = -2\Delta d \frac{\cos \Theta}{R} \quad (6.1)$$

with

$R$  Radius of the goniometer circle

The following estimation demonstrates how important it is to place the sample exactly. The cosine is around 1 for small angles. Let the radius of the goniometer circle be 175mm. In this case an error of 100 $\mu$ m during positioning of the sample would result in an angular deviation of around 0.065°.

To place the sample with an accuracy of less than  $\pm 50\mu\text{m}$  in the axis of rotation we need special arrangements. As a rule the **EPS2** parameter should always be released during Rietveld analysis. This parameter describes the angular deviation due to the sample eccentricity. **EPS2** is recommended for general use unless the angular range to be evaluated is  $< 40^\circ$ . In this case **EPS1** and **EPS2** would correlate strongly.

A reliable compromise between surface roughness and preferred orientation of the sample could be the application of the “side filling” technique, but other methods can also be appropriate, depending on the sample material.

For comprehensive description of sample preparation techniques see chapter 4, in [6].



# Chapter 7

## Measuring strategy

To achieve precise results in Rietveld analysis, careful measurement on a well-adjusted device is absolutely necessary. The quality of measuring data can be enhanced by destined choice of measuring parameters. Selection of measuring parameters is explained in the chapter below.

### 7.1 Diffractometer control

The program expects counts which have been obtained by stepwise scanning. The user is recommended not to use a continuous scan: In these cases the deviations between the real angle and the stored one are increasing as a function of rising angle. For default you would set equidistant angular steps at constant measuring time for each step. But this measuring strategy is not necessary, because the program is able to cope with both non-equidistant angular steps and arbitrary measuring times for each step.

As a rule of thumb let the angle step size be around a fifth of the half width of the narrowest peak, that are normally  $0.02$  to  $0.05^\circ$ . Keep the angular range in a way, that the peaks of low-indexed lattice planes are always contained. For improved fitting of the background, a background range of some degrees should lie in front of the first peak. For analysis of phases and real structures without refinement of atomic positions and anisotropic temperature factors, an upper boundary of about  $90^\circ$  is commonly sufficient. This boundary means that there are no intensive peaks above this angular value. For structure refinement, try to cover the entire angular range, which is in most cases up to  $160^\circ$ . To get a precise analysis, choose a measuring time value that enables a minimum of 2500 counts for a greater number of peaks.

#### Variable counting time

There are a lot of factors reducing the measured intensity towards higher diffraction angles. The Lorentzian polarisation factor, the Debye-Waller-factor and the atomic scattering factors are the most important ones. Partly, their influence is compensated by the multiplicity of peaks, which is increasing in with the angle  $2\theta$ . In cases of cylindrical sample geometry the absorption of the sample also acts for balancing.

Despite of this intensity slope, Rietveld measurements are commonly carried out with constant counting time per step. As a result, the accuracy of the measuring values is higher for low angles than for higher angles. This effect is mostly unfavourable since the peak density is essentially higher in the case of greater diffraction angles.

Unfortunately it is not possible to establish a universal simple rule to modify the measuring time as a function of the angle. The atomic scattering factors, the Debye-Waller-factor and multiplicity depend

on sample material. Therefore, it is recommended to determine the expected intensities in a short preliminary measurement. Based on this pattern, a new measuring instruction with several intervals can be elaborated, whose measuring time increases with each interval.

To calculate variable measuring times, you may use a software of Madsen and Hill [19]. Necessary entry parameters: The average value for thermal diffuse scattering, the mass attenuation coefficient, the predominant crystal system and the average chemical formula of the sample.

## Variable (automatic) divergence slits

Variable divergence slits are used to expose a constant sample length independent of the angle. Consequently, a formulation of the  $2\Theta$ -dependency of the divergence angle (or equatorial slit dimension) has to be used. This is easy to do by the program **GEOMET** when calculating the geometry function.

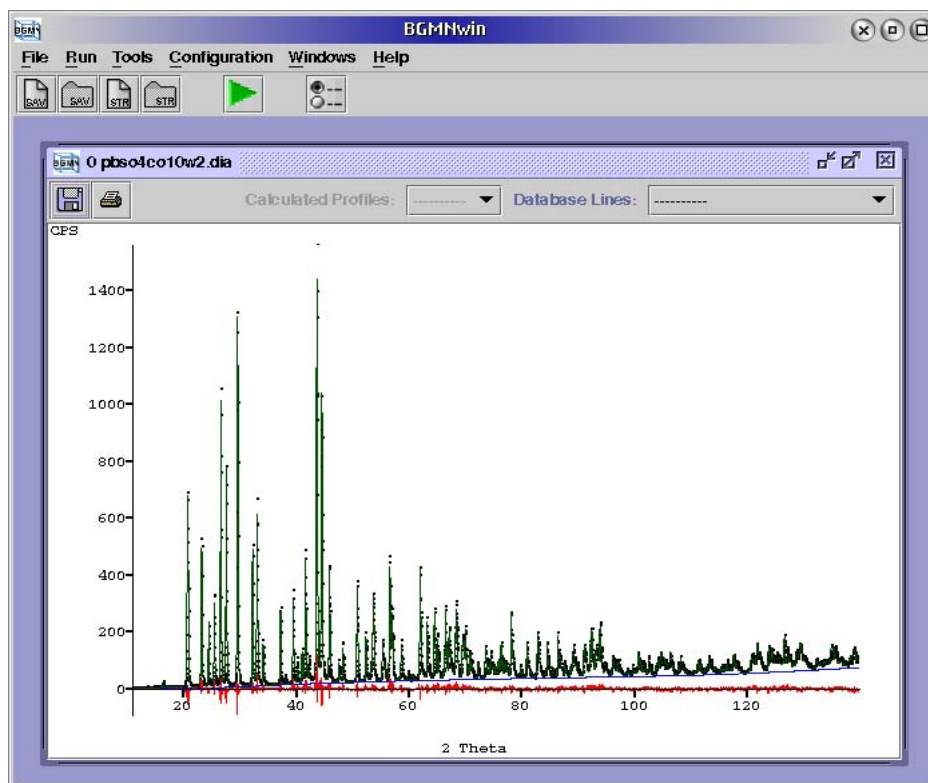


Figure 7.1: Exemplary diagram measured by means of a variable divergence slit and evaluated by **BGMN**. Illuminated specimen length 10mm,  $R_{wp}=6.48\%$

Therefore the slit aperture must be represented as a function of the angle, and **GSUM** has to be used. We give an example for 10mm exposed sample length:

```

HSlitR=250-152
HSlitW=(2*152*10*sin(pi*zweiTheta/360))/(2*250+10*cos(pi*zweiTheta/360))
GSUM=Y

```

In contrast to other Rietveld programs, the data do not have to be subjected to *any further correction*. The calculated geometry function includes the profile changes and the intensity corrections. As for fixed slits the error data are computed correctly.

An example is the refinement of the structure of anglesite (see Chapter 4) using automatic divergence slit measurements. The refinement results of two ADS measurements and one fixed slit measurement

(same sample, all  $15\text{--}140^\circ 2\Theta$ , step  $0.03^\circ$ , 10 sec/step on an XRD 3000TT instrument without secondary Soller slits) are compared to the data cited from [13], and computed from the original data set using **BGMN**, resp. The own fixed slit measurement has an irradiated sample length of 10 mm at about  $30^\circ 2\Theta$ , the region of the most intense lines. The results in tab. 7.1 are comparable, although the number of the acquired measuring points and the measuring time are reduced compared to [13].

The advantages of the variable divergence slits are:

- Correct intensity values in the entire angular range because of the sample holder is not irradiated
- Higher intensity in the case of high angles in comparison to the fixed slit
- Better grain statistics especially for higher angles
- Lower angular limit due to prevention of irradiation of sample boundaries
- Low intensity of the background at low angles

Therefore, it is explicitly recommended to use automatic divergence slits in structure refinement and phase analysis.

*Note:*

*If you are working with a fixed anti-scatter slit, you should select a sufficient slit width that does not limit the beam path even for large angles! Additionally, if you are working with a variable anti-scattering slit plus **TubeTails**-Correction, you must use the **SSlitW** plus **SSlitR** entries in the profile describing \*.str-file for the **GEOMET** run.*

Table 7.1: Comparison of fixed and automatic divergence slit measurements, resp.

Value	RR	RR-BGMN	F1	V5	V10	X
$R_{exp}$	1.5%–7.0%	5.36%	6.16%	4.96%	3.70%	—
$R_{wp}$	8.2%–20%	7.84%	8.36%	7.91%	6.48%	—
a/Å	8.4764–8.4859	8.4760(2)	8.4789(6)	8.4786(5)	8.4786(4)	8.482(2)
b/Å	5.3962–5.4024	5.3958(2)	5.3991(4)	5.3989(3)	5.3986(3)	5.398(2)
c/Å	6.9568–6.9650	6.9564(2)	6.9589(5)	6.9588(4)	6.9588(4)	6.959(2)
Pb: x	0.1875–0.1883	0.18790(7)	0.1880(1)	0.1881(1)	0.18790(7)	0.1879(1)
Pb: z	0.1669–0.1683	0.1672(1)	0.1672(2)	0.1674(2)	0.1671(2)	0.1667(1)
Pb: B/Å <sup>2</sup>	0.9–2.39	1.55(2)	1.44(2)	1.30(2)	1.63(2)	1.48
S: x	0.0621–0.0673	0.0631(4)	0.0636(6)	0.0632(5)	0.0636(4)	0.0633(6)
S: z	0.6799–0.6860	0.6849(5)	0.6878(7)	0.6852(7)	0.6851(5)	0.6842(7)
S: B/Å <sup>2</sup>	0.29–1.37	0.83(7)	1.0(1)	0.7(1)	1.04(7)	0.74
O1: x	0.902–0.924	0.906(1)	0.907(2)	0.909(1)	0.907(1)	0.908(2)
O1: z	0.585–0.601	0.597(1)	0.598(2)	0.599(2)	0.598(2)	0.596(3)
O1: B/Å <sup>2</sup>	0.50–4.2	1.2(2)	0.8(2)	0.8(2)	1.0(2)	1.87
O2: x	0.177–0.200	0.191(2)	0.192(2)	0.191(2)	0.191(2)	0.194(2)
O2: z	0.523–0.548	0.547(2)	0.546(2)	0.543(2)	0.545(2)	0.543(2)
O2: B/Å <sup>2</sup>	0.1–5.8	1.4(2)	1.6(3)	0.6(2)	1.4(2)	1.76
O3: x	0.071–0.080	0.0786(6)	0.0808(8)	0.0810(8)	0.0790(6)	0.082(1)
O3: y	0.018–0.041	0.026(1)	0.024(2)	0.026(2)	0.026(1)	0.026(2)
O3: z	0.806–0.819	0.811(1)	0.807(2)	0.805(2)	0.807(1)	0.809(2)
O3: B/Å <sup>2</sup>	0.8–4.6	0.9(2)	0.7(2)	0.7(2)	0.8(2)	1.34

Table columns are marked as follows:

1. column RR: Range of results given by HILL (1992).
2. column RR-BGMN: Data as distributed, re-evaluated using **BGMN**.
3. column F1: Own measurement of RR sample PbSO<sub>4</sub> using fixed divergence slit 1 mm.
4. column V5: Own measurement of RR sample PbSO<sub>4</sub> using variable divergence slit, 5 mm irradiated sample length.
5. column V10: Own measurement of RR sample PbSO<sub>4</sub> using variable divergence slit, 10mm irradiated sample length.
6. column X: Single crystal data as described *ibid*.

## 7.2 Sample illumination

If possible, let the sample be greater than the area illuminated by the primary beam (the “infinite large” sample). Select the divergence slit width correspondingly narrow.

However, the sample may be too small. Under these circumstances, it may be necessary that the sample surface is illuminated as far as possible, that the beam really overflows the sample.

In that case the sample size and shape must be considered during calculation of the device function. Use **GEOMET** (parameters **SampleW** and **SampleH** for width and height, **SampleD** for sample diameter, resp.) for consideration. For samples of irregular shape, take average values. Note that **GSUM** must be set “Y” in the case of small samples. You should also reduce angle step sizes for running **GEOMET** in order to get a more precise interpolation of the profile parameters.

## 7.3 Measurement geometry

There are three sample geometries to be selected. Each of them has its particular advantages and disadvantages.

### Reflection

Reflection (Bragg-Brentano), which is often predefined by sample consistency, is regarded as standard geometry. Problems resulting from the profile shape mostly occur in the case of low angles. This problem results from the sample roughness, which can only nearly be modelled. Weighted least squares sums  $R_{wp}$  of 5% are attainable in reflection mode.

You should take into consideration transmission geometry, if this is possible for the reasons of applied device and sample material.

### Transmission

Although used more seldom, transmission is clearly more advantageous than reflection. Transmission can be modelled much more exactly and also particle statistics can be controlled much better. Sample roughness is irrelevant for small angles. Another advantage, that is essential for practice, is the weaker preferred orientation in comparison to reflection mode.

The specific profile shape for transmission geometry (smeared box profile with asymmetric tails displaced in  $2\Theta$ ) is modelled very exactly. Weighted least-squares sums  $R_{wp}$  of 2% have already been achieved.

Figure 7.2 illustrates a profile calculated to evaluate the sample metashale Böhlscheiben.

### Capillary

Capillary stands for the third introduced geometry. In some cases, e.g. for high temperature investigations, it can be the only possible geometry.

Until now experiences on accuracy have not been made available yet. Mistakes may result from a lot of causes such as:

- non-axial and/or tumbling sample in the range of  $10 \mu\text{m}$ .
- non-homogeneous sample due to particle statistics. The errors observed in reflection may multiply themselves.

- Density fluctuations in longitudinal capillary direction (by uneven filling of the capillary) result in profile errors.

Consequently capillary geometry should be used in cases where the sample is available as homogeneous stick, e.g. as thin wire or fibre. Provided that another geometry can be realised, do not use a real capillary with powder filling. This recommendation is based on the above mentioned causes.

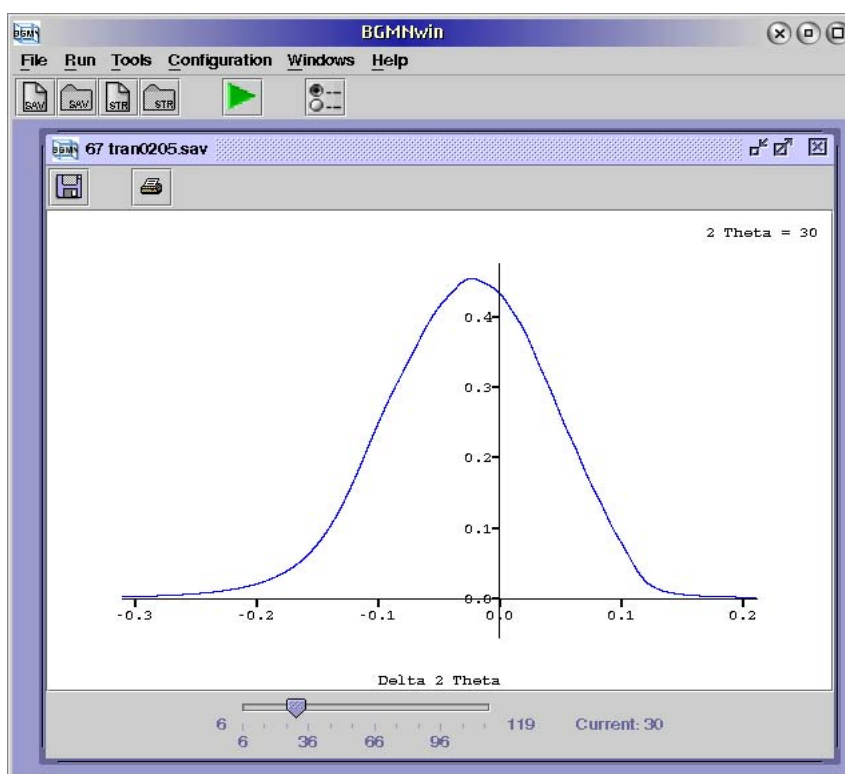


Figure 7.2: Exemplary device function in transmission ( $2\Theta = 30^\circ$ )

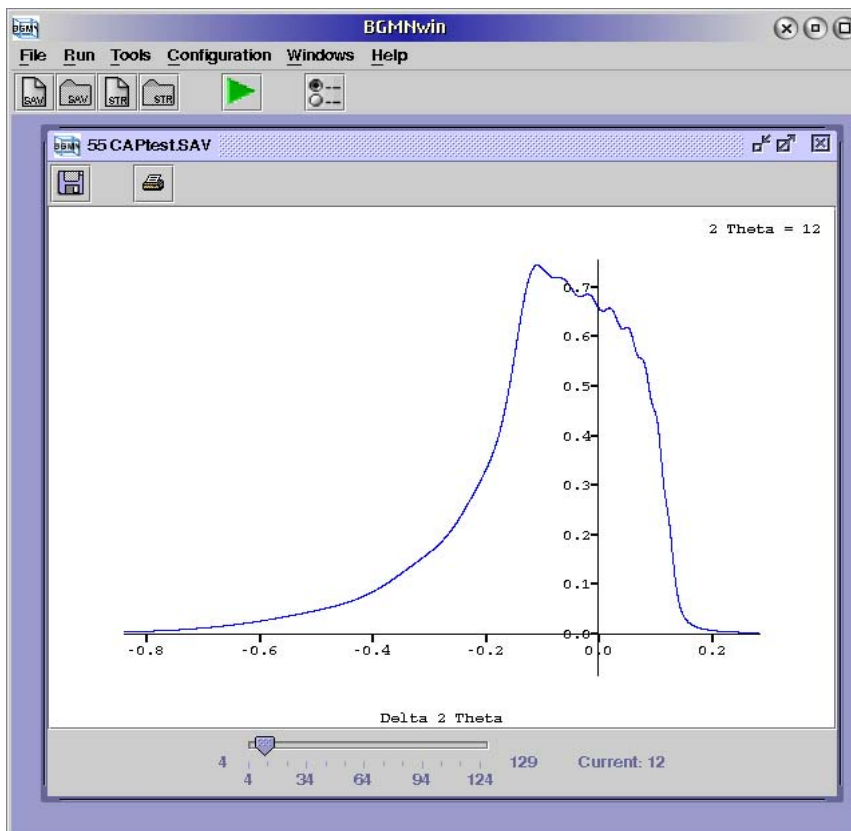


Figure 7.3: Example device function as calculated for a gypsum filled capillary at  $2\Theta = 12^\circ$



# Chapter 8

## General restrictions

### 8.1 Physical and mathematical restrictions

How powerful a software may be, it is not able to model all physical effects which can occur. We need assumptions for approximations, which limit either the accuracy to be achieved or the range of application. The following chapter includes the essential restrictions resulting from the applied models.

#### Obtainable precision of intensities and phase contents

Deviations of the electron density from the spherical shape result from influencing bonding electrons. Consequently the deviation of real intensity from theoretical intensity ranges from 2 to 5%. Due to averaging over all reflections we can achieve a relative accuracy of maximally 1 to 2% for the phase contents.

#### Preferred orientation at grazing incidence

All implemented models of preferred orientation describe an inverse two-dimensional pole figure. The diffraction vector (medians between primary and secondary beam) is assumed either in fixed orientation related to the sample or subjected to constant averaging. For example, constant averaging is performed for a rotating transmission sample. In the special case of grazing incidence both suppositions are not guaranteed. The deviation of the diffraction vector from the sample's normal is proportional to the increase of the angle  $2\Theta$ . For this case a texture correction must describe the entire three-dimensional texture. Such texture corrections are much more complicated and also react much more sensitively upon parameter correlation. There is no adequate model implemented for the description of PO in grazing incidence geometry, until now.

#### Primary monochromator

The **BGMN** program is based on a folding of wavelength distribution with the device function for an ideal profile. This assumption is based on the condition that the different beam paths (shaping the device function) are the same for all wavelengths. This is not the case for beams diffracted by a single-crystal primary beam monochromator. For that reason the profile model of **BGMN** cannot be applied for primary monochromators. Some other reasons are:

- In cases of readjustment of the monochromator crystal the wavelength distribution can be modified in a not reproducible manner

- Even if one would refuse the separation in wavelength distribution and geometry function within the profile model, the profile shape to be computed would not remain reproducible

Provided that one is trying to do the structure analysis without the full **BGMN** profile model, one can analyze data obtained by a primary monochromator. In this case, the profile is based on a special wavelength distribution (Delta function) and a simple goniometer function formula. The numerical advantages of the program are still alive. For example, such an approach can be applied for the analysis of synchrotron data.

### **Neutrons (constant wavelength and time of flight)**

The **BGMN** program system was tailored for use in the X-ray lab, because most of the Rietveld analyses are performed in such laboratories.

With respect to the profile shape to be modelled, neutron diffraction patterns are easier to treat than X-ray diagrams. For that reason, neutron diffraction patterns can be analyzed quite well by means of the simple analytical profile functions as used in traditional Rietveld programs. The new optimization algorithm as well as the sample model would be the only advantages resulting directly from **BGMN**. Therefore, the option of refinement of neutron data is not implemented in **BGMN**.

## **8.2 Restrictions due to software**

The program was newly developed from the roots. It does not take reference to any published Rietveld code. Basing on an entirely new way of programming, the program does not cause any restrictions for the user concerning the volume of the analysis subject. Number of free parameters, of measuring points, of diffraction reflections and phases are the most essential parameters that will not be restricted any more.

The only existing limitation of the software is the number of the characters per item in the *\*.sav* and *\*.str* files. An item is the least unit that is limited by delimiters (space, new line). But, an item can also be written over a lot of lines, without any blanks, and if there remains at least one open bracket at the end of line, which has not yet been closed. Maximally 8000 characters per item are permitted.

The *only practical restriction* arises from the CPU time, which naturally increases with the number of the parameters/peaks/measuring points. In case of bad (low statistic) measurement or strongly correlating parameters in the starting model the necessary CPU time increases also.

Example:

About 1min 30s min CPU time, when using a Pentium 4 2.4 GHz for a phase analysis with 2101 pattern data length; phases: 2 triclinic, 2 monoclinic, 1 hexagonal and 1 tetragonal phase with 997 reflections and 84 parameters in total (see figure 9.11).

# Chapter 9

## Phase analysis

Some examples are introduced to clarify practical problems of quantitative phase analysis. The principle is described for a mixture of two phases. The second example deals with the determination of the amorphous part in a sample making use of an internal standard. The analysis of metashale being a very sophisticated application is taken for example. At the end of this chapter you will read about the experience gained by using **BGMN**.

### 9.1 Mixture of goethite and quartz

Take a 50/50 mixture of goethite and quartz as a simple example of phase analysis. The sample was prepared in an aluminium cuvette to be filled from the front. The sample holder was filled with low pressure only. The remaining material was drawn off laterally.

Measurement was carried out on an URD 6 diffractometer (reflection geometry) with sample rotating unit. A Co fine focus X-ray tube, automatic divergency with irradiated sample length of 15mm (see subsection 7.1), a primary soller collimator with 15mm axial width and a 0.25mm receiving slit were used. The diffracted radiation was analyzed by a graphite secondary monochromator.

Measurement was performed in a range of 5 to 80° (step size 0.03°, time preselection 5 sec, that is 2501 data points). Such values are common for standard phase analysis.

By **Geomet** and **MakeGEQ**, the device function was calculated using the *URDco15ph.SAV* control file. This file will be visible by opening **BGMNwin**, selecting

File→Open Control File

browsing to the *URDco15ph.SAV* file and opening it. See figure 9.1. Note that the calculation with **Geomet/MakeGEQ** is only necessary, if the required device function has not yet been computed. When using **MakeGEQ** for computation, consider, that you have to enter explicitly the average penetration depth of the X-rays. Average penetration depth is a correction, which represents the profile deformation better than parameter **EPS3** for angle correction. An average value of the two phases, the sample consists of, was introduced for **D**. For the calculation, use again **BGMNwin** and enter

Run→Geomet

browse to the *URDco15ph.SAV* file and open it. When **Geomet** has finished, start **MakeGEQ** in the same way:

Run→MakeGEQ



```

% file containing the geometric functions, output of the Monte-Carlo simulation
VERZERR=urdc015ph.ger
% file containing the interpolated geometric functions, output of the interpolation by MAKEGEQ
GEQ=urdc015ph.geq
% file of the TubeTails measurement
TubeTails=focph11ff1.val
% goniometer radius
R=220
% estimated penetration depth
D=0.1
% position (distance from goniometer axis) of the equatorial divergence slit, mm
HSlitR=220-101
% automatic divergence slit width, 15 mm irradiated length, distance from focus to slit is 101
HSlitW=(2*101*15*sin(pi*zweiTheta/360))/(2*220+15*cos(pi*zweiTheta/360))
% position (distance from goniometer axis) and width of an axial divergence slit, mm
VSlitR=220-70
VSlitH=15
% beam length between sample and secondary graphite monochromator
MonR=220+59
% axial dimension of the monochromator crystal, mm
MonH=15
% axial dimension (length) and optical breadth (1/10 of the nominal) of the line focus, mm
FbcusH=12
FbcusW=0.04
% width of the receiving slit, mm
DetW=0.25
% diameter of the sample holder, mm
SamplD=25
% primary soller slits, distance/length (mm) or half the acceptance angle (radians)
PColl=0.5/20
% angular positions for the MonteCarlo simulation, 2theta
zweiTheta [1]=5
zweiTheta [2]=8
zweiTheta [3]=13
zweiTheta [4]=20
zweiTheta [5]=30
zweiTheta [6]=42
zweiTheta [7]=56
zweiTheta [8]=76
zweiTheta [9]=90
zweiTheta [10]=105
zweiTheta [11]=120
zweiTheta [12]=135
zweiTheta [13]=150
% angular range and step width for the interpolation of the geometric profiles
WMIN=5
WMAX=150
pi=2*acos(0)
WSTEP=3*sin(pi*zweiTheta/180)
% switch for applying the intensity correction for beam overflow resp. ADS function
GSUM=Y

```

Figure 9.1: Control file *URDco15ph.SAV* as used for the **Geomet** and **MakeGEQ** run

browse again to the *URDco15ph.SAV* file and open it.

In the following step the structure files of the present phases were provided. Since there was no information available on the real structure, the width parameters **B1**, **k1** and **k2** were released during both the fitting phases. Literature values were taken as values for the Debye-Waller-factors (TDS). As a rule in phase analysis the temperature factors are maintained as preset instead of released. Pay attention to entries such as `GOAL : . . . =GEWICHT`. In this term the identifiers between **GOAL** and the equal mark are required for output of the phase parts into the result file. For output, the corresponding formulae are entered into the control file for Rietveld analysis. Figure 9.3 shows both the structure files *Goethite.str* and *Quartz.sav* as visible in **BGMNwin** using the Command

File→Open Structure File

Due to preferred orientation, for both the structure descriptions

GEWICHT=SPHAR4

was selected. The control file *GoethiteQuartz.sav* was generated for Rietveld analysis. Figure 9.2 shows it as visible within **BGMNwin** by selecting

File→Open Control File

To obtain just the weight contents of the phases in the output file, the lines of the type `GOAL [x] = . . .` were inserted. Note, that you have to use even the same identifier, that has been entered to the structure files by the terms `GOAL : . . . =GEWICHT`.

**BGMN** requires 14 seconds for the calculation with 53 parameters.

Figure 9.4 shows the first lines of the *GoethiteQuartz.lst* result file from which all the phase contents as well as the associated random errors may be obtained, it will be shown by selecting

Tools→Show Results

and opening the *GoethiteQuartz.lst* file. The errors represent a lower boundary of the esd (estimated standard deviation) as defined by the error propagation rules from only counting statistics of the pattern data. In reality the total error of analysis is greater than the computed one. This difference is caused by systematic deviations that e.g. may occur during sample preparation.

Figure 9.5 shows good coincidence of measured and computed diagrams. Presumably the observed intensity deviations are caused by inaccuracies of the used Debye-Waller-factors. The user is recommended not to refine the TDS parameters, because of possibly strong correlation of the parameter of the temperature factors and possible preferred orientations.

	Goethite	Quartz	Parameter count	$1 - \rho$	$R_{wp}$
quant. phase analysis	49.30(18)%	50.70(18)%	53	0.524%	5.20%
prepared quantity	50%	50%	—	—	—

Table 9.1: Estimated and prepared phase contents in comparison

```

% device file containing the geometric profile
VERZERR=urdc015ph.ges
% estimated particle size for microabsorption correction
d=6
% polarisation factor of the graphite monochromator, angle 31.0 deg for Co radiation
pi=2*acos(0)
POL=sqr(cos(31.0*pi/180))
% measuring data
VAL [1]=GoethiteQuartz.val
% structures
STRUC [1]=Goethite.str
STRUC [2]=Quartz.str
% denom is an arbitrary chosen helper variable
denom=Goethite+Quartz
% calculation rules for phase quantification, simply relating the phases
GOAL [1]=Goethite/denom
GOAL [2]=Quartz/denom
% peak list
OUTPUT=GoethiteQuartz.par
% diagram output file
DIAGRAMM=GoethiteQuartz.dia
% result file
LIST=GoethiteQuartz.lst
% refining the zero point deviation
PARAM [1]=EPS1=0_-0.0003^0.0003
% refining the sample displacement correction
PARAM [2]=EPS2=0
PROTOKOLL=Y

```

Figure 9.2: Control file *GoethiteQuartz.sav* as used in the example

```

PHASE=Goethite SpacegroupNo=62 HermannMauguin=F2_1/n2_1/m2_1/a //
Group=Oxides Formula=Fe_O_OH ICDD=290713 Reference=71810 //
PARAM=A=0.996_0.99^1 PARAM=B=0.3023_0.298^0.307 PARAM=C=0.4605_0.455^0.465 //
//
RP=4 PARAM=B1=0_0^0.02 PARAM=k1=0_0^1 PARAM=k2=0_0^0.0001 GOAL=GrainSize(1,0,0) GOAL=sqrt(k2) //
GEMICHT=SPHAR4 GOAL:Goethite=GEMICHT*ifthenelse(ifDef(d), exp(ny*d*3/4), 1)
E=(FE+3(1)) Wyckoff=c x=0.3539 y=0 z=0.4523 TDS=0.01
E=(O-1(1)) Wyckoff=c x=0.6996 y=0 z=0.792 TDS=0.01
E=(O-1(1)) Wyckoff=c x=0.5531 y=0 z=0.296 TDS=0.01

```

```

PHASE=Quartz SpacegroupNo=154 //
Group=Oxides Formula=Si_O2 ICDD=331161 Reference=34636 //
PARAM=A=0.4913_0.49^0.4935 PARAM=C=0.5404_0.538^0.545 //
//
RP=4 PARAM=B1=0_0^0.01 PARAM=k2=0_0^0.00001 GOAL=GrainSize(1,0,0) GOAL=sqrt(k2) //
GEMICHT=SPHAR4 GOAL:Quartz=GEMICHT*ifthenelse(ifDef(d), exp(ny*d*3/4), 1)
E=(SI+4(1)) Wyckoff=a x=0.47 y=0 z=0 TDS=0.0056
E=(O-2(1)) Wyckoff=c x=0.415 y=0.268 z=0.786 TDS=0.0096

```

Figure 9.3: Both the structure files *Goethite.str* and *Quartz.str* as used in the example

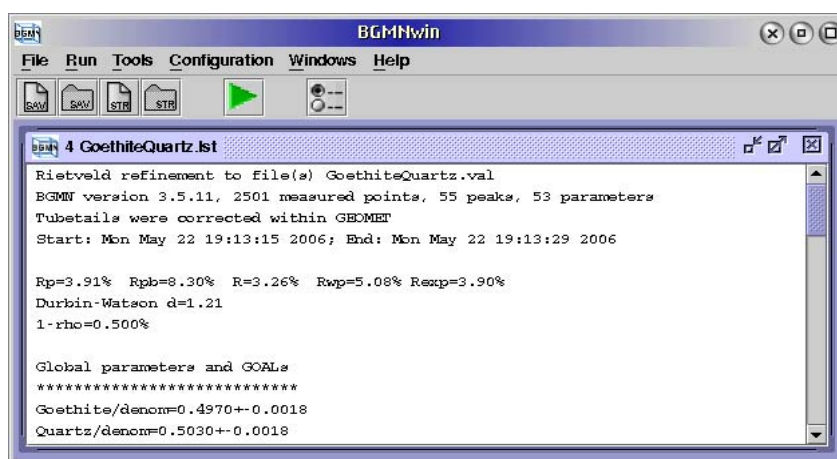


Figure 9.4: First lines of the result file *GoethiteQuartz.lst* giving the estimated phase contents of both the phases including their random errors

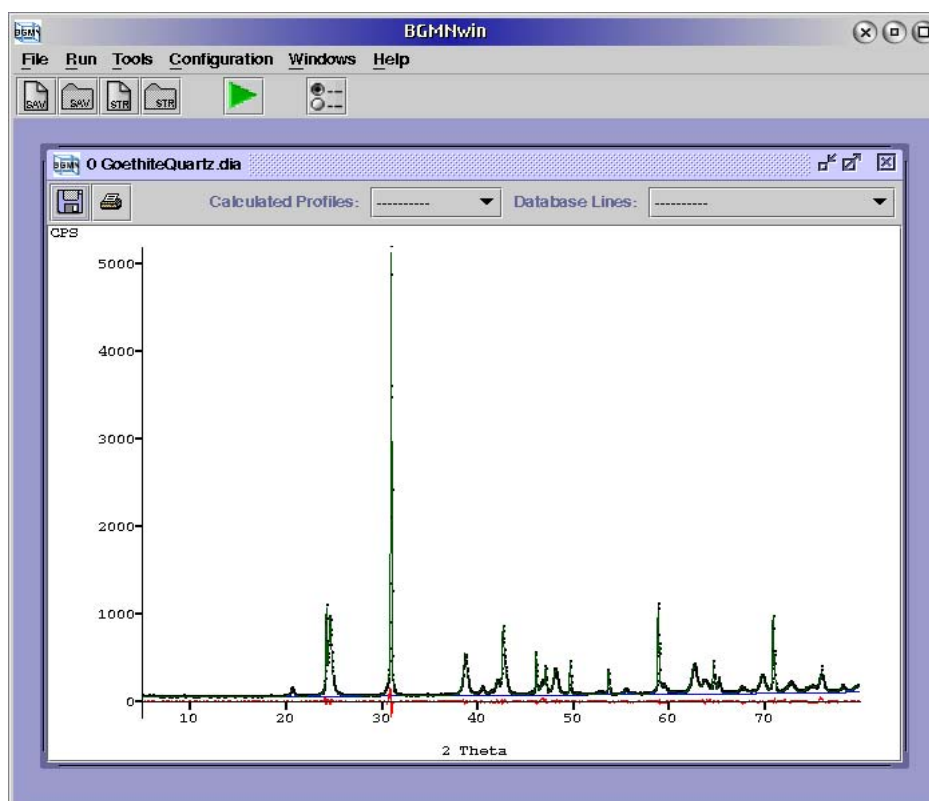


Figure 9.5: Measurement (in reflection on URD 6) and difference curve of a mixture of goethite and quartz ( $R_{wp}$  5.20%)

## 9.2 Determination of amorphous content by using an internal standard

A mixture of 40% glass, 30% quartz, 10% adularia, 10% Albite and 10% calcite was used for trying to estimate the amorphous content (glass) by an internal standard. Therefore, 10% zincite powder were added to 90% of the sample material. The same device as in the example above was used. The structure files as used are shown in figure 9.9. They may be inspected by opening **BGMNwin**, selecting

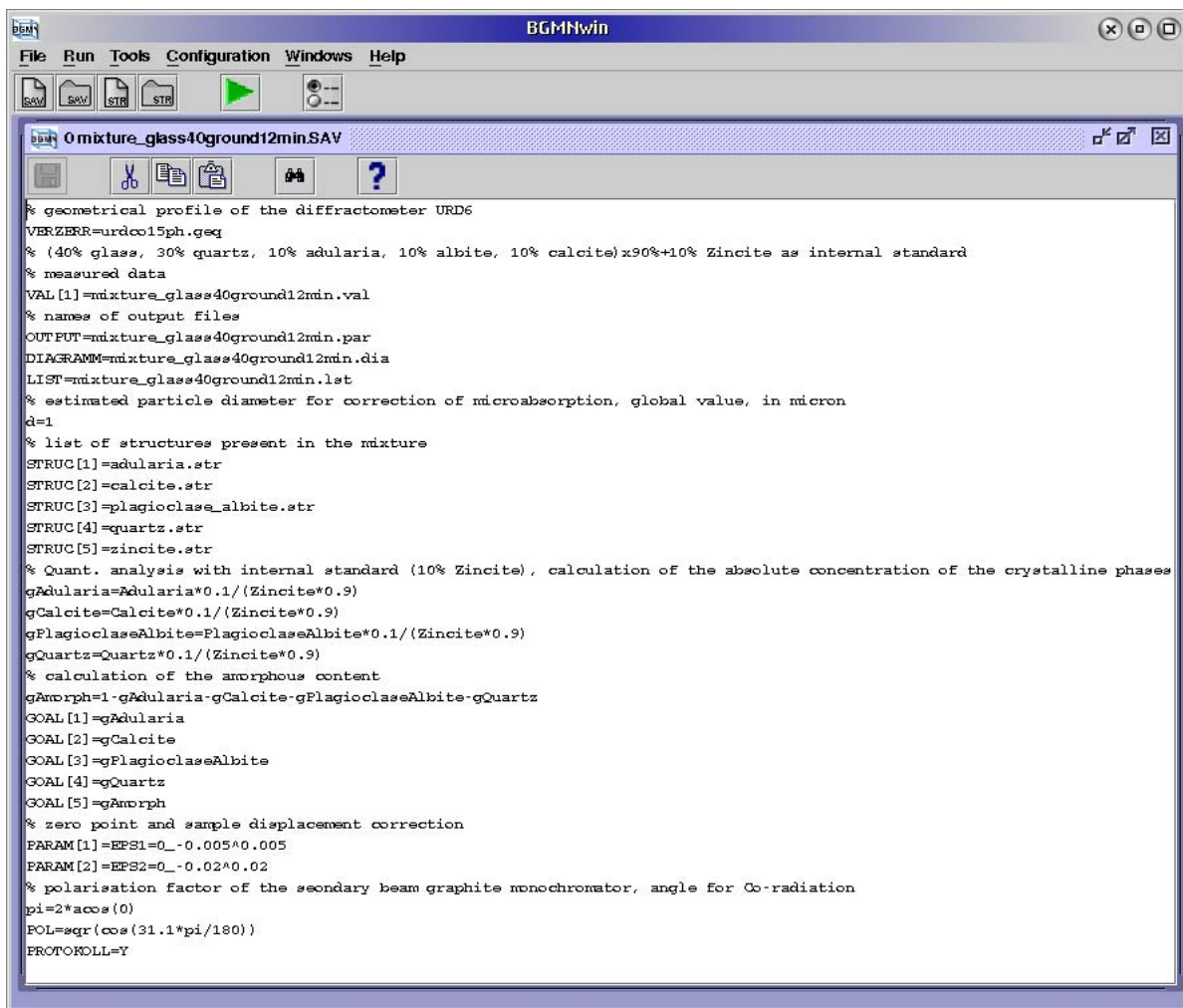
File→Open Structure File

browsing to the structure files and opening them.

Figure 9.6 control *glass40ground12min.sav* file was created for Rietveld analysis. It may be inspected by opening **BGMNwin**, selecting

File→Open Control File

browsing to the *glass40ground12min.sav* file and open it.



```

% geometrical profile of the diffractometer URD6
VERZERR=urdc015ph.geq
% (40% glass, 30% quartz, 10% adularia, 10% albite, 10% calcite)x90%+10% Zincite as internal standard
% measured data
VAL[1]=mixture_glass40ground12min.val
% names of output files
OUTPUT=mixture_glass40ground12min.par
DIAGRAM=mixture_glass40ground12min.dia
LIST=mixture_glass40ground12min.lst
% estimated particle diameter for correction of microabsorption, global value, in micron
d=1
% list of structures present in the mixture
STRUC[1]=adularia.str
STRUC[2]=calcite.str
STRUC[3]=plagioclase_albite.str
STRUC[4]=quartz.str
STRUC[5]=zincite.str
% Quant. analysis with internal standard (10% Zincite), calculation of the absolute concentration of the crystalline phases
gAdularia=Adularia*0.1/(Zincite*0.9)
gCalcite=Calcite*0.1/(Zincite*0.9)
gPlagioclaseAlbite=PlagioclaseAlbite*0.1/(Zincite*0.9)
gQuartz=Quartz*0.1/(Zincite*0.9)
% calculation of the amorphous content
gAmorph=1-gAdularia-gCalcite-gPlagioclaseAlbite-gQuartz
GOAL[1]=gAdularia
GOAL[2]=gCalcite
GOAL[3]=gPlagioclaseAlbite
GOAL[4]=gQuartz
GOAL[5]=gAmorph
% zero point and sample displacement correction
PARAM[1]=EPS1=0_-0.005^0.005
PARAM[2]=EPS2=0_-0.02^0.02
% polarisation factor of the secondary beam graphite monochromator, angle for Co-radiation
pi=2*acos(0)
POL=sqr(cos(31.1*pi/180))
PROTOCOLL=Y

```

Figure 9.6: Control file for the estimation of the amorphous content

The amorphous part is determined in the lines below:

```

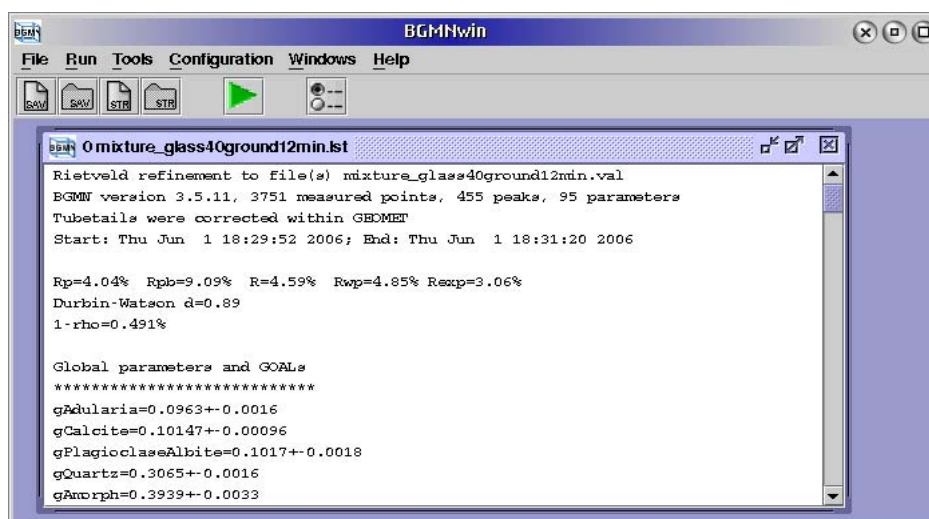
...
gAdularia=Adularia*0.1/(Zincite*0.9)
gCalcite=Calcite*0.1/(Zincite*0.9)
gPlagioclaseAlbite=PlagioclaseAlbite*0.1/(Zincite*0.9)
gQuartz=Quartz*0.1/(Zincite*0.9)
% calculation of the amorphous content
gAmorph=1-gAdularia-gCalcite-gPlagioclaseAlbite-gQuartz
GOAL[1]=gAdularia
GOAL[2]=gCalcite
GOAL[3]=gPlagioclaseAlbite
GOAL[4]=gQuartz
GOAL[5]=gAmorph
...

```

First the contents of all the well crystallized phases, related to the known part of the internal standard, are calculated. To make these contents values also available in the output file (result file), they are assigned to the corresponding GOALS. This division into auxiliary variables and GOAL assignment makes the contents values also available to just another GOAL statement for the amorphous part.

Last but not least, the amorphous part gAMORPH is computed by simple subtraction: Hereby 1 (corresponding to 100%) is diminished by the determined phase contents and the content of the internal standard.

The calculation takes about 2 min CPU time. Then we obtain the following result:



```

BGMN 0 mixture_glass40ground12min.lst
Rietveld refinement to File(s) mixture_glass40ground12min.val
BGMN version 3.5.11, 3751 measured points, 455 peaks, 95 parameters
Tubetails were corrected within GEOMET
Start: Thu Jun 1 18:29:52 2006; End: Thu Jun 1 18:31:20 2006

Rp=4.04% Rpb=9.09% R=4.59% Rwp=4.85% Rexp=3.06%
Durbin-Watson d=0.89
1-rho=0.491%

Global parameters and GOALS
*****
gAdularia=0.0963+-0.0016
gCalcite=0.10147+-0.00096
gPlagioclaseAlbite=0.1017+-0.0018
gQuartz=0.3065+-0.0016
gAmorph=0.3939+-0.0033

```

Figure 9.7: Result file of the amorphous content estimation

Consequently the amorphous content is about 39.4(3)%. Note that the errors caused by all the other phase contents do also impact due to error propagation.

As already mentioned, the specified failures are only *random errors*. Systematic errors cannot be computed by the program. The denominated errors are to be understood as a minimum value, which often may be much higher due to the systematic errors occurring in each case.

Figure 9.8 shows the internal fitting of the background caused by the amorphous content. Fitting can be abstracted from the background curve, which is bulged upwards amongst 20 and 40°.

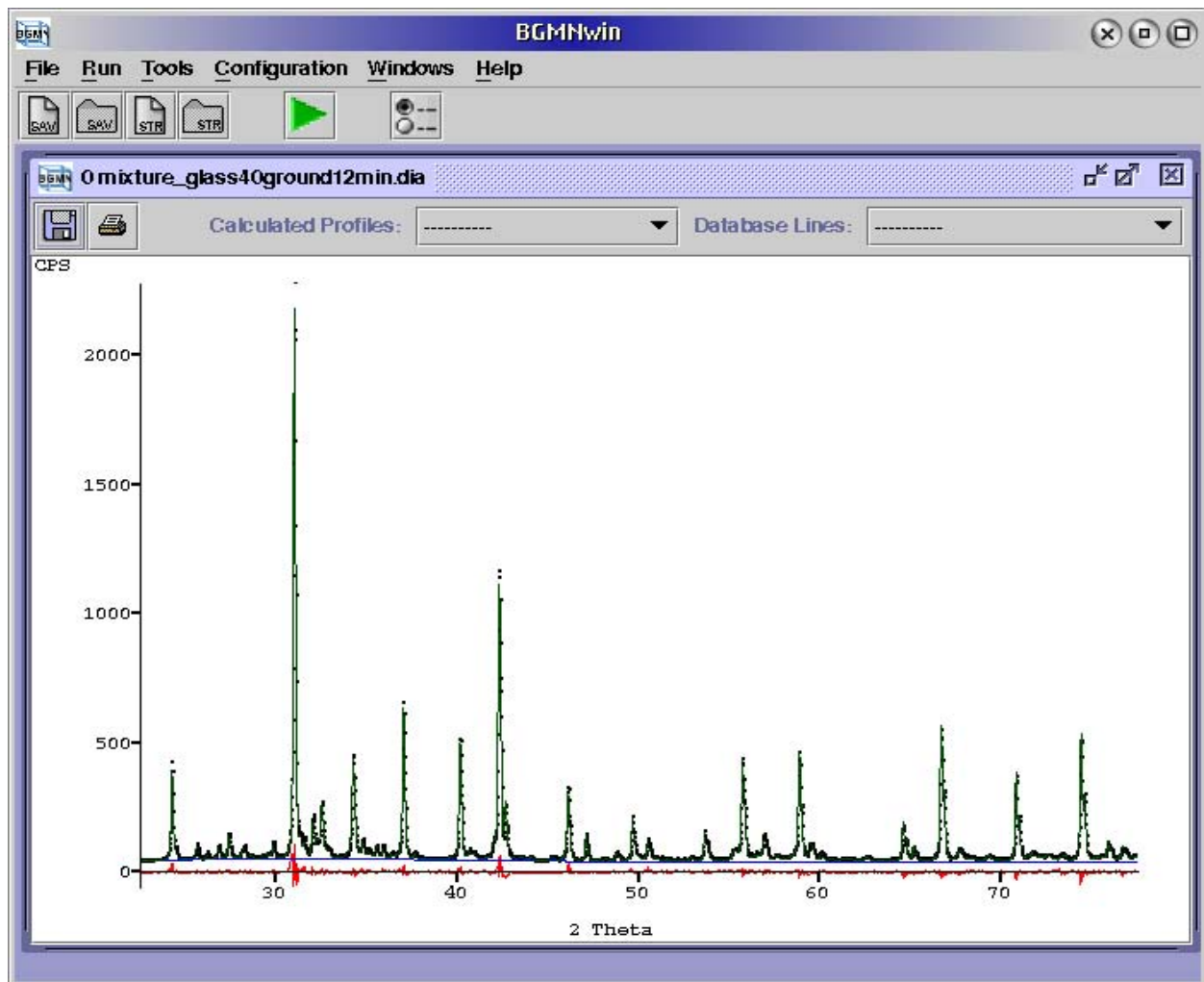


Figure 9.8: Measurement, difference and background curve of the amorphous content example with internal standard zincite (section); CPU time approx. 2 min.

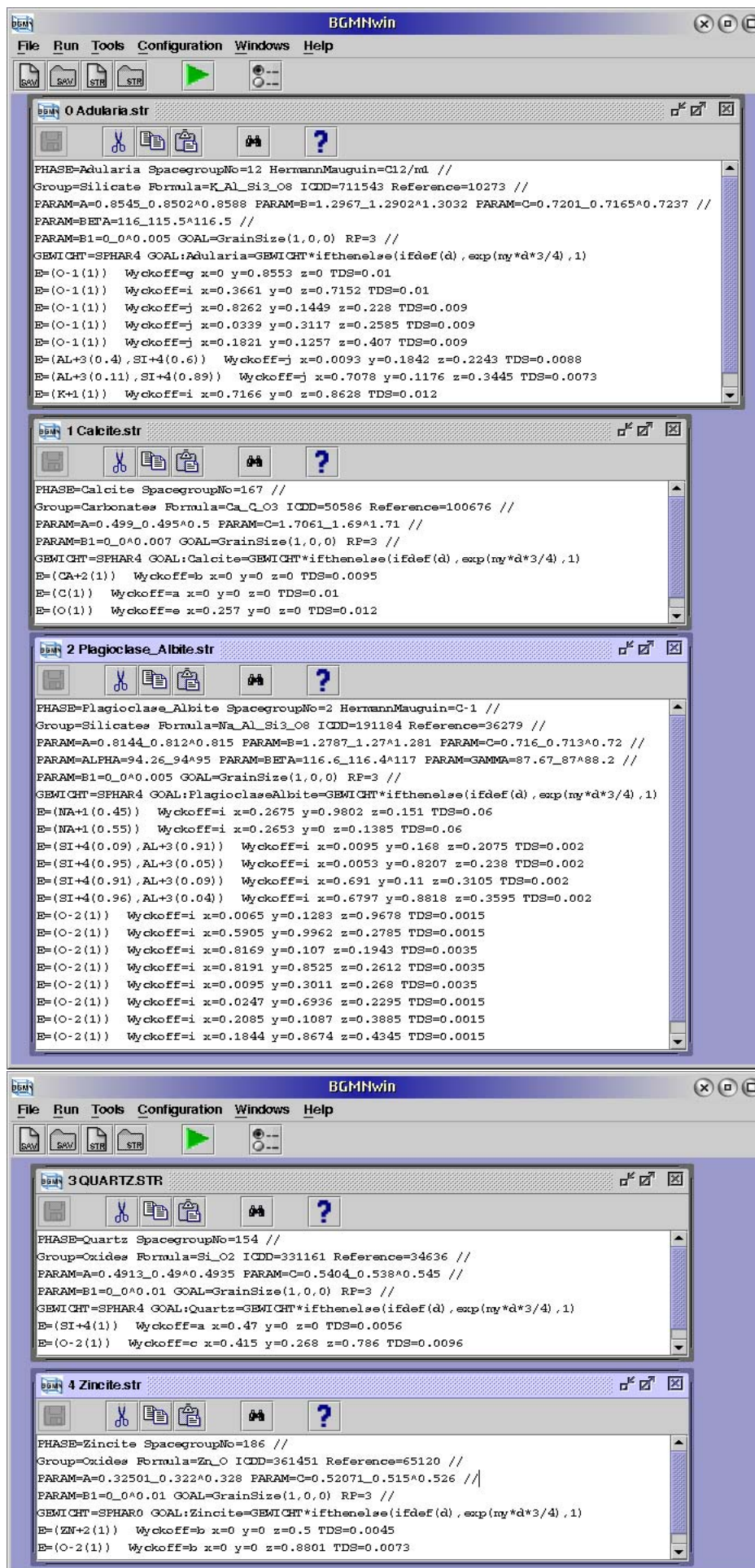


Figure 9.9: Structure files as used in the amorphous content example

### 9.3 Metashale Böhlscheiben

This standard rock sample examined well was selected in order to test the convergence behavior of the BGMN program on a real sample with several low symmetrical phases and to compare different measuring geometry.

The measurements were carried out at a sample of particle fraction  $< 30\mu\text{m}$  (step by step ground and sieved) both in Bragg-Brentano geometry (reflection, URD 6) and in Debye-Scherrer geometry (transmission through flat sample, XRD 3000 TT). For the case of transmission measurement, the measurement parameters (goniometer radius, slits, sample thickness, step width, counting time) were chosen so that a resolution sufficient for qualitative phase analysis was reached. Pulse statistics and peak profiles useful for normal peak search programs were still achieved in spite of smaller intensities compared to reflection geometry (see fig. methashale2). Consequently, the measuring time was in contrast to HILL et al. (1993) in the order of magnitude of the “normal” measurements in reflection geometry.

Refinement was carried out with muscovite as a  $2M_1$ -polytype as above, chlorite (ripidolite) 1MIIb and albite with isotropic width model and complex texture correction as well as with quartz. The difference curve of first refinement showed weak remaining peaks at 0.324 nm. That corresponds to a small potassium feldspar content presumed already in former times already. Therefore, microcline (without texture modeling and with limited peak broadening) was included in the model during the second refinement.

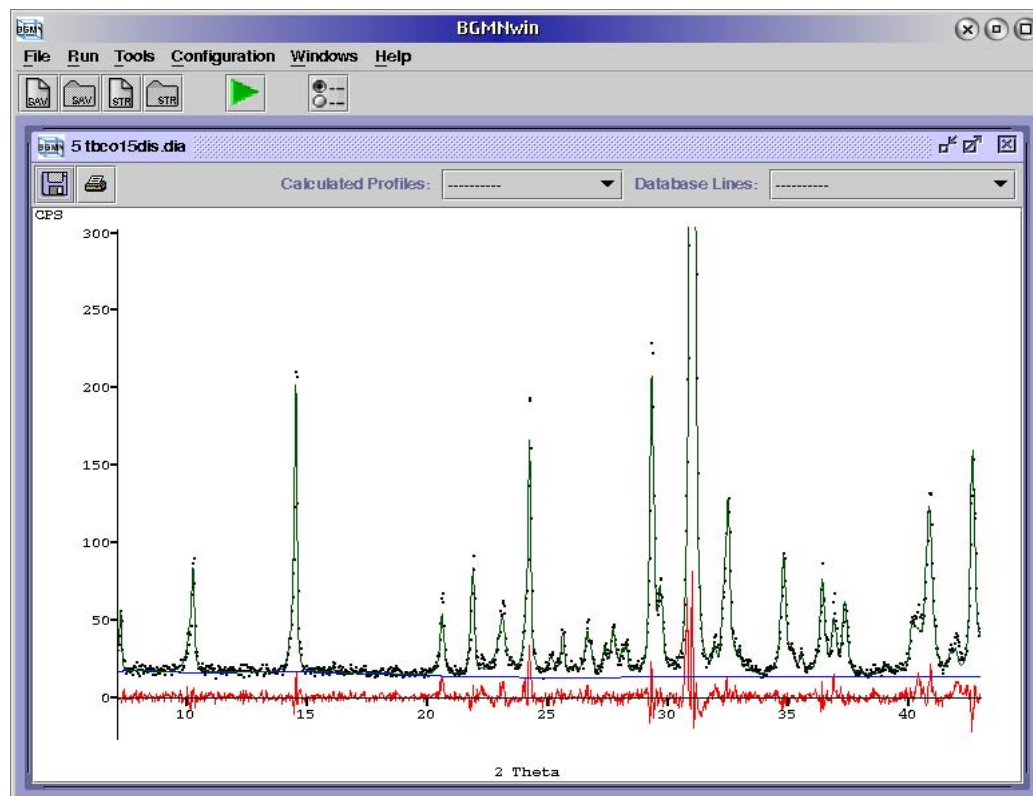


Figure 9.10: XRD 3000 TT measurement in reflection and difference curve (metashale Böhlscheiben — section); Muscovite, chlorite, albite and quartz ( $R_{wp}=9.87\%$ , CPU time approx. 5 min)

The difference plot shows some weak residual peaks, especially at 0.325 and 0.169 nm (fig. 9.10). This can be interpreted by the presence of rutile and/or potassium feldspar (microcline). These structures were inserted in a second calculation, including upper limits for peak broadening and a PO

correction model. For these minor phases the PO correction model was reduced automatically to isotropy during refinement. The second calculation diminished  $R_{wp}$  by 0.4%. Considering the low microcline content of about 1.1% and the rutile content of 0.9%, this could be taken as a quite certain indication for the presence of these phases in the sample.

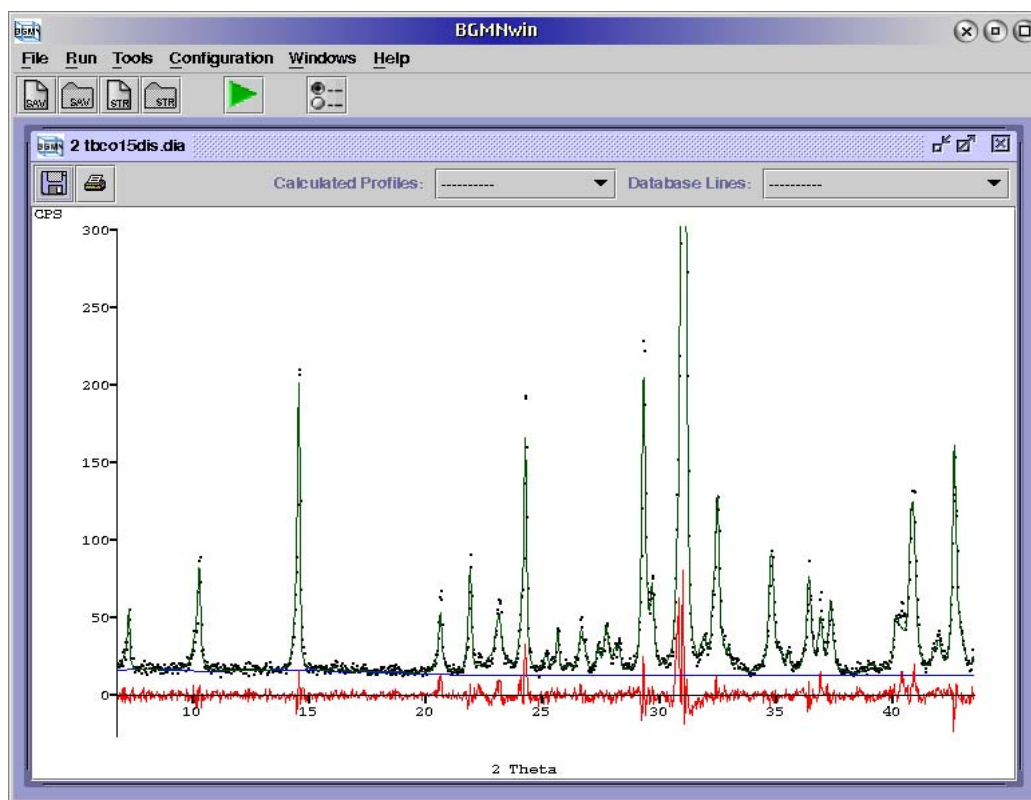


Figure 9.11: XRD 3000 TT measurement in reflection and difference curve (metashale Böhlischeiben — section); Muscovite, chlorite, albite, quartz, microcline, rutile ( $R_{wp}=9.46\%$ , CPU time approx. 3 min)

The probability of the potassium occupation in muscovite is fitted to 0.84(1), which is a very plausible value. This is another indicator for the correctness of the used model. The PO correction factor (see table 9.2) for the 002 reflections of muscovite and chlorite being especially sensitive to preferred orientation are 2.5 resp. 2.0. This means, that the refined counting rate of the associated reflection is about 2.5/2.0 times higher than the ideal one without preferred orientation.

To decrease preferred orientations and to check the correction model, the sample was additionally measured and analyzed in transmission geometry (see before). The results (table 9.2) correspond to the expectations. The direction of preferred orientation is reversed. Because of the low intensity, the calculated errors are higher than in reflection mode and the detection of microcline became nearly impossible.

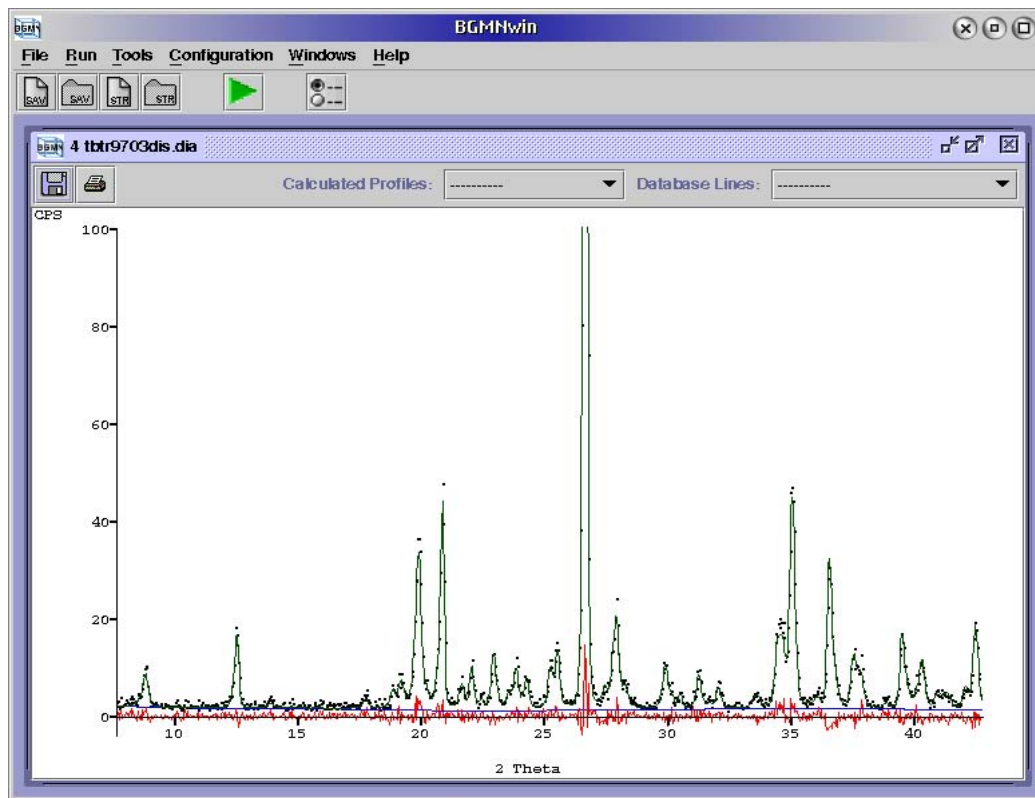


Figure 9.12: XRD 3000 TT measurement in transmission and difference curve (metashale Böhlischeiben — section); Muscovite, chlorite, albite, quartz, microcline, rutile ( $R_{wp}=15.38\%$ , CPU time approx. 5 min)

Table 9.2: Analysis results of metashale Böhlischeiben

Phase	STARKE [28]	BGMN reflection		BGMN transmission	
	wt-%	wt-%	texture/hkl	wt-%	texture/hkl
Quartz	30	31.4(3)		32.6(4)	
Muscovite	39	41.2(4)	2.10/002	40.1(6)	0.38/002
Chlorite	19	18.5(3)	2.42/002	17.2(6)	0.44/002
Albite	10	6.95(23)	0.88/020	7.8(3)	1.08/020
Microcline	—	1.1(2)		1.4(3)	
Rutile	—	0.86(7)		0.88(14)	
Accessories	2				

## 9.4 Rules for phase analysis

When using **BGMN** for phase analysis, the following rules proved to be very useful (see [3]):

The program is extremely robust, even to achieve convergence. For that reason all parameters can be determined in only one calculating step.

The cell parameters demand for initial values as precise as possible. Lower and upper boundaries should be defined especially for those phases with small contents.

Atomic positions are defined as constants and should not be refined at all.

There are no defaults necessary for weights, peak widths and the background parameters. These parameters start at zero.

Probabilities of occupation and temperature factors should only be refined for the main phases and heavy elements. Upper boundaries are often useful. Be especially careful when refinement of temperature factors and fitting of preferred orientation are carried out simultaneously. In this case the **TDS** parameters correlate strongly with the parameters of preferred orientation.

As a rule, peak broadening resulting from crystallite size and micro strain (**B1**, **k1** and **k2**) should always be refined. Upper boundaries should be defined for low phase contents and complex diagrams. In the case of high phase contents, anisotropic **B1** parameters should be applied. In special cases, you can also try to use anisotropic **k2**.

Complex models for preferred orientation (**SPHARx** with  $x \geq 4$ ) are useful for minerals with multiple cleavage. The single models **ANISO** or **SPHAR2** are to be preferred for phases that are strongly oriented but of low content. Obviously it is better to avoid preferred orientation by a suitable experimental procedure (preparation, transmission geometry).

In general the angle correction parameters **EPS1** for zero offset and **EPS2** for sample eccentricity should be released. If the real structure of the phases is hardly disturbed and thus causes problems when fitting large angles, only **EPS1** should be refined.

If using the internal standard, its lattice constants may be kept constant. However you should release **EPS1** and **EPS2**, in some cases also **EPS3**, for correction of the sample transparency.



# Chapter 10

## Size/strain analysis

### 10.1 Analysis of a virgilite sample

For a round robin test concerning different size/strain analysis methods, measurements of a glass ceramics sample were made. The glass ceramics material consisted of virgilite. We had to determine crystallite size and micro strain.

Measurement of the compact sample was made on an XRD 7 diffractometer (BRAGG-BRENTANO geometry) in an angular range of 15 to 140°, step width 0.02°, measuring time of 10 sec. We used a Cu – K $\alpha$  normal focus tube, a primary and a secondary collimator as well as a graphite secondary monochromator. The device function was computed by means of **GEOMET** and **MAKEGEQ** using the following control file:

*Rd7nf31.sav*

```
% theor. Verzerrungsfkt. f. Messung am RD7 Dr. Kleeberg
VERZERR=rd7stdkl.ger
GEQ=rd7stdkl.geq
R=175
D=0.12
HSlitR=175-113
HSlitW=0.92
VSlitR=175-72
VSlitH=10
FocusH=10
FocusW=0.1
DetH=15
MonR=175+50
DetW=0.31
SamplD=25
PColl=0.5/29
SColl=0.5/20
zweiTheta [1]=10
zweiTheta [2]=16
zweiTheta [3]=24
zweiTheta [4]=34
zweiTheta [5]=48
zweiTheta [6]=60
zweiTheta [7]=90
zweiTheta [8]=120
```

```

zweiTheta [9]=150
WMIN=10
WMAX=150
pi=2*acos(0)
WSTEP=3*sin(pi*zweiTheta/180)

```

In size/strain analysis the profile shape has to be modelled as precisely as possible. For that reason an average penetration depth of 0.12 mm was considered for the calculation with **MAKEGEQ**.

The structure of virgilite is described in the following file:

#### *Virgilit.str*

```

PHASE=virgilite SpacegroupNo=180 //
PARAM=A=0.5156_0.51^0.52 PARAM=C=0.54134_0.536^0.546 //
GAMMA=120 PARAM=GEWICHT=0_0 PARAM=X=1.5_0^3 //
RP=4 B1=ANISO PARAM=k1=0_0^1 PARAM=k2=0_0 //
GOAL=GrainSize(1,0,0) GOAL=GrainSize(0,0,1)
E=LI+1(X/3) Wyckoff=a PARAM=TDS=0_0
E=(AL+3(X/3),SI+4((3-X)/3)) Wyckoff=c TDS=ANISO
E=O-2 Wyckoff=j PARAM=x=0.2055_0.1^0.3 TDS=ANISO

```

The chemical formula of virgilite is  $\text{Li}_x\text{Al}_x\text{Si}_{3-x}\text{O}_6$ . Si is partially replaced by Al. Li is placed on another lattice position in the same way as Al. According to recommendations by the manufacturer, the mixing parameter  $x$  should be around 1.5. This value was set as the start value. The limits for fitting the mixture parameters correspond to those values physically just possible.

An anisotropic crystallite size was expected due to the hexagonal lattice. For that reason anisotropic crystallite size (B1=ANISO) and isotropic micro strain (PARAM=k2=0\_0) were chosen as the peak width model. We used the functions GOAL=GrainSize(h,k,l). Subsequently it was not necessary to manually calculate the crystallite size from the individual peak widths. The mentioned functions were applied to compute the crystallite size in the specified lattice direction. As another advantage, this notation also allows to calculate error values.

Anisotropic temperature factors are introduced for the heavy ions  $\text{O}^{2-}$ ,  $\text{Al}^{3+}$  and  $\text{Si}^{4+}$ . For the  $\text{Li}^{1+}$  ions of lower weight, isotropic temperature factors are implemented.

The measuring diagram shows a special feature: a wide peak to be assigned to the amorphous rate in the sample lies between  $29^\circ$  and  $34^\circ$ . To fit the curve without any disturbance, this region was excluded from fitting by the statement CUT [1] = 29 : 34. Now, the *rts.sav* control file does not show any further special effect:

#### *rts.sav*

```

VAL [1]=rts031
% Exclude the range between 29 and 34 deg
CUT [1]=29:34
VERZERR=rd7stdkl
STRUC [1]=virgilit
PARAM [1]=EPS1=0
PARAM [2]=EPS2=0
PROTOKOLL=Y
pi=2*acos(0)
POL=sqr(cos(26.6*pi/180))
LIST=rts.lst
OUTPUT=rts

```

Passing calculation (it runs about 1 min), the following file *rts.lst* is provided:

*rts.lst*

```
Rietveld refinement to file(s) rts031.val
BGMN version 4.0.15, 6000 measured points, 67 peaks, 37 parameters
Start: Sun Sep 21 20:04:12 2008; End: Sun Sep 21 20:04:21 2008
24 iteration steps

Rp=6.15% Rpb=12.55% R=2.71% Rwp=8.78% Rexp=7.40%
Durbin-Watson d=1.43
1-rho=1.32%

Global parameters and GOALS
*****
EPS1=-0.00030+-0.00093
EPS2=0.00029+-0.00089

Local parameters and GOALS for phase virgilite
*****
SpacegroupNo=180
HermannMauguin=P6_222
XrayDensity=2.502
Rphase=6.40%
UNIT=NM
A=0.51568+-0.00014
C=0.54314+-0.00015
GEWICHT=0.02430+-0.00017
X=1.411+-0.043
k1=0.74+-0.16
k2=0.00000539+-0.00000029
GrainSize(1,0,0)=34.67+-0.44
GrainSize(0,0,1)=61.8+-4.1
B1=ANISOLIN, MeanValue(B1)=0.00836896, sqrt3(det(B1))=0.00793716
Atomic positions for phase virgilite
-----
  3 a    0.0000  0.0000  0.0000    E=(LI+1(0.4703))
TDS=0.0587+-0.0068

  3 c    0.5000  0.0000  0.0000    E=(AL+3(0.4703),SI+4(0.5297))
TDS=ANISO, vibrational matrice for 1st atomic position:
(beta dimensionless, U in nm**2)
beta[i,j]=(0.02613, 0.00974, 0.00000 U[i,j]=(0.0002640, 0.0000984, 0.0000000
          0.00974, 0.01948, 0.00000          0.0000984, 0.0001968, 0.0000000
          0.00000, 0.00000, 0.01171)          0.0000000, 0.0000000, 0.0001749)

  6 j    0.2078  0.4157  0.5000    E=(O-2(1.0000))
x=0.20785+-0.00016
TDS=ANISO, vibrational matrice for 1st atomic position:
(beta dimensionless, U in nm**2)
beta[i,j]=(0.05015, 0.02168, 0.01413 U[i,j]=(0.0005067, 0.0002190, 0.0001737
          0.02168, 0.04336, 0.00000          0.0002190, 0.0004381, 0.0000000
          0.01413, 0.00000, 0.04671)          0.0001737, 0.0000000, 0.0006980)
```

This result is to be estimated as follows:

- Within the error limits the computed mixing parameter  $x = 1.56 \pm 0.037$  is equal to the default of 1.5
- The crystallite size ( $\|A$ :  $35.5 \pm 0.4$  nm,  $\|C$ :  $48 \pm 1.9$  nm) is anisotropic
- Obvious peak broadening as a result of micro strain ( $k_2 = 4.6 \pm 0.2 * 10^{-6}$ )
- In comparison with  $R_{exp}$  (7.5%), the  $R_{wp}$  value (9.2%) is satisfying.

Using the statement `k2=ANISO4`, you may also consider anisotropic micro strains. This test has been evidenced. Furthermore the micro strain values in A and C lattice direction can be calculated automatically by the following statement:

```
GOAL=sqrt(k2(1,0,0)) GOAL=sqrt(k2(0,0,1))
```

Additionally one must add the items

```
ANISOLIMIT=0 ANISO4LIMIT=0
```

for preventing anisotropies from switching off.

The changes can be taken from the following section of the result file:

*rts.lst*

```
Fit to file(s) rts031
EGMN version 2.5.3, 6000 measured points, 66 peaks, 51 parameters
Start: Tue Apr 27 19:59:03 1999; End: Tue Apr 27 20:00:14 1999

Rp=6.15% Rpb=12.37% R=3.59% Rwp=9.00% Rexp=7.54%
Durbin-Watson d=1.45
1-rho=1.72%

Global parameters and GOALS
*****
EPS1=-0.00075+-0.00090
EPS2=0.00068+-0.00086

Local parameters and GOALS for phase virgilitite
*****
XrayDensity=2.512
Rphase=6.88%
UNIT=NM
A=0.51576+-0.00014
C=0.54322+-0.00015
GEWICHT=0.02474+-0.00015
X=1.549+-0.036
k1=0.246+-0.066
GrainSize(1,0,0)=40.34+-0.87
GrainSize(0,0,1)=38.3+-1.4
sqrt(k2(1,0,0))=0.00324+-0.00010
sqrt(k2(0,0,1))=0.00084+-0.00030
k2=ANISO4, MeanValue(k2)=0.00000546550
B1=ANISOLIN, MeanValue(B1)=0.00953425, sqrt3(det(B1))=0.00952953
parameter and GOALS for atomic position 1
-----
E=(LI(0.5165))
TDS=0.0538+-0.0056
parameter and GOALS for atomic position 2
-----
E=(AL(0.5165),SI(0.4835))
TDS=ANISO, vibrational matrice for 1st atomic position:
(beta dimensionless, U in nm**2)
beta[i,j]=(0.02638, 0.00919, 0.00000 U[i,j]=(0.0002666, 0.0000929, 0.0000000
          0.00919, 0.01838, 0.00000          0.0000929, 0.0001857, 0.0000000
          0.00000, 0.00000, 0.01312)          0.0000000, 0.0000000, 0.0001961)
parameter and GOALS for atomic position 3
-----
E=(O(1.0000))
x=0.20715+-0.00017
TDS=ANISO, vibrational matrice for 1st atomic position:
(beta dimensionless, U in nm**2)
beta[i,j]=(0.03558, 0.01587, 0.01703 U[i,j]=(0.0003596, 0.0001603, 0.0002093
          0.01587, 0.03173, 0.00000          0.0001603, 0.0003207, 0.0000000
          0.01703, 0.00000, 0.04117)          0.0002093, 0.0000000, 0.0006154)
```

The result is amazing:

- The  $R_{wp}$  value is slightly diminished by 0.2%
- Within the error limits the crystallite size is almost isotropic ( $\|A: 40.3 \pm 0.9$  nm,  $\|C: 38.3 \pm 1.4$  nm)
- The micro strain ( $\sqrt{k_2}\|A: 3.24 \pm 0.10E-3$ ,  $\sqrt{k_2}\|C: 0.84 \pm 0.30E-3$ ) is strongly anisotropic.

From that we may conclude, that the anisotropy of the peak widths is mainly based on anisotropic micro strain effects. To get the differences between anisotropic broadening caused by crystallite size and micro strain much clearer, we should do more precise measurements.

Finally the fitting result is shown in a diagram:

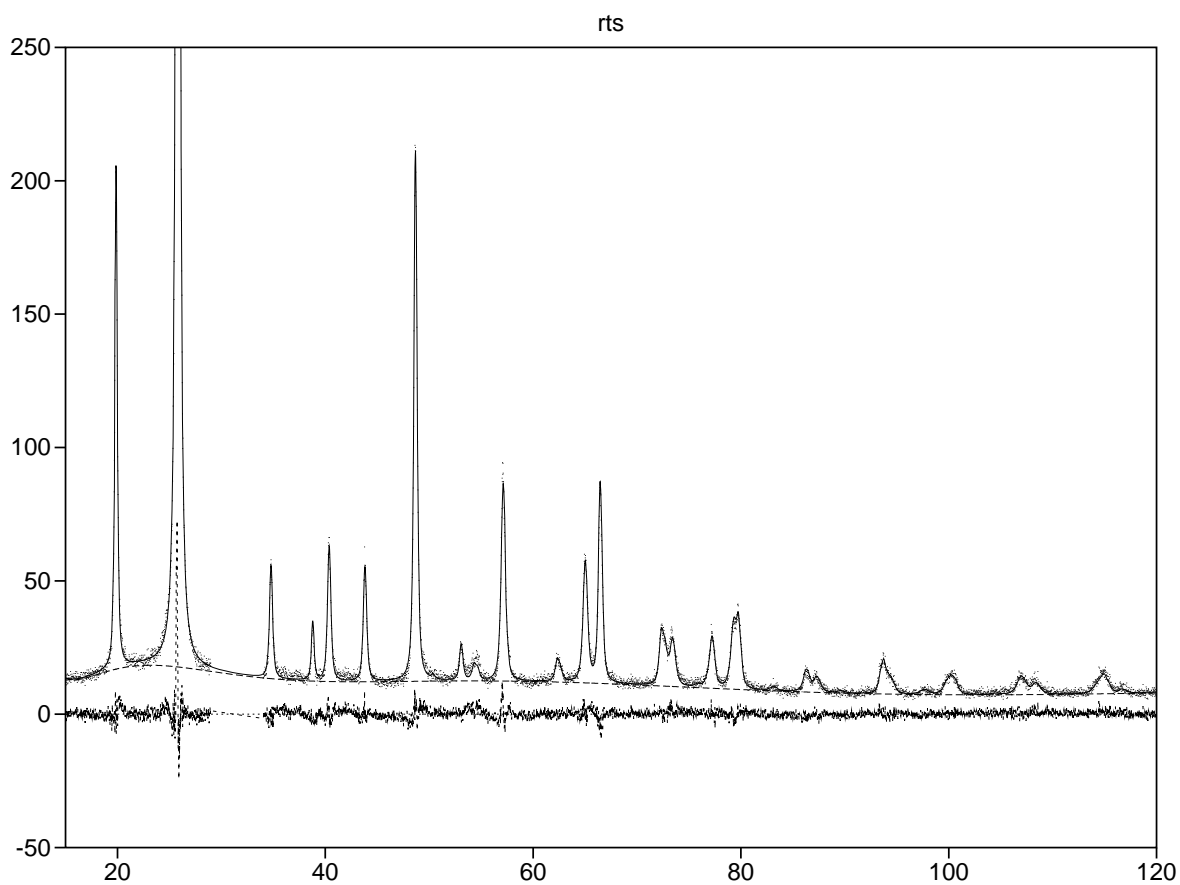


Figure 10.1: Measurement and difference curve of the virgilite sample (section)

Excluding the range between 29 to 34°, measurement and calculation coincide very well.

## 10.2 Tube tails correction

Using the raytraced geometric profiles in accurate size/strain analysis demands for some further correction. Tube tails mean: A small part of the X-rays emitted by the tube originates not inside the focus, but up to 1mm outside the focus. This means 1mm equatorial broadening towards both sides of the optical focus. If not corrected, these tube tails may totally disturb the profile shapes calculated by fundamental parameters, because the fundamental parameter model uses an ideal box shaped profile for the focus contribution. See figure 10.2.

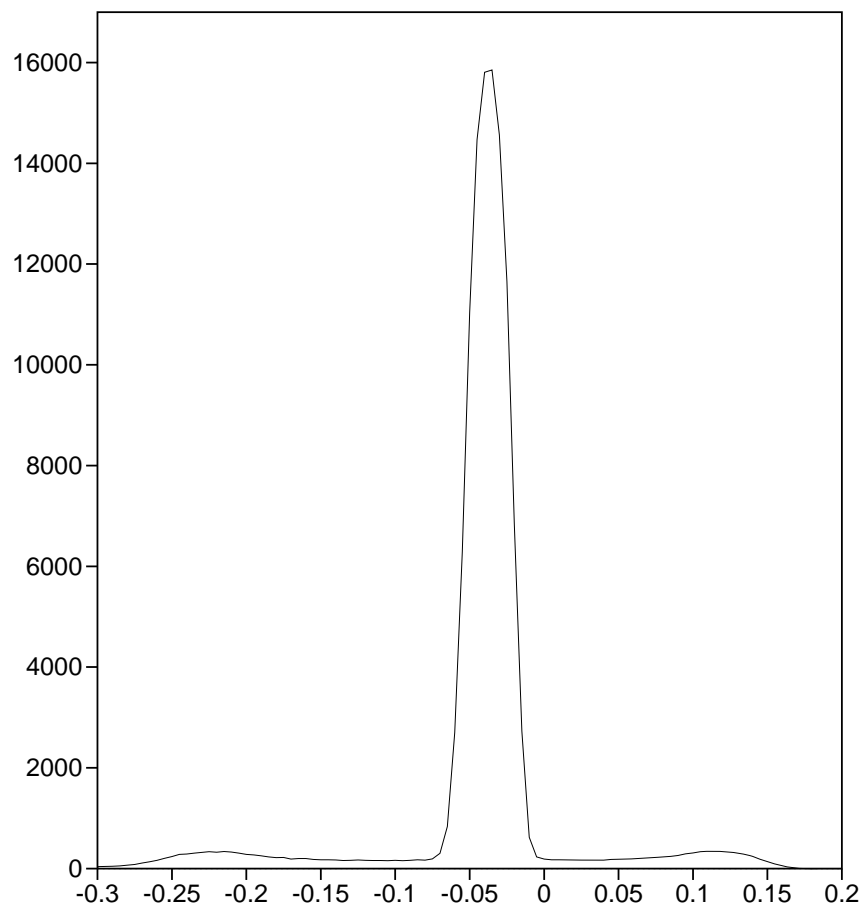


Figure 10.2: Tube tails as measured for an AEG fine focus tube. A lead foil containing a  $50\ \mu\text{m}$  hole placed on sample position was used for reproduction of the tube focus onto the receiving slit.

Different tube types show different tube tails:

- An AEG long fine focus Cu anode tube shows 15.8% of intensity emitted outside the focus. For sharp lines, fundamental parameters profile shape models as used by **BGMN** fail strongly.
- A glass tube from Seifert (made by Röhrenwerk Rudolstadt), also long fine focus, shows only 6.7 % tube tails. But this tube is an older one. Today the Röhrenwerk Rudolstadt produces only Siemens ceramic tubes. These tubes are not checked. Hopefully they show low tube tails, too.
- A Philips long fine focus Co anode tube (produced in 1993) shows 5.7% tube tails.

**BGMN** is able to correct for tube tails. To do so, use the switch

```
TubeTails=...
```

in the \*.sav file for the GEOMET run. Give a tube tails pattern as shown above. **Attention:** You must use a narrow grid (small stepwidth) of 0.005 deg or, if your diffractometer doesn't support such a small stepwidth, at least 0.01 deg. You may use the same file formats as for VAL [1] = . . . pattern data input. The paths of the X-rays emitted by the tube tails often are restricted by a secondary anti-scattering slit. Therefore use the entries

```
SSlitW=...
SSlitR=...
```

for description of equatorial dimension (width) and radius of a secondary anti-scattering slit. Equivalent to HSlitW, the entry SSlitW may depend from zweiTheta ( $2\Theta$ ). Thus a variable anti-scattering slit is supported.

For explanation we show the measurement of SRM 660 standard ( $\text{LaB}_6$ ) without (left) and with (right) tube tails correction for the AEG tube mentioned above (figure 10.3)

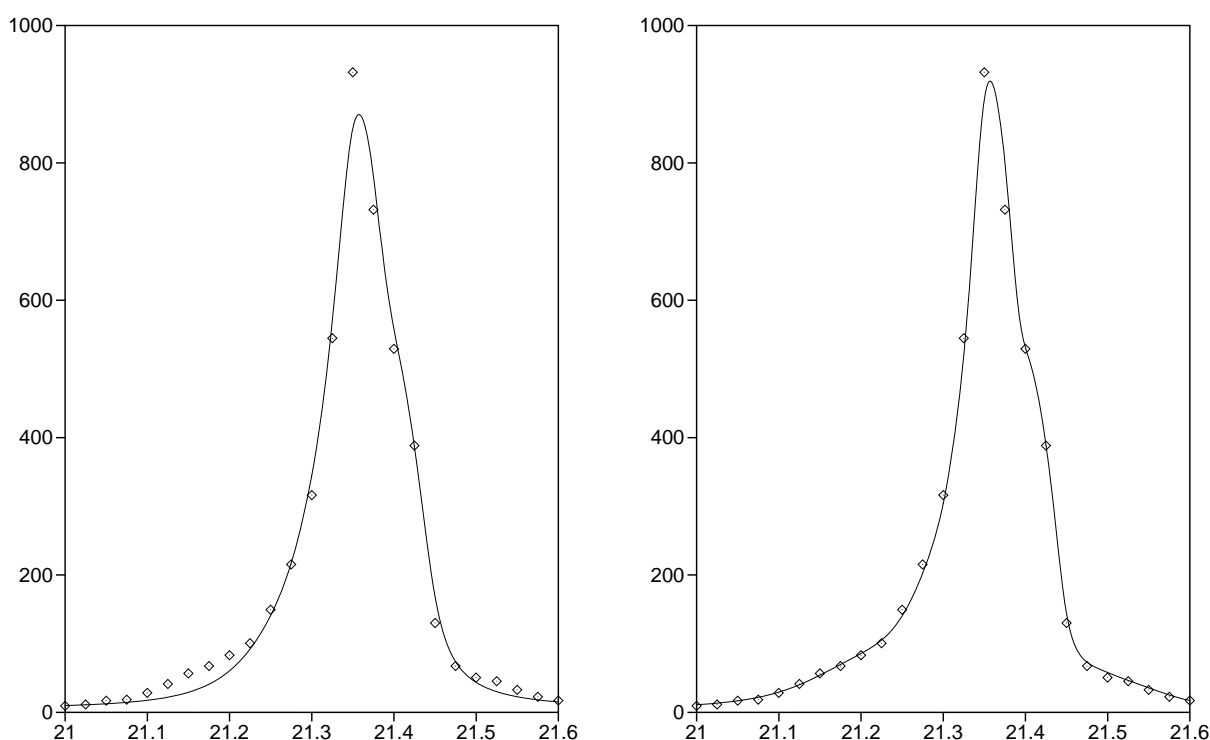


Figure 10.3:  $\text{LaB}_6$  (SRM660) as measured and refined without (left) and with (right) tube tails correction.

We measured the SRM 660 ( $\text{LaB}_6$ ) standard with three different tubes ( $\text{Cu-K}_\alpha$  and  $\text{Co-K}_\alpha$  radiation) using three different slit set-ups on two different diffractometers. For demonstration of the remaining errors we give results using two different  $\text{Cu-K}_\alpha$  spectra as cited from [1] resp. [14]. Table 10.1 shows the results.

Table 10.1: Comparison of size/strain values of SRM 660 as gained using three different tube types, two different Cu-K $_{\alpha}$  data sets and deconvoluted without resp. with tube tails correction

$\Lambda$	Cu K $_{\alpha}$ [1]			Cu K $_{\alpha}$ [14]			Co K $_{\alpha}$ [14]
	AEG	Rudolstadt	XRD3000TT	AEG	Rudolstadt	URD6	
Diffractometer	XRD3000TT						URD6
Tube type	AEG	Rudolstadt	AEG	Rudolstadt	Philips		
equatorial divergence slit	fixed	variable	fixed	variable	fixed	fixed	
	without tube tails correction						
size/nm	324(4)	496(6)	510(8)	308(4)	468(6)	474(5)	610(10)
micro strain $\times 10^6$	0	0	0	0	0	0	0
	with tube tails correction						
size/nm	1109(51)	995(38)	1056(37)	884(31)	793(23)	824(21)	944(34)
micro strain $\times 10^6$	156(7)	152(7)	157(5)	115(8)	105(8)	113(6)	96(10)
[10]	size: 1.3(7) $\mu\text{m}$						

This table greatly illustrates the success of the tube tails correction. At our opinion, tube tails are the strongest fault of classical fundamental parameter profile description. Obviously the inaccuracies of different Cu- $K_{\alpha}$  spectra overdominate the standard uncertainties of the fundamental parameter approach. On the other hand our measurements clearly show the imperfectness of line profile standards. The total error of our approach, including  $K_{\alpha}$  inaccuracy, is much less compared to line standard imperfectness.

Obviously the  $\Lambda$  data given in [1] are somewhat too broad compared to [14]. Data given in [14] give comparable results for different anodes. Therefore we recommend using the data given in [14], which are available for Cr-, Fe-, Co- and Cu-Anodes.

Using tube tails correction, one may think about using **BGMN** for line profile analysis (size/strain analysis).

### 10.3 Learnt device functions

The raytraced fundamental parameters method may be used for modelling conventional X-ray diffractometers. However, the ray paths of modern X-ray optics, as well as PSDs resolution functions, may not be described well using these techniques. For such devices, extraction of the geometric part **G** of the device from reference lines (learnt peak profile approach) is required. This learned geometric part may be used instead of a raytraced **G**.

The NIST peak position and peak profile reference material SRM 660a was certified for homogeneity and lattice parameter [11]. Efforts were undertaken to achieve a minimum line broadening due to size/strain and optimum grain statistics. A domain size of 2.0  $\mu\text{m}$  and a microstrain below detection limit were given as non-certified values. Electron-microscopic crystallite sizes were observed from 2 to 5  $\mu\text{m}$  [11].

Due to the applied sieving procedure, the aggregated grains were restricted in size to 15  $\mu\text{m}$ . This was confirmed by LASER diffraction. Therefore (and due to the excellent purity), the reference material SRM 660a is suitable for profile extraction. For doing so, first set up an parameter file *srm660a.par* as follows:

```
PEAKZAHL=14 LAMBDA=CU POL=0.79951
4 3.589195E+001 2.4051308 0.0005705 0.000000036 F=37.266 H=6 1 0 0
4 6.007939E+001 3.4013685 0.0005316 0.000000071 F=48.772 H=12 1 1 0
4 2.713306E+001 4.1658087 0.0004443 0.000000107 F=48.923 H=8 1 1 1
4 3.396980E+001 5.3780359 0.0003047 0.000000178 F=40.833 H=24 2 1 0
4 1.893594E+001 5.8913431 0.0002399 0.000000214 F=33.389 H=24 2 1 1
4 7.517191E+000 6.8027371 0.0002199 0.000000285 F=34.504 H=12 2 2 0
4 2.000985E+001 7.2153923 0.0002388 0.000000321 F=26.380 H=6 3 0 0 F=42.092 H=24 2 2 1
4 1.038069E+001 7.9769163 0.0001902 0.000000392 F=33.422 H=24 3 1 1
4 6.856976E+000 8.6718223 0.0001643 0.000000463 F=29.654 H=24 3 2 0
4 1.410475E+001 8.9991752 0.0001658 0.000000499 F=31.165 H=48 3 2 1
4 6.335432E+000 9.9166081 0.0001527 0.000000606 F=27.816 H=24 4 1 0 F=32.507 H=24 3 2 2
4 3.618046E+000 10.4837219 0.0001328 0.000000677 F=26.042 H=24 3 3 1
4 9.094819E+000 11.0216937 0.0001427 0.000000749 F=30.611 H=48 4 2 1
4 4.216217E+000 11.2810632 0.0001393 0.000000784 F=30.175 H=24 3 3 2
```

Please take special attention to the lines at  $\frac{1}{d}$  of 7.2153923 and 9.9166081. Both these lines appear twice in the \*-output of the BGMN run, they must be unified each pair to one line. Otherwise, VERZERR will run into trouble.

Simply set up a control file like:

```
STANDARDPAR=srm660a.par
VAL[1]=val\lp660afx150201.val
VAL[2]=val\lp660afx150202.val
VAL[3]=val\lp660afx150203.val
```

```

VAL[4]=val\lp660afx150204.val
VAL[5]=val\lp660afx150205.val
VAL[6]=val\lp660afx150206.val
VAL[7]=val\lp660afx150207.val
VAL[8]=val\lp660afx150208.val
VAL[9]=val\lp660afx150209.val
VAL[10]=val\lp660afx150210.val
VERZERR=lab6
pi=2*acos(0)
POL=sqr(cos(26.6*pi/180))
WMIN=21.4
WMAX=120.7
WSTEP=3*sin(pi*zweiTheta/180)

```

The **STANDARDPAR** entry refers to the above file. For learning profiles on a conventional lab diffractometer, one needs for a very accurate, multiple days measurement. For hiding the results from long-term variations of the atmospheric etc. conditions, it is a good idea for measuring several scans for one and the same setup. In the above example, the whole scan was measured 10 times. The data will be accumulated by the **VERZERR** program. Another good idea is producing multi scan data files, about seconds per step for the strong reflections and about minutes per step for the weakest reflection. All that is of no need in case of more intensity (position sensitive detectors and/or synchrotron radiation).

For the calculation, simply select Run→**Verzerr**, browse to the above file and hit OK. You will see some lines of output. As a result, a file *lab6.ger* (similar to that produced by **GEOMET**) is created. Similar to raytraced profiles, select Run→**MakeGEQ** and produce the interpolated profiles for usage in **BGMN**.

## 10.4 Rules for profile analysis (size/strain analysis)

Our knowledge about size/strain analysis is still under heavy improvement. Nevertheless we want to give some general hints on this theme:

- Real structure analysis/real structure description is a much wider area than just size/strain analysis. And, **BGMN** may answer much more real structure questions than just size/strain measurements. For example have a look at [3].
- The first question is that about quality of real structure. Therefore you must check several different real structure models, as we have done in the virgillite example. Giving an “exact” value with low errors, but using a wrong model, is almost nonsense.
- Have special care in case of nearly perfect crystallites. In such cases you *must* use **TubeTails** correction and a correct  $K_\alpha$  description as given e.g. in [14].

Table 10.2: Comparison of raytraced fundamental parameters vs. learnt profiles

	Raytraced profiles (fundamental parameters)	Learnt profiles
Advantages	<ul style="list-style-type: none"> <li>• More accurate</li> <li>• None or only a short time measurement needed</li> <li>• Wide angular range (including very low) available</li> </ul>	May handle many geometric goniometer set-ups
Disadvantages	<p>Restricted to the three common geometric conditions</p> <ul style="list-style-type: none"> <li>• Symmetric reflection (Bragg-Brentano)</li> <li>• Symmetric transmission (planar sample)</li> <li>• Capillary</li> </ul>	<ul style="list-style-type: none"> <li>• Less accurate</li> <li>• Needs for a multiple day calibration measurement</li> <li>• Restricted to the angular range of the reference lines</li> </ul>



# Appendix A

## Short reference

This chapter concerns the functions of the utilities including input parameters. The following explanations are given as concluding remarks summarising and adding the content of the chapters before. Possible text redundancies are written for your better understanding.

### A.1 GEOMET

In **GEOMET**, the geometric profile shapes are modelled from theoretic data (slit positions, sample size and collimator widths). For description of the device geometry, the program demands for a number of necessary inputs to the control file *\*.sav*. Denomination of divergence slits is based on a horizontal configuration of the diffractometer measuring circle. Lengths and/or radii are input in millimeters, angles in ° (with the exception of Soller slits divergence angles: their units are radians). The necessary and optional parameters are listed in the control file below:

**AirScat** may be set for defining an air scatter blocker (a metal plate perpendicular to the sample surface, the goniometer axis within the plane of the plate). **AirScat** should be set to the height of the blocker above sample surface. Valid only for **GEOMETRY=REFLEXION**.

**DetW, DetH**

Axial and equatorial dimensions of the detection slit; input necessary

**DetArrayW**

total equatorial dimension of a 1D array of detectors such as Vantec-1, Lynxeye (Bruker) or X'Celerator (Panalytical). In such cases, **DetW** should be assigned the equatorial dimension of a single detection unit and **DetH** the axial dimension of the detection units.

**EPSG** Target precision of fitting;

Default: 0.007, that corresponds to 0.7%

**FocusH, FocusW**

Axial and equatorial dimension of the X-ray tube's focus; input necessary

**FocusW** means the optical focus width. Usually, the thermal focus dimensions are printed on the X-ray tube. The optical focus width is reduced due to the take-off angle (usually 6°) between X-ray beam and anode surface. Usually the optical focus width (equatorial dimension) is assumed as the 10<sup>th</sup> part of the thermal one.

**FocusS, FocusA**

Corrections for the focus, axial shift in mm and rotation around the radial axis through the centre of the focus in °; optional

**GEOMETRY**

Default REFLEXION;

If TRANSMISSION is input, the sample is computed in a position turned by 90 degrees.

In the case of CAPILLARY input, a capillary sample is taken for calculation.

**GSUM** Logical switch.

Default: N.

If it is true (Y) (GSUM=Y | Y | J | j), an intensity correction of the form GSUM= . . . is put out for each calculated profile. The intensity correction value is written to the file \*.ger in cases of, e.g., variable equatorial divergence slit or if the margins of the sample are irradiated.

**HSlitR, HSlitW**

Radius (ex centre of the sample) and width of the equatorial divergence slit; necessary parameter specification. The equatorial slit width may depend on  $i$  (no. of the calculated profile in \*.ger) or `zweiTheta` ( $2\Theta$ ) thus enabling the description of a variable vertical divergence slit (with GSUM=Y).

**MonR** Distance between secondary monochromator and the goniometer axis, where the secondary monochromator limits the beam path. Take `DetH` as axial dimension of the monochromator crystal;

Default: R.

**MonH** Axial dimension of a secondary monochromator.

**PColl** Divergence angle of the primary collimator, e.g. 0.5/25, where 0.5 is the laminar distance and 25 is the collimator length;

Default: no collimator, unit: radian.

**R** Radius of the goniometer circle; necessary parameter specification

**SamplD**

Diameter of a round sample; standard: infinite (greater than the illuminated area). Assuming that the input value is too low, the sample will be irradiated. In this case, you should use GSUM=Y. In the case GEOMETRY=CAPILLARY, `SamplD` or `SamplH` stand for the axial capillary dimension.

**SamplW, SamplH**

Length and axial dimension of a rectangular, non-spinning sample;

Default: infinite.

**SColl** Divergence angle of the secondary collimator, see `PColl`;

Default: no collimator, unit: radian.

**SSlitR, SSlitW**

Radius (ex centre of the sample) and equatorial dimension (width) of a secondary anti-scattering slit. The equatorial slit width may depend on  $i$  (no. of the calculated profile in \*.ger) or `zweiTheta` ( $2\Theta$ ) thus enabling the description of a variable anti-scattering divergence slit (with GSUM=Y). Should be used, when using `TubeTails` correction. See section 10.2).

**TSlitH** Axial dimension of a divergence slit limiting the focus immediately in front of the tube window; optional. If `TSlitH` is specified, its radius must also be specified:

**TSlitR** Specified radius.

**TubeTails**

File containing the measurement of tube tails, see section 10.2.

**VERZERR**

Name of the *\*.ger* output file

**VSlitR, VSlitH**

Radius (ex centre of the sample) and axial dimension of the axial divergence slit. You must specify either axial divergence slit or primary collimator.

**ZweiTheta[1], zweiTheta[2]. . .**

for  $i = 1 \dots$  Angular positions, at which the device function is calculated by **GEOMET**; necessary parameter specification

When using **GSUM**, note, that this value is interpolated according to the step width **WSTEP**. In the subsequent programs the geometry function is only subjected to linear interpolation. For that reason, use angle step values that are sufficiently narrow.

## A.2 VERZERR

In **VERZERR**, the geometric profile shapes are modelled from accumulated reference line measurements. For this purpose, the program demands for a number of necessary inputs to the control file *\*.sav*. The necessary and optional parameters are listed in the control file below:

**VERZERR**

Name of the *\*.ger* result file.

**GSUM** optional parameter, see section above.

**STANDARDPAR**

Name of the *\*.par* file containing the residual line widths of the reference sample.

**VAL[i]** Reference peak measurements to be accumulated.

**LAMBDA**

wavelength in case pattern data do not contain that.

**SYNCHROTRON**

wavelength of a synchrotron source, changes some of the internal behaviour of **VERZERR**.

**NEUTRONS**

wavelength of neutron CW data.

## A.3 MAKEGEQ

As a next step the device function is interpolated. This is necessary, since **GEOMET** provides the device function only for discrete angles. This interpolation is very time consuming. It should be carried out before **BGMN** runs by means of **MAKEGEQ**. Corrections of the profile shape to consider sample features (penetration depth of the radiation and finite sample thickness) are already carried out in this interpolation.

VERZERR is the only parameter necessary in the \*.sav control file. To save storage capacity, the interpolation result is output in binary form into the \*.geq file. In the control file, the following additional information is possible:

- D        Reciprocal linear attenuation coefficient of the sample material,  
          unit: mm
- EPSG    Default 0.007, demanded precision of interpolation
- GEQ     This parameter is used to generate the \*.geq-file for the output. For default the name of the  
          VERZERR file is used.
- R        Radius of the goniometer
- T        Sample thickness or diameter of the capillary in the case of  
          GEOMETRY=CAPILLARY
- WMIN    Lower angle limit of interpolation;  
          Default: 20°
- WMAX    Upper angle limit of interpolation;  
          Default: 140°
- WSTEP   Step width for interpolation;  
          Default: 0.01°
- When setting this parameter, it is quite possible to use even 0.1° or 1°, if the calculation of  
          **MAKEGEQ** will take too much time. This value may be a function of `zweiTheta`. For  
          example, `2*sin(zweiTheta*pi/180)` could be a reasonable function.

## A.4 BGMN

The Rietveld refinement is executed by the program **BGMN** standing for the name of the overall system itself.

The kind of evaluation is determined by the \*.sav control file. This file summarizes information on the device function, measurement data and the sample structures to be refined. Additionally the program uses global variables and parameters being valid for all phases.

We introduced the assignment statement `PARAM= . . .` to declare variables as parameters. You may enter initial values that are necessary in most cases. These initial values may also be represented by variables. But you may also enter static lower and upper limits of the following form:

```
PARAM=variable=initialvalue_lowerlimit^upperlimit
```

Note, that the last three elements can be written in any order.

### Control file

The parameters necessary to control the calculation are described in the following list:

ANISOLIMIT  
          see LIMIT2

**ANISO4LIMIT**

see LIMIT2

**CUT**[*i*] Common format: CUT [*i*] =wmin:wmax

It represents the corresponding angular sector (in  $2\Theta$ ) which is to be eliminated from fitting.  
*i*=1... (continuously without any gap)

**DIAGRAMM**

Enables the output of a file after each iteration step; this file consists of *m* lines with *m* = number of measuring points. Each line contains  $2\Theta$ , measured intensity and fitted intensity. This information is foreseen for further processing by other programs, e.g. for presentation.

**EPS1...EPS4**

These parameters describe angle corrections of the diagram: **EPS1** is a constant to correct malpositions of the tube or the detector. **EPS2** is a factor proportional to  $\cos(\Theta)$  ( $\sin(\Theta)$  during transmission) to correct eccentricity of the sample. **EPS3** is proportional to  $\sin(2\Theta)$  to correct penetration depth. **EPS4**, is a factor of the  $\cot(2\Theta)$  type foreseen to correct divergence. Interpretation of parameters: **EPS1**: zero point, **EPS2**: sample displacement, **EPS3**: sample transparency, **EPS4**: divergence shifting.

The use of **ESP4** is recommended only for calculation without device function. Please do not enter **EPS3** in cases if the device function is corrected according to penetration depth. Furthermore you should reasonably specify **EPS3** only in the case of GEOMETRY=REFLEXION.

**FCFOUT**[*i*]

Output of observed and calculated F values plus phase angle in **ShelX** format. I have chosen the No. 5 format from the **ShelX 97** manual. Cited from those manual:

Write h, k, l, Fo, Fc, and f (phase angle in degree)... This is indented for input to some standard macromolecular FFT programs (such as W. Furey's PHASES program), thereby providing a possible route to a graphical display of the electron density.

All Fs and the phase angles are corrected for dispersion. This means: They really are Fourier coefficients of electron density maps. See (newest) ShelX manual.

This output is disabled if the *i*-th phase uses the "user calculated structure amplitudes" feature by defining **FMult** in its \*.str file.

**GOAL**[*i*] Global goal, e.g. for experimental design, common format:

GOAL=term [=value] [+error]

=value is inserted after calculation and ignored during input.

+error remains unchanged to be taken for output. It demands for subsequent experimental design.

**ITMAX** Maximal number of iteration steps, valid for all iteration runs; reasonable default values are used by the program automatically; change in extreme circumstances only.

**LAMBDA**

Some pattern data formats do not contain information concerning the used wavelengths (GSAS or DAT) or are restricted to common X-ray anode materials. In such cases, one may introduce such an entry for declaring the used wavelength. May point to common

anode materials (e.g. LAMBDA=CU) or may set to a wavelength in Nanometers. In the latter case, a sharp line with zero width (delta distribution) will be assumed.

#### LIMIT2, LIMIT4, LIMIT6, LIMIT8, LIMIT10, ANISOLIMIT and ANISO4LIMIT

These parameters are useful when using the SPHARx texture descriptions and/or any other anisotropies ANISO during phase analysis. As explained on page 5.4, BGMN uses an automatic, Laue Group dependent switch-off of SPHARx/ANISOx. But there may be need for a phase specific switch-off, this is done by the LIMITx values.

After initial computation, if the isotropic weight of a phase and/or the isotropic variable value drops down below the LIMITfold of its error, then it is simplified from SPHARx and all more complex models. Below LIMIT2, simplification is carried out to an internal model SPHAR0 corresponding to an isotropic scale factor. Below LIMIT4, it is simplified to SPHAR2, below LIMIT6 to SPHAR4, below LIMIT8 to SPHAR6 and below LIMIT10 to SPHAR8. Below ANISO4LIMIT, ANISO4 is simplified to ANISOSQR and below ANISOLIMIT to an isotropic substitute. Assigning a value of 0 will cause switch-off only if the isotropic value from the first iteration becomes zero.

**LIST** Result file with information on the refinement result. In cases of missing file name (\*.lst), the output will be in the screen.

#### NEUTRONS

should be used in cases of Neutron CW pattern data. Thus, bgmn uses bounded neutron scattering lengths instead of atomic form factors. Simply assign the neutron's wavelength.

#### NTHREADS

Number of threads as used by BGMN in parallel. Some parts of BGMN may calculate in parallel on multi core processors. Depending on your problem, the computation time may shrink down. You must tell BGMN how many threads it may use by

```
NTHREADS= . . .
```

You should specify the number of cores in your PC or less.

#### ONLYISO

If this parameter is different from "N" or "n", a quick run is started. In this run only isotropic iteration is performed no matter if there are anisotropies or preferred orientations that might be specified. Note that anisotropies are calculated but not refined. That means, they correspond to isotropy.

If a numerical value is specified for ONLYISO, then it is used as a relative termination limit of isotropic iteration (default  $10^{-4}$ ). The parameter is first of all used for testing complex refinement models.

#### OUTPUT

Result file with all peak and background parameters (\*.par). This is a text file with parametric representation of internal format.

#### PARAM[i]

Global parameter definition of the following form:

```
PARAM[i]=name
PARAM[i]=name=initial value
PARAM[i]=name_lower limit
PARAM[i]=name^upper limit
```

The last three attachments can be combined in any sequence, `initialvalue` must be available. The parameter `name` is refined by calculation according to the specified limits.

**POL** Polarisation factor of the secondary monochromator. Not for parameterisation since the graphite monochromator mostly used is an ideal mosaic crystal. Consequently it has the polarisation factor of an ideal polycrystal that diffracts kinetically. Deviations in other programs obviously result from insufficient profile shape. Its polarisation factor corrects profile shape errors as a function of  $2\theta$ .

$\cos^2(2\theta_{\text{monochromator}})$  should be specified for **POL**. Specify `POL=sqr(cos(26.6*pi/180))` with `pi=2*acos(0)` for graphite and copper radiation.

Default: 1 (without secondary monochromator).

### PROTOKOLL

Controls the protocol of the optimization algorithm. Screen protocol is enabled by Y or J.

Standard: N

### PDBOUT[i] and RESOUT[i]

Result file of the individual phases in the format of the Brookhaven protein database (\*.pdb) or of **ShelX** (\*.res). The pdb format is foreseen for use by **RasMol** (Sayle 1996). The atomic identifiers are determined in accordance with the following ranking sequence:

- AtomName, a variable specified to atomic positions
- Identifier in molecular crystals, used in X(...), Y(...), Z(...)
- Corresponding entered atomic type in E= . . .

If necessary, these identifiers are given a number and a letter to mark them unambiguously.

**PLAN** List of measuring points as a result of experimental design.

### RESOUT[i]

see PDBOUT[i]

**RP** Standard peak model, if not specified in the structure file; range of values: {2 | 3 | 4}.

**RU** Number of background parameters. In following the Lagrangian polynomial as used for the background is of degree RU-1. If not specified – chosen automatically depending on the extension of the diagram (proportional to  $\ln \frac{W_{MAX}}{W_{MIN}}$ ).

In most cases, it is not necessary to enter **RU**.

### STRUC[i]

\*.str structure files of the individual phases *i*.

### STRUCOUT[i]

Result files of the individual phases in the structure file format \*.str. The results are only entered as new start values. The structure of the input file (line feed, sequence of explanations) will be widely taken over. Thus you can continue a calculation using the results of the last calculation. This result file does not replace the result file \*.lst since it does not contain any information on the anisotropic parameter values.

**SimpleSTRUCOUT[i]**

Simple structure output. May be used as new input structure, as above. In contrary to above, these structure files will contain no atomic positions data. Instead of, a full list of structure amplitudes depending from  $h\ k\ l$  (and  $iref$  for compatibility) will be provided.

In case you want to convert a LeBail structure refinement into a Simple Structure output, you must provide non-zero values of **GEWICHT** and **density**. They should contain values as expected. E.g. while refining an 50:50 mixture of an internal standard and an unknown phase, you should place an assignment of the **GEWICHT** value as refined for the internal standard to **GEWICHT** inside the unknown phase (LeBail) structure.

**SYNCHROTRON**

should be used in case of synchrotron data, please assign the synchrotron wavelength in Nanometers. Using **SYNCHROTRON** instead of **LAMBDA** changes some of the internal behaviour of **BGMN**, for example Synchrotrons do not generate tube tails.

**UNIT** Output format for peak positions and peak widths by means of **OUTPUT**. It can be used for output in Å units via **UNIT=ANGSTROEM**.

Default: **UNIT=NM**

**UNT** Background diagram with measured values in any of the possible **VAL** formats. It may be used to correct an amorphous background or a phase of unknown structure, but available pattern data. If this file is specified, a background polynomial is taken from only **RU-1** parameters. The last background parameter refers to the rate of this **UNT** file. In case of an amorphous background this file may have a greater increment and measurements for this file could be carried out at wider divergence than the diagram to be analyzed. As a recommendation, considering each measuring point, this file should be more precise than the measurement itself.

**UNTC** Background diagram with measured values in any of the possible **VAL** formats. It may be used to correct an amorphous background or a phase of unknown structure, but available pattern data. In contrary to **UNT**, this pattern will be added unscaled, no background parameter will be used for scaling.

**DDM** If set to **DDM=Y**, the **DDM** method as described in

L. A. Solovyov  
Full-profile refinement by derivative difference minimization  
J. Appl. Cryst. 37 (2004), pp. 743-749  
[http://www.geocities.com/l\\_solovyov/ddm.html](http://www.geocities.com/l_solovyov/ddm.html)

will be used. As inherent to this Method, the number of background parameters **RU** is set to zero. The **DDM** method is indented to cases with complicated background.

**VAL[i]** specifies the file(s) containing the raw pattern data. **BGMN** assumes patterns in free **XY[E]** format, in general: Leading comments starting with **#** will be ignored, all following lines may contain

1. angle  $2\Theta$
2. intensity (cps)
3. (optionally) esd.

If esd is omitted, it will be calculated as the square root of the intensity.

Special file formats are chosen depending from the filename suffix:

- \*.val files will be assumed to be in the APX file format of the firm SEIFERT FPM.
- \*.rd files will be assumed to be in an old PHILLIPS format. In this case, the variable STEPWIDTH may be used to assign a non-raster stepwidth ( $STEPWIDTH \neq n * 0.005$ ) of the pattern data (e.g. PHILLIPS format in conjunction with a scanning PSD from SIEMENS).
- \*.raw files will be assumed to be in an old SIEMENS format.
- \*.gsa files will be assumed in GSAS format, restricted to equidistant angular steps (both the variants STD and ESD of the GSAS data format).

Assignments must start with VAL [1] = . . . , the next file must be assigned with VAL [2] = . . . and so on. Data are not allowed to be smoothed,  $K_{\alpha}$  stripped, background corrected or corrected in any other way. The files must contain the original measured data.

There will be no iteration if no pattern data are specified or if 0 data points remain (WMIN, WMAX, CUT[i]), since all measuring points have been deleted. In these cases theoretical results are calculated instead of iteration. The parameters are kept constant at their initial values. No errors are computed. GOALS can be set and evaluated.

#### WMIN, WMAX

lower and/or upper angle limit in  $2\Theta$  of the diagram to be processed.

Any other variables can be defined — maybe as parameters. Subsequently these variables have global effect for all structures.

#### Special case: Unknown device function

One can work without device function, if analyzing measurement data have been obtained by an unknown device or if no device function has been determined yet. However the precision enabled by the peak model is lost at large extent.

VERZERR=term is specified in the control file for BGMN. THETA is permitted as a part of the term. This term becomes a squared Lorentzian width, specifying the peak width in  $\Theta$  (unit radian). A reasonable estimation disregarding all other influences could be as follows:

$$\text{receivingslitwidth} / (2 * \text{goniometerradius} * \text{sqrt}(12))$$

In the control file, PARAM [i] = k3 = 0\_0 and PARAM [j] = EPS4 = 0 should be specified together for all phases. k3 describes line broadening as a result of divergence and EPS4 line shift resulting from divergence. Please do not introduce parameters k3 and EPS4 if a device function is given!

## Structure file

### Anisotropic parameters

ParameterName=ANISOSQR and/or ParameterName=ANISOLIN automatically generates each 6 parameters for description of a positively definite symmetrical matrix. Thus the value of the parameter is calculated as a quadratic form via  $hkl$ . As guaranteed by the program, the corresponding ellipsoid always fulfils the demands of symmetry of the crystal (e.g. in the case of B1, k2 and GEWICHT see below) and/or the special point position (TDS). For this purpose the general position

must be known. In cases without spacegroup the general position must be specified explicitly (see below).

A quadratic form is introduced by ANISOSQR, the square root of a quadratic form by ANISOLIN. The extension

$$x=\text{ANISOLIN}^{\text{upperlimit}} \text{ and/or } x=\text{ANISOSQR}^{\text{upperlimit}}$$

is implemented for both types. `upperlimit` is only valid for the initial iteration (isotropic approximation). It is foreseen to overcome maybe false secondary minima.

### Spacegroup, lattice constants and further phase-specific parameters

All phase-specific information is contained in the 1st line. Often the volume of one line is exceeded. If the line limit is extended, terminate the partial line via continuation statement “//” and continue with the next partial line. All characters behind “//” will be ignored.

**Phase identification** Phase identifiers are entered via `PHASE= . . .`. The name assigned this way is used for the identifier in the output list and output table in the phase column. If `PHASE` is not specified, the name of the *\*.str* file is used as identifier of the output.

**Spacegroup and lattice** One can work with spacegroups and the corresponding Wyckoff notations. Select a spacegroup by entering `SpacegroupNo=` and/or `HermannMauguin=` into the 1st line of the *\*.str* file. `BASIS`, `Lattice`, `CellChoice`, `OriginChoice` and/or `UniqueAxis` can be specified additionally. All parameters result in the selection of a spacegroup from the *spacegrp.dat* file.

All entries listed must also be specified explicitly in the file *spacegrp.dat*. If `BASIS` e.g. is not specified and is implicitly abstracted from `HermannMauguin`, then this parameter cannot be used for the selection.

Entries of the lattice constants `A`, `B`, `C`, `ALPHA`, `BETA`, `GAMMA` are required in a usual manner according to the lattice, e.g. only `A` and `C` for hexagonal or tetragonal spacegroups.

If there is no spacegroup specified, you may also specify the lattice by

$$\text{Lattice}=\{\text{Triclinic}|\text{Monoclinic}|\text{Orthorhombic}|\text{Tetragonal}|\text{Trigonal}|\text{Hexagonal}|\text{Rhombohedral}|\text{Cubic}\}$$

as well as the corresponding term

$$\text{UniqueAxis}=\{a|b|c\}.$$

If there is no information available on `Lattice` (even not taken from a specified spacegroup), then the default settings `B=A`, `C=A`, `ALPHA=90`, `BETA=ALPHA` and `GAMMA=ALPHA` are accepted. The `Lattice` and `uniqueAxis` parameters are determined automatically according to the initial values of the lattice constants. Even though the `Lattice` and `uniqueAxis` are not specified explicitly at all, the necessary entries are predetermined for the ongoing calculation and corresponding information is output. Take for example the hexagonal system, then the term `PARAM=GAMMA=120` is ineffective. `GAMMA` is constantly maintained at 120.

`A`, `B` and `C` are to be specified in nm (or, specify `UNIT=ANGSTROEM`).

When entering `BASIS={P|I|F|A|B|C|R}`, a lattice base is selected. Depending on the context, different effects are possible:

- When entering a spacegroup, `BASIS` is considered for selection of the spacegroup.

- If there is no entry on a spacegroup, the specified general and special co-ordinates are multiplied by this **BASIS** value.
- If there is no entry on a structure (lattice is given without atomic positions), **BASIS** is used to determine the reflection conditions.

If entering `Pack={Y|y|J|j}`, then the specified co-ordinates at PDB output are reduced to the unit cell built up by **RasMol**.

If entering `GeneralCondition=logical_term`, those reflections whose `logical_term` will become `FALSE` are omitted for calculations without atomic positions. The term may include the Miller indices *h, k, l*.

**Peak model** A peak model for the phase is selected by **RP**. Default: **RP=4**.

The following peak models can be selected:

**RP=2** : Ideally crystalline substance, the peak model of the sample function (divergence and other geometrical influences as well as spectral broadening have been eliminated) is a Delta function with 2 parameters: Intensity and  $s=1/d$

**RP=3** : Real crystalline substance with broadening resulting from crystallite size and similar influences. The model of a peak contains 3 parameters: Intensity,  $s=1/d$  and width parameter of the Cauchy function (**B1** Lorentzian width). **B1** must be specified either isotropic - for spheric or specified cubic-shaped crystallites:

`PARAM=B1=0_0`

or anisotropic for sticks or platy crystals:

`B1=ANISO` respective `B1=ANISOLIN` (no `PARAM=`)

**RP=4** : Real crystalline substance, in addition to **RP=3** with Cauchy square broadening (squared Lorentzian) by the square of the width parameter **B2** which corresponds to  $\sigma^2$  of a Gaussian function. Use in case of internal strain, dislocation densities, paracrystals (see **k2** parameter) and more precise description of crystallite size distribution in addition to **B1** (see **k1** parameter). Either **B2** or **k1** or **k2** or **k3** must be specified.

If not specified as a formula, the standard notation of **B2** is:

$$B2=k1*sqr(B1)+k2*sqr(sk)+k3*sqr(cot(2*THETA)*cos(THETA))$$

As an option, the user may define the parameters **k1** . . . **k3** either as constants or parameters. Default value in each case: 0. **k1** and **k2** describe the crystallite size distribution and internal strain. **k2** can be defined as anisotropic:

`k2=ANISO` respective `k2=ANISOSQR`  
`k2=ANISO4`

**k3** describes a shift resulting from divergence. Use of **k3** is only permitted for calculations without device function (in this case, however, use **k3** in the `*.sav` files for all structures in conjunction one with each other).

The `ANISOxxx^upperlimit` notation is possible for **B1** and **k2**.

If you want to test your own width functions, you may enter the variables **B1** (Lorentzian width), **B2** (squared value of the squared Lorentzian width) and the constant **RP** into the first line of the *\*.str* file. The variables **sk** ( $=1/d$ ) and **h, k, l** (Miller indices) can be used in the terms of **B1, k1, k2** and **B2**.

It is not necessary to manually calculate the crystallite size from the **B1** values. Use the `GrainSize(h, k, l)` function instead of manual calculation (see also chapter “GOALs and experimental design”).

**Phase content** The **GEWICHT** parameter is a scale factor to adapt the diagram computed in theory to the measured diagram. In addition, we may use this parameter to control whether preferred orientation should be available or not.

**GEWICHT** must be specified if the atomic positions are specified. Parameterisation of an isotropic **GEWICHT** (without preferred orientation) should have the following form:

```
PARAM=GEWICHT=0_0 or GEWICHT=SPHAR0
```

If the *weight.mol* file containing the molecular weights is available, then this scale corresponds to the weight content of the phase. If this file is not available or the atoms are not registered inside, then the scale corresponds to the volume content of the phase.

Use the statements **GEWICHT=ANISO**, **GEWICHT=SPHAR2**, **GEWICHT=SPHAR4**, **GEWICHT=SPHAR6**, **GEWICHT=SPHAR8** and **GEWICHT=SPHAR10** to control modelling of the preferred orientation.

- **ANISO** describes common (weakly changing) preferred orientations. In particular, this type is not able to describe preferred orientations for cubic crystallites. Furthermore, it is also not suitable for description of the equatorial dependence of the preferred orientation of hexagonal crystallites.
- **SPHAR2, SPHAR4, SPHAR6, SPHAR8** or **SPHAR10** introduce a symmetrical tensor of the 2nd, 4th, 6th, 8th and/or 10th level. Using this tensor, all even spherical harmonics up to the 2nd, 4th, 6th, 8th and/or 10th order are implemented. As a result, we obtain 6, 15, 28, 45 and/or 66 parameters which even may demand for independent definition in the triclinic case. In the Laue groups resting, constraints are introduced upon general positions. Those constraints result in obviously less parameters.

**SPHAR** stands for **S**pherical **H**ARmonics. In simple cubic substances, **ANISO/SPHAR2** only describes isotropy. In trigonal symmetries with **SPHAR4** as well as in hexagonal symmetries with **SPHAR6**, even equatorial dependencies can be described. For example, for the point group of quartz which may be left/right screwing, left and right reflections are assigned differing scales (preferred orientations).

**SPHAR8/SPHAR10** were introduced for very strong preferred orientations, but it requires extreme CPU time for adjustment of symmetries.

**ANISO** and **SPHAR2** are differential concerning their structure: Whereas **ANISO** is based on a quadratic positively definite matrix, **SPHAR2** is based on the exponents of a quadratic common matrix. Note, that in linear approximation (for weak preferred orientation), both approaches are identical. In contrast to **ANISO**, **SPHAR2** can be used to represent sharp textures in low-symmetric Laue groups.

**Debye-Waller-factor** You may input a phase-specific parameter **TDS** for the temperature factor (Debye-Waller-factor) into the first line of the structure file. The value of **TDS** corresponds to the common *B* value, divided by 100 (because the default **UNIT=NM**)

**LIMIT2, LIMIT4, LIMIT6, LIMIT8, LIMIT10, ANISOLIMIT and**

**ANISO4LIMIT** Analogously to the global limits specified in the control file, you may also enter phase-specific limits for the anisotropies. For description of these limits, see chapter “Entries into the control file”.

**GOALS** For the entire phase, you may enter **GOALS** of the `GOAL= . . .` type. For this topic, see chapter “GOALS and experimental design”.

**UNIT** Related to a phase, you may decide to process all data in Å via `UNIT=ANGSTROEM`. Default: `UNIT=NM`.

**Atomic positions (optional):**

The atomic positions are defined in the following lines. If there have not been specified any atomic positions, then only the lattice constants, the peak shape parameters as described in the structure file and one parameter for every peak (its intensity) parameters are refined. This is what we call “LeBail refinement”.

In all else cases, atomic positions follows.

In case `RefMult>1` is set, a LeBail refinement may be set for a single subphase by assigning its number to `LeBail`:

```
LeBail=i
```

Multiple such assignments may be given to set multiple subphases to LeBail refinement.

**Atomic type/ion** Every atomic position begins with the entry `E= . . .` information. Mixed occupations may be entered, even parameterised. For example, the following equation

```
E=(CA+2, MG+2 (p) ) PARAM=p_0_0^1
```

indicates a mixed allocation by Ca- and Mg ions. The proportion of components is refined via `p` parameter.

Isotopic numbers may be given, and isotopic numbers may be combined with ionic charges. Example:

```
E=C12+4
```

**Specific position** When working with the spacegroup, specify the Wyckoff position `Wyckoff=x` (`x={a . . . α}`) for each atomic position.

**Atomic temperature factors** Analogous to an entire phase, the calculation of the temperature factors can be controlled for each atom upon the **TDS** parameter.

If **TDS** is preset, an isotropic temperature factor of the form

$$T_k = e^{-\text{TDS} \sin^2 \frac{\Theta_k}{\lambda}}$$

is multiplied to the atomic form amplitudes. Except the unit  $\text{nm}^2$  instead of  $\text{Å}^2$  (in writing by decimals, shift the value 2 places to the right). Thus **TDS** corresponds to the common *B*.

To automatically introduce the set of six anisotropy parameters including start values and limits, we use the entry `TDS=ANISO`. Constraints that consider the special position's symmetry are abstracted from the relation amongst special and general positions. In this case, an amplitude attenuation by

$$e^{-\left(h^2\beta_{11}+k^2\beta_{22}+l^2\beta_{33}+2hk\beta_{12}+2hl\beta_{13}+2kl\beta_{23}\right)}$$

is used.  $\beta_{ij}$  stands for six independent components of the symmetric tensor as identified in the result list. In contrast to the isotropic TDS, there are no problems with units at all, because the  $hkl$  are without dimension.

`TDS=ANISO^upperlimit` can be used for TDS to omit maybe possible faulty minima. This upper limit is valid for the first isotropic iteration run of **BGMN**.

**GOALS** You may enter goals of the type `GOAL=...` also for atoms. For this task see chapter "GOALS and experimental design".

### Sequence of evaluation

The sequence of parameters to be processed one after the other corresponds to the sequence of parameters in the file. GOALS are computed later.

The lattice will be computed just when it is necessary first, but no later than behind the end of the first line (see molecules). Parameter declarations using `ANISO` or `SPHARx` must be local to one structure and declared after lattice definition. All other parameters may be declared as global.

### Intensity and position corrections

For example, if a common TDS or the `EPSx` parameters are insufficient for user-specific corrections, then we may also specify the variables `DELTAzweiTheta` or `DELTAk` (optional) as well as `GEWICHT[1]` in the first part of the `*.str` file. They may depend on `sk` ( $\frac{1}{d}$ ), `zweiTheta` (in  $^\circ$ ), `H`, `F`, `Finv` and `h`, `k`, `l` (if there is only one reflection type of constant intensity). These variables result in reflection shifts and/or changes of intensity following the `GEWICHT[1]` factor. Example:

```
PARAM=g=1^2_0.5
GEWICHT [1] =p*GEWICHT
```

`GEWICHT[1]` holds an expression dependent on `GEWICHT` and other stuff.

### Computation with structure amplitudes

One may even set `FMult` to a positive integer. In that case, **BGMN** will provide `F[i]` and `phi[i]` for the absolute value resp. phase angle (in degree 0...360) of complex structure amplitudes ( $i=1 \dots \text{RefMult}$ ). From that, one may do arbitrary operations and at the end set the structural amplitude `F` of the whole phase, which will then used for intensity calculation. Having set e.g. `FMult=3`, one may define an extended version of the atomic position descriptor like:

```
E(1,0,0)=CA+2
```

That example means: This atomic position contributes to `F[1]` with weight 1.0 and not to `F[2]`, `F[3]`.

The values for the inverse reflection are set to `Finv[i]` and `phiinv[i]`.

**BGMN** serves a function `F(phi, ...)` for dynamic computation of complex structure amplitudes. For clarification: The atomic positions in part 2 of the structural description are evaluated prior to

all Peak parameter evaluations. In difference, the atomic positions as defined in  $F(\text{phi}, \dots)$  are evaluated for every call to that function. There are several advantageous applications of that function. Among them, a combination with `cintegral` allows computation of arbitrary distributions of atoms/molecules in a given structure. Example:

```

FMult=1
F=cat (fmittelbetrag==cintegral (fi, F(psi,
D2 (r1, r2, rot, EOZ1, eoz1, EOZ2, eoz2, EOZ3, eoz3, EOZ4, eoz4, EOZ5, eoz5, EOZ6, eoz6) ,
E=NA+1 (pCA) , Wyckoff=c, XYZ (ECA) , TDS==tdsint ,
E=O-2 (pOZ) , Wyckoff=c, XYZ (eoz1) , TDS==tdsH2O,
E=O-2 (pOZ) , Wyckoff=c, XYZ (eoz2) , TDS==tdsH2O,
E=O-2 (pOZ) , Wyckoff=c, XYZ (eoz3) , TDS==tdsH2O,
E=O-2 (pOZ) , Wyckoff=c, XYZ (eoz4) , TDS==tdsH2O,
E=O-2 (pOZ) , Wyckoff=c, XYZ (eoz5) , TDS==tdsH2O,
E=O-2 (pOZ) , Wyckoff=c, XYZ (eoz6) , TDS==tdsH2O) ,
psi, rot, 0, 120) /120,
sqrt (sqr (F[1] *cos (pi*phi [1] /180) +fmittelbetrag*cos (pi*fi/180) ) +
sqr (F[1] *sin (pi*phi [1] /180) +fmittelbetrag*sin (pi*fi/180) ) ) )

```

calculates the structure amplitude for an arbitrary structure including a rotatin octahedron.

## Sub-phases

Sub-phases represent a special approach. A multiplet of peaks for each reflection may be generated setting `RefMult` to that value, e.g.

```
RefMult=3
```

These peaks consist of the scales `GEWICHT[i]`, the width parameters `B1[i]` and `B2[i]` (for default abstracted from `k1[i]`, `k2[i]` and `k3[i]`) as well as the correction parameters `DELTAask[i]` and/or `DELTAzweiTheta[i]`.

By default, we use the values that are not subscribed or 0 (latter except for `GEWICHT`). The sub-phases have common preferred orientations and lattice constants, in this way, it is for instance possible to represent sub-phases of the real structure. These sub-phases may share arbitrary common parameters (also `ANISO`) since they are declared inside one `*.str` file. Sub-phases are also suitable for description of asymmetric peaks. Default: `RefMult=1`, enabling to correct intensity by entering of `GEWICHT[1]=f(GEWICHT)`. The actual peak index is available as the variable (`iref=1, \dots, RefMult`), which can be used for selection within the non-subscribed variables `B1`, `B2`, `k1`, `k2`, `k3`, `DELTAask`, `DELTAzweiTheta`.

In case one uses both `FMult` and `RefMult`, you may achieve different values for `F` by using `iref` in the calculation. The simplest form is e.g.

```
F=f[iref]
```

and then defining `f[i]`.

In case there is no use of `FMult`, the extended version of `E(a,b,c)=` changes its sense. Having set e.g. `RefMult=3`,

```
E(1, 0, 0)=CA+2
```

means: This atomic setting is present for the structure factor calculation of sub-phase 1 with weight 1 and not present for all the other two sub-phases. In following, the sub-phases may have different structures at all. The weights may be any real values, even negative!

## Density and linear attenuation coefficient

BGMN provides the X ray densities and linear attenuation coefficients of the **FMult** sub-settings of atomic positions in the pre-defined variables **density[i]** (in  $\frac{\text{g}}{\text{cm}^3}$ ) and **my[i]** (in  $\mu\text{m}^{-1}$ ). In case **FMult** is not set, their values refer to the **RefMult** subphases.

In addition, BGMN provides predefined X ray density and linear attenuation coefficients **density** and **my**. In case of **FMult**, **density** and **my** are set to the sum of all atomic positions. Otherwise, **density** and **my** are set to them calculated from the first sub-phase.

In many cases, one needs **density[i]** and **my[i]** to assign new values to **density** and/or **my**.

## LeBail-refinement

Sometimes, one needs to refine all peak intensities as extra parameters. This may be done by assigning the number of the wanted subphase `1...RefMult` to the variable **LeBail**. Multiple assignments are possible for multiple subphases. In case no atomic positions are given at all, **LeBail** will be set automatically for all subphases.

## Molecules with known structure

Molecules can be defined in their Cartesian and/or atomic co-ordinates. Subsequently, these molecules may be subjected to some general displacements in space. This includes translation as a whole and rotation around 3 Eulerian angles. Parts of molecules may be turned around freely definable axes of rotation (which are defined by 2 atoms or virtual positions that are introduced for definition purposes — to define an axis of rotation, only). Subsequently, the resulting co-ordinates can be assigned to the lattice coordinates. To carry out these manipulations, the following standard procedures have been developed. Call these procedures upon the 1st line of the *\*.str* file instead of using an assignment statement.

### angle(A,B,C)

computes the angle enclosed by the 3 atoms A, B, C

### angle(A,B,C,D)

computes the torsion angle of the 4 atoms following the convention of signs in accordance with the IUPAC-IUB convention in:

Biochemistry 9 (1970), 3471

### angle(vec1,vec2)

computes the angle between the vectors **vec1** and **vec2** in  $^{\circ}$  ( $0 \leq \text{angle} \leq 180$ ). An error occurs if one of both vectors is too small (about 0).

### cross(p1,p2,p3,p4)

**p1**, **p2** and **p3** should be atomic identifiers specified via **set**. **cross** computes **p4** as a symbolic position, the **p2–p4** link is orthogonal to **p1–p2** and orthogonal to **p2–p3** (cross product). If **p1**, **p2** and **p3** are collinear, point **p4** coincides with point **p2**.

### D(p1,p2,fi,E...)

turns all **E...** positions around the **p1–p2** axis (2 position identifiers) around the angle **fi**. An error occurs if **p1** and **p2** are coincident.

### D(p1,p2,fi,Ein,Eout...)

with odd parameter count is an abbreviation for `cpXYZ(Ein,Eout...)` `D(p1,p2,fi,Eout...)`

`diffvec(p1,p2,vec)`

assigns the difference of the `p2–p1` position vectors to the `vec` vector (also a non-subscribed name).

`distance(p1,p2)`

results in the scalar distance between the two atomic positions `p1` and `p2`.

`normvec(vec1,vec2)`

assigns the unit vector to `vec2` in the `vec1` direction:

$$\text{vec2} = \text{vec1} / |\text{vec1}|$$

An error occurs if `vec1` is too small (around 0).

`skalpro(vec1,vec2)`

computes the inner product of `vec1` and `vec2`

`set(E,x,y,z)`

defines the `E` position. `E` is a general position identifier, e.g. `C6` stands for the 6th carbon atom with its Cartesian co-ordinates `x`, `y`, `z`.

`setgitter(E,x,y,z)`

defines the `E` position from its lattice (or fractional or atomic) co-ordinates `x`, `y`, `z`.

`cpXYZ(a,b. . .)`

with even parameter count: within each pair of parameters, the co-ordinates of the left one are copied to the right-one. The right-one parameter may be a comma-separated list in brackets:

$$\text{cpXYZ}(a, (b, c, d), e, f)$$

By this way, multiple copies are generated from one source.

`T(x,y,z,theta1,theta2,theta3,E. . .)`

rotates all `E. . .` positions for the 3 Eulerian angles `theta1. . . theta3` around zero point. As the second step, all `E. . .` positions are shifted by the Cartesian vector `x`, `y`, `z`.

`T2(x,y,z,theta1,theta2,theta3,Ein,Eout. . .)`

with even parameter count is an abbreviation for

$$\begin{aligned} &\text{cpXYZ}(Ein, Eout. . .) \\ &\text{T}(x, y, z, theta1, theta2, theta3, Eout. . .) \end{aligned}$$

Angles are given in  $^{\circ}$ , co-ordinates and displacements in Cartesian coordinates in nm (according to the default value `UNIT=NM`) or  $\text{\AA}$  (if `UNIT=ANGSTROEM` is set). Note, that all coordinates, displacements and angles may be arbitrary parameters and terms.

Modify valency angle inside a molecule by angle `fi` as following:

$$\begin{aligned} &\text{cross}(p1, p2, p3, p4) \\ &\text{D}(p2, p4, fi, p3, e1, e2, e3, e4. . .) \\ &\text{D}(p2, p4, fi, ex, . . .) \end{aligned}$$

For stretching and/or compressing of a `p1–p2` valency via coefficient `s` ( $-1 < s < 0$ : compressing,  $s > 0$ : stretching), use the formulations below:

```
diffvec(p1,p2,t)
T(s*t[1],s*t[2],s*t[3],0,0,0,p2,e1,e2,e3,e4,...)
T(s*t[1],s*t[2],s*t[3],0,0,0,ex,...)
```

Use the following parameter combination to twist a molecule around the p1–p2 valency around the angle fi:

```
D(p1,p2,fi,e1,e2,e3,...)
D(p1,p2,fi,ex,...)
```

The large number of introduced functions in molecule- and other lattices should be evaluated by means of the vector functions **cross**, **diffvec**, **normvec**, **skalpro** and **angle**, if necessary making use of the **setgitter** conversion function explained below. Some examples are:

1. Valency length A–B:

```
l==distance(A,B)
```

2. A–B–C valency angle

```
w==angle(A,B,C)
```

3. A–B–C–D torsion angles

```
w==angle(A,B,C,D)
```

4. Distance of point D beyond the ABC plane:

```
cross(A,B,C,x) diffvec(B,x,x) normvec(x,x)
diffvec(B,D,y) l==skalpro(y,x)
```

5. Out-of-plane angle of point D of B of the ABC plane:

```
cross(A,B,C,x) diffvec(B,x,x) diffvec(B,C,y)
w==angle(x,y)-90
```

6. Angle between 2 planes, each given by 3 points:

```
cross(A,B,C,x) diffvec(B,x,x)
cross(D,E,F,y) diffvec(E,y,y)
w==angle(x,y)
```

Remark: The authors paid special attention that the functions can be decomposed into several short individual statements. In addition to the corresponding special function, we introduced the **CROSS** auxiliary function for modification of a valency angle.

As to be seen in the example mentioned above, an **E** atomic position identifier which can be noted as any non-indexed name introduces the 3 Cartesian co-ordinates **E[1]**, **E[2]** and **E[3]** automatically.

These co-ordinates are applied via **X**, **Y** and **Z** coordinates which are assigned to the lattice coordinates in the structure part of the \*.*str*-file:

Hereby, **X(E)**, **Y(E)** and **Z(E)** provide the corresponding **x**, **y** or **z** coordinates of the **E** position in atomic coordinates. The inverse is **setgitter(E,x,y,z)** whereby the atomic coordinates are represented by **x**, **y**, **z**. To avoid errors, lattice type and lattice constants should already be defined when using **X**, **Y** and **Z** or **setgitter**.

You may use an abbreviation for

$$x=X(E) \quad y=Y(E) \quad z=ZE$$

, simply write XYZ (E) .

Hereby, it is important to know the possibility of output in the \*.pdb-format which is especially essential for molecules.

## Format of the \*.lst result file

The LIST=. . . file includes all computation results, i.e. the computed parameter values and corresponding errors. Errors are not indicated in cases if the parameter coincides with one of its limits or if it is declared as anisotropic.

The number of the measuring points is indicated in the head. The four items following contain commonly used  $R$  values. The value of Durbin-Watson statistics is in the succeeding line. It is followed by 1-rho (quality parameter). In opposite to all  $R$  values, 1-rho should not depend on the effect background ratio extremely.

1-rho is followed by all global parameters, these are the parameters specified in the \*.sav control file.

As a next part, a local parameter set is given for each involved phase. The parameters of the file head are specified first. The anisotropic GEWICHT is specified by average value (without errors). An arithmetical as well as a geometric average (without errors) are indicated for anisotropic parameters as B1=ANISOLIN or k2=ANISOSQR.

If one is interested to display errors for the GEWICHT average value, he can use a suitable GOAL (see section "GOALS and experimental design"). This error calculation is only disabled for reasons of computing time.

As a next part, the parameters of all atomic positions of the corresponding phase are given. For TDS=ANISO, the complete symmetrical oscillation tensor is pointed out for the first atomic position (without errors).

## Automatic refinement strategy

Assume that there is a parameter specified by =ANISO, =ANISOLIN or =ANISOSQR or GEWICHT=SPHARx for  $\geq 1$  phase or, respectively, TSD=ANISO for  $\geq 1$  atomic positions, then refinement is performed in a lot of iteration runs. In the first run, to find out suitable initial values for ongoing runs, isotropic approximations are used rather than anisotropic parameters.

The number of necessary iteration steps is calculated by the program automatically. In this way, wrong parameter sets caused by premature termination of iteration are avoided. In cases of especially insufficient convergence, a satisfying number of iteration steps is set as criterion for abortion.

## A.5 Output

An output table for observation of the refined peaks is available at Tools→Show Peak List.

The output table consists of the following columns:

2 Theta

Angle of the peak (weighted average of alpha1 and alpha2)

Int

Intensity in cps  $\times$  ° in the diagram; does *not* correspond to the first peak parameter in the peak list \*.par, but is recalculated from this and other parameters. To carry out *all*

corrections regularly, **OUTPUT** reads the **VERZERR** variable and the associated files analogously to **BGMN**.

%	Intensity normalized to maximum peak=100%
d	Lattice plane distance of the reflection
1/d	Reciprocal lattice plane distance, corresponds to the 2nd peak parameter in the *.par peak list
b1	if $RP > 2$ for this phase: <b>B1</b> corresponds to the Lorentzian width in the sample function. If not specified otherwise: 0
$b2^2$	if $RP > 3$ for this phase: <b>B2</b> corresponds to the square of the squared Lorentzian width in the convolution product of the Lorentzian and the squared Lorentzian which is used as sample function. If not specified otherwise: 0
PHASE	Phase identifier, corresponds to <code>PHASE= . . .</code> in the *.str structure file
H	Multiplicity
h, k, l	Miller indices; each is a representative for peaks equivalent according to symmetry
TEXTURE	Factor describing the deviation between reflection intensity and isotropic distribution. Specified for anisotropic scales, only. Corresponds to the inverse pole figure on reflection position.
F	associated variable identifying data, absolute of the $ F $ structure amplitude

d is given in nm, 1/d and **B1** in  $\text{nm}^{-1}$ ,  $b2^2$  is given in  $\text{nm}^{-2}$ .

## A.6 Formula interpreter

All control files with .sav extension and structure files with .str extension are evaluated by a formula interpreter. That means, most of control values can be assigned variables or complex expressions rather than constants, only.

We explain the function of the formula interpreter by means of the calculation of the polarisation factor

$$POL = \text{sqr}(\cos(26.6 * \text{pi} / 180)),$$

taken as a simple example with variable pi which was assigned a value previously.

The \*.sav control file consists of assignments and comments. Assignments are statements to link any (sometimes indexed) variable names to values. A value may be a numerical value or a character string. In special, character strings may hold arithmetical terms. A term may consist of: + - \* /, pairwise ( ) nested into arbitrary depth, arbitrary variables, standard functions described below, specific user functions. Concerning time and frequency, these terms are analyzed then and only then if request and as often as demanded in the program. In cases the program requests this value of the variable as a numerical value, then the program tries to analyze the character string as a term. In this case, maybe further variables are analyzed as a term (recursive approach). Specific user functions which are

ranking at the same priority as also the standard functions can also be assigned. Standard functions may be overwritten by definitions of the user.

One can decide whether a variable is analyzed partially or completely just during its definition. The multiple entry of the “=” assignment operator is used for this determination:

`A==B` Variable A is assigned the value of variable B.

`A==(B)`

Variable B is evaluated as a term. The obtained result is assigned to A.

`A=2*acos(0)`

Variable A is assigned the character string `2*acos(0)` that will be evaluated for  $\pi$  by the program whenever necessary.

`A==2*acos(0)`

The value of  $\pi$  is directly numerically assigned to variable A (to be evaluated faster).

`A=` Variable A is deleted.

`A==` Variable A is assigned the empty character string of length 0.

`A[1,2,3]=12`

Assignment statement to an indexed variable.

`factorial(1):ifthenelse(gt(#1,0),#1*factorial(#1-1),1)`

Definition of  $n!$ , (factorial n) which is no standard function of the program. `factorial(1)` means that this definition is only used, if called in conjunction with one parameter. For instance, `Prod(-2)` means that the definition of `prod` is applied whenever it is called with at least  $\geq 2$  parameters.

\*.sav control files may include comments beginning with “%” on the first line position. Concerning logic membership, those comments are part of the assignment statement following. These comments are deleted in conjunctions with the assignment statement. Consequently, more than one comments cannot be placed one after the other. Otherwise, the comments would overwrite each other.

The following standard functions are available for general use:

**numerical functions** `abs`, `sqr`, `sqrt`, `sin`, `cos`, `tan`, `asin`, `acos`, `atan`,  
`log`, `exp` with 1 argument;

**numerical functions** `mod`, `power` with 2 arguments;

**min, max functions** with variable argument number;

**comparison functions** with variable argument number: This functions accept at least two arguments: `ge`, `gt`, `le`, `lt`, `eq` return 1.0 (TRUE), if the condition holds for each neighboured pair of arguments, starting from the first. If some pair does not hold the condition, 0.0 (FALSE) will be returned immediatly, errors in following arguments will not cause this function to cause errors.

`ne` looks for inequality between any pair (also not neighboured) of arguments. If two arguments are equal, `ne` returns 0.0 (FALSE). Otherwise, `ne` returns 1.0 (TRUE);

**logic operators** `and`, `or` with variable number of arguments: evaluation is carried out in an abridged manner, that is arguments in more right position remain unconsidered as soon as the result has been found.

**cat function for command concatenation** with variable number of arguments: the arguments are evaluated in order, depending on its kind (term or assignment): the assignment statements are executed, the terms are evaluated. At least one argument should be a term (no assignment statement). The last of these terms is provided as result.

**assignment function ergibt** with 1 argument: transfers the argument in form of an assignment statement to formula interpreter. TRUE result, if allocation was successful, otherwise FALSE;

**ifdef function** with variable argument number: it returns TRUE if all arguments may be evaluated as a term (and connection, abridged evaluation occurs);

**conditional function ifthenelse** with 3 arguments: if the first argument is TRUE, the 2nd argument is analyzed and returned as result. Otherwise, the 3rd argument is given as result. As also in the logic functions, there are analyzed only those arguments required! Thus, possible error responses of the formula interpreter can be avoided;

**function select** with variable argument count: Depending on the value of the first argument  $i$ , the value of the Argument number  $i + 1$  will be returned. All the other arguments will not be evaluated and therefore cause no error if undefined. An error occurs if the first argument will be zero or below or exceeds the number of arguments as given for selection. Examples:

```
i=3
select(i, a, b, c)
```

will return the value of the variable  $c$  (if defined).

**conditional loop while** with variable argument number: The first argument must be an expression. As long as its value is non-zero and no error occurs, all following arguments are evaluated. Returns the number of loop iterations;

**logic function not** with 1 argument;

**linear equation system solver gauss, cgauss** are high-level standard functions for solving linear equation systems. Called as

```
gauss(A, x, b, eps, n)
cgauss(Areal, Aimag, xreal, ximag, breal, bimag, eps, n)
```

$A, x, b$  are placeholders for arrays, therefore only non-indexed names are allowed. Both the standard functions solve the inhomogen linear equation system

$$\mathbf{Ax} = \mathbf{b} \quad (\text{A.1})$$

where

$$\mathbf{A} = \begin{pmatrix} A[1, 1] & \cdots & A[1, n] \\ \vdots & \ddots & \vdots \\ A[n, 1] & \cdots & A[n, n] \end{pmatrix} \quad (\text{A.2})$$

$$\mathbf{x} = \begin{pmatrix} x[1] \\ \vdots \\ x[n] \end{pmatrix} \quad (\text{A.3})$$

$$\mathbf{b} = \begin{pmatrix} b[1] \\ \vdots \\ b[n] \end{pmatrix} \quad (\text{A.4})$$

`eps` is a limit for the pivot element. If any pivot element has an absolute value smaller than `eps` the equation leaves unsolved and zero (false) will be returned. If the equation system has been solved and `x[1]...x[n]` hold the solution, 1 (true) will be returned.

`cgauss` is the complex equivalent to `gauss`. Therefore six placeholders are necessary, each one for the real part and one for the imaginary part of `A,x,b`.

**numeric integration function `integral`, `cintegral`** implement a seven-point numeric integral with adaptive step width.

- `integral(y,x,xu,xo)` integrates the values as given in the first position (`y`), the integration is carried out for `x` between `xu` and `xo`. An optionally fifth parameter will be used for definition of the numeric integral's precision. It defaults to 1E-13. Due to the fast convergency of the 7-point formulae, the default value will serve a total precision of about 1E-15.
- `cintegral(phi,yabs,yphase,x,xu,xo)` is the equivalent function for complex `y` values and therefore complex result. `yabs` is the absolute value of `y`, `yphase` is it's phase angle in degree. The result value is the absolute value of the complex result, it's phase angle will be set to the variable as given in the first position (`phi`). An optionally seventh parameter will be used for definition of the numeric integral's precision. It defaults to 1E-13. Due to the fast convergency of the 7-point formulae, the default value will serve a total precision of about 1E-15.

Functions are written with parentheses, therefore: `A=abs(a)`.



# Appendix B

## Examples

### B.1 Files for the example in chapter “User’s Guide”

#### Control file *Ringverz.sav* for the GEOMET and MAKEGEQ run

```
% Titel of Calculation
TITEL=PbSO4_Round_Robin
% Name of 'Raytraced' Goniometer Function
VERZERR=ringverz.ger
% Name of Interpolated Goniometer Function
GEQ=ringverz.geq
% Helper Variables
pi=2*acos(0)
rh=100
% Rowland Circle Radius
R=173
% Tube
FocusH=8
FocusW=0.04
% Divergence Slit
HSlitR=rh
HSlitW=(R-rh)*1*pi/180
% Primary Collimator
PColl=0.5*4.45*pi/180
% Sample
SamplH=20
SamplW=20
% Secondary Collimator
SColl=0.5*4.45*pi/180
% Detector Slit
DetH=15
DetW=0.2
% Secondary Monochromator
MonR=R+51
% 2Theta List for GEOMET
zweiTheta[1]=10
zweiTheta[2]=14
zweiTheta[3]=20
zweiTheta[4]=28
zweiTheta[5]=40
zweiTheta[6]=65
zweiTheta[7]=90
zweiTheta[8]=115
zweiTheta[9]=135
zweiTheta[10]=150
zweiTheta[11]=160
% Angle Range for MAKEGEQ
WMIN=10
WMAX=160
WSTEP=2*sin(zweiTheta*pi/180)
```

**Result file *ringverz.ger* to evaluate geometry function via GEOMET**

```
GEOMETRY=REFLEXION
TITEL=PbSO4_Round_Robin
R=173
FocusH=8
FocusW=0.04
HSlitW=(R-rh)*1*pi/180
HSlitR=rh
PColl=0.5*4.45*pi/180
SamplH=10
SamplW=20
SColl=0.5*4.45*pi/180
DetH=15
DetW=0.2
MonR=R+51
THETA=5.0000 N=12
0.15029 0.0004560 0.00022151
0.09919 0.0006639 0.00028144
0.10133 0.0001843 0.00014601
0.08871 0.0009174 0.00036578
0.15725 0.0003011 0.00017542
0.01497 -0.0001888 0.00007240
0.06047 0.0027498 0.00146893
0.03136 -0.0001070 0.00008825
0.08190 0.0018203 0.00080576
0.07880 0.0000755 0.00012315
0.05246 -0.0000202 0.00010421
0.08946 0.0012665 0.00051647
THETA=7.0000 N=10
0.11571 0.0001373 0.00014872
0.14213 0.0004026 0.00019653
0.07351 0.0000197 0.00012589
0.16688 0.0002672 0.00016906
0.10144 0.0012086 0.00057307
0.01793 -0.0001772 0.00008101
0.11236 0.0008308 0.00037168
0.15595 0.0005702 0.00025667
0.07996 0.0018626 0.00107819
0.04043 -0.0000846 0.00010287
THETA=10.0000 N=10
0.16742 0.0004456 0.00021716
0.15125 0.0006214 0.00028793
0.03316 -0.0001201 0.00008712
0.10693 0.0009208 0.00044910
0.01432 -0.0001990 0.00006813
0.18791 0.0002963 0.00017310
0.07286 0.0014023 0.00079962
0.12350 0.0001780 0.00014594
0.05923 -0.0000308 0.00010621
0.09002 0.0000693 0.00012579
THETA=14.0000 N=9
0.24005 0.0002849 0.00018334
0.14767 0.0001622 0.00015007
0.20381 0.0004456 0.00023963
0.04425 -0.0001290 0.00008570
0.09688 0.0006824 0.00034901
0.01901 -0.0002065 0.00006816
0.07537 -0.0000423 0.00010428
0.06318 0.0010287 0.00058034
0.11664 0.0000537 0.00012518
THETA=20.0000 N=9
0.18636 0.0003849 0.00022832
0.03930 -0.0001703 0.00006867
0.01918 -0.0002318 0.00006088
0.09558 0.0006355 0.00042449
0.24984 0.0002593 0.00017111
0.15209 0.0001396 0.00013769
0.08574 -0.0000383 0.00009278
0.11992 0.0000441 0.00011342
0.05836 -0.0001065 0.00007839
THETA=32.5000 N=7
0.49435 0.0002374 0.00021946
0.05226 -0.0002064 0.00007004
0.11666 0.0001041 0.00013001
```

```

0.11426 -0.0000663 0.00009947
0.08779 -0.0001410 0.00008388
0.01708 -0.0002656 0.00005927
0.12366 0.0000160 0.00011377
THETA=45.0000 N=6
0.21084 0.0002578 0.00014555
0.10599 -0.0002313 0.00011009
0.18764 0.0001515 0.00014439
0.18421 0.0000491 0.00013795
0.14546 -0.0001478 0.00011634
0.17217 -0.0000520 0.00012873
THETA=60.0000 N=6
0.05260 0.0002803 0.00008250
0.37340 -0.0002022 0.00018033
0.14859 -0.0000736 0.00013164
0.14920 0.0001252 0.00011352
0.10459 0.0002108 0.00009458
0.17711 0.0000268 0.00012904
THETA=67.5000 N=8
0.31690 -0.0002222 0.00016752
0.19494 -0.0000922 0.00014477
0.06104 0.0002317 0.00006957
0.14885 0.0000097 0.00011943
0.06425 -0.0004403 0.00027262
0.08504 0.0001677 0.00008228
0.02542 0.0002898 0.00005972
0.10962 0.0000955 0.00009776
THETA=75.0000 N=9
0.34209 -0.0002267 0.00017856
0.06584 0.0001713 0.00007437
0.04052 0.0002317 0.00005897
0.05845 -0.0006777 0.00039022
0.17571 -0.0000869 0.00014331
0.12559 0.0000150 0.00011520
0.09258 0.0000996 0.00009289
0.01482 0.0002839 0.00004751
0.09116 -0.0004358 0.00025167
THETA=80.0000 N=11
0.30574 -0.0002360 0.00017688
0.13293 -0.0001059 0.00013307
0.12210 -0.0004378 0.00025168
0.02890 0.0002335 0.00005248
0.05688 0.0001235 0.00007345
0.05534 -0.0010403 0.00056861
0.09494 -0.0000168 0.00010604
0.07273 0.0000586 0.00008686
0.01000 0.0002813 0.00004198
0.08320 -0.0006801 0.00035079
0.04366 0.0001816 0.00006258

```

## Structure file for *pbso4ani.str* anglesite

```

PHASE=PbSO4 SpacegroupNo=62 PARAM=A=0.847 PARAM=B=0.539 PARAM=C=0.695
B1=ANISO PARAM=k1=1_0^1 PARAM=k2=0_0 GEWICHT=SPHAR2 Pack=Y ANISOLIMIT=0
E=PB Wyckoff=c PARAM=x=0.188 PARAM=z=0.168 TDS=ANISO
E=S Wyckoff=c PARAM=x=0.063 PARAM=z=0.684 TDS=ANISO
E=O Wyckoff=c PARAM=x=0.910 PARAM=z=0.595 TDS=ANISO
E=O Wyckoff=c PARAM=x=0.185 PARAM=z=0.540 TDS=ANISO
E=O Wyckoff=d PARAM=x=0.077 PARAM=y=0.025 PARAM=z=0.813 TDS=ANISO

```

## Control file *pbso4ani.sav* for refinement calculation via BGMN

```

% Geometry function
VERZERR=ringverz.geq
% Measuring values in APX format
VAL[1]=pbso4.val
% Polarisation factor for sec. graphite monochromator
pi=2*acos(0)
POL=sqr(cos(26.6*pi/180))
% Starting structure
STRUC[1]=pbso4.str

```

```

% Resulting structure
STRUCOUT[1]=pbso4.sto
% RasMol output
PDBOUT[1]=pbso4.pdb
% Shelx output for PowderCell
RESOUT[1]=pbso4.res
% Peak list
OUTPUT=pbso4.par
% Result listing
LIST=pbso4.lst
% Protocol output after every iteration step
PROTOKOLL=Y
% Zero point with starting value and limits
PARAM[1]=EPS1=2.88724209182800E-003_-0.005^0.005
% Sample displacement with starting value
PARAM[2]=EPS2=-2.70422552073637E-003_-0.005^0.005
EPS1==2.8872420918280000E-003
EPS2== -2.7042255207363740E-003

```

## PowderCell result graph

For output of crystal structure, the *pbso4.res* file must be read in. Afterwards, enter spacegroup 62 and Wyckoff positions.

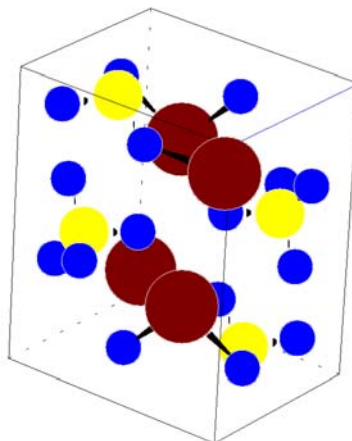


Figure B.1: Graphic representation of  $\text{PbSO}_4$  structure obtained via **PowderCell**

## RasMol result graph

To display the unit cell as a black line against white background, insert the following entries in the **RasMol** command line:

```

background white
set unitcell true
color axis black

```

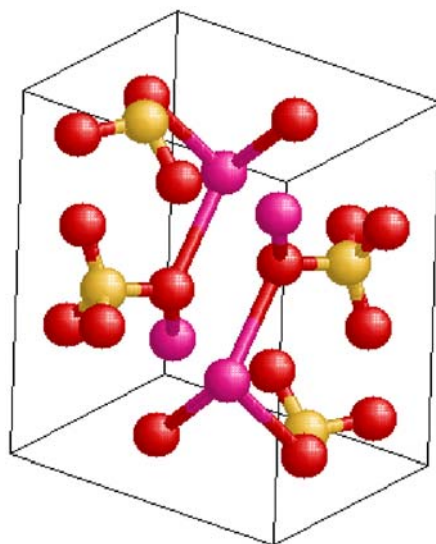


Figure B.2: Graphic representation of PbSO<sub>4</sub> structure obtained by **RasMol**

### ShelX result graph

P2\_12\_1m2\_1a No.62 PbSO4

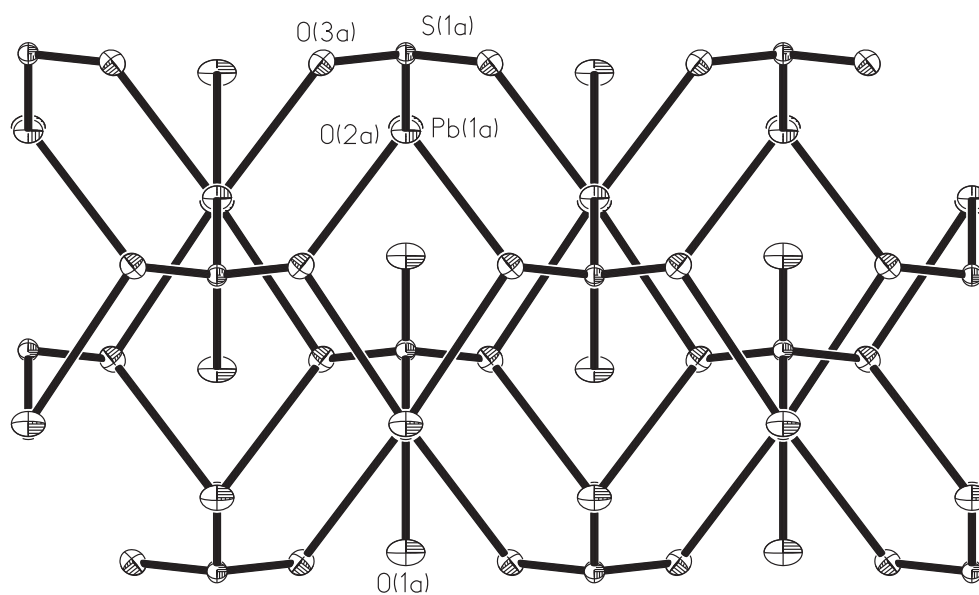


Figure B.3: Graphic representation of PbSO<sub>4</sub> structure using ellipsoids in accordance with the anisotropic temperature factors

## B.2 Files for the example “Metashale Böhlscheiben” in transmission geometry

### Control file *Tran0205.sav* for the GEOMET and MAKEGEQ run

```
% Device function XRD 3000TT in transmission
VERZERR=tran0205.ger
GEQ=tran0205.geq
GEOMETRY=TRANSMISSION
R=250
D=0.08
T=0.2
HSlitR=250-152
HSlitW=0.2
VSlitR=250-80
VSlitH=17
FocusH=12
FocusW=0.04
DetH=14
MonR=250+50
DetW=0.5
SampLD=20
PColl=0.5/25
zweiTheta [1]=6
zweiTheta [2]=10
zweiTheta [3]=16
zweiTheta [4]=24
zweiTheta [5]=34
zweiTheta [6]=48
zweiTheta [7]=60
zweiTheta [8]=90
zweiTheta [9]=120
WMIN=6
WMAX=120
GSUM=Y
pi=2*acos(0)
WSTEP=3*sin(pi*zweiTheta/180)
```

### Quartz structure file *quarz.str*

```
PHASE=Quarz SpacegroupNo=154 //
PARAM=A=0.4913_0.485^0.5 PARAM=C=0.5405_0.53^0.55 GAMMA=120 //
PARAM=B1=0_0 PARAM=k1=0_0^1 PARAM=k2=0_0 //
PARAM=GEWICHT=0_0 GOAL:quarz=GEWICHT
E=SI+4 Wyckoff=a x=0.465 TDS=0.002
E=O-2 Wyckoff=c x=0.415 y=0.268 z=0.786 TDS=0.0015
```

### Chlorite structure file *aphrol.str*

```
PHASE=Aphrosiderit SpacegroupNo=5 HermannMaugin=C121 //
UniqueAxis=b //
PARAM=A=0.537_0.53^0.54 PARAM=B=0.93_0.92^0.94 //
PARAM=C=1.425_1.42^1.435 PARAM=BETA=96.28_96.0^97.5 //
PARAM=B1=0_0^0.005 PARAM=k1=0_0^1 PARAM=k2=0_0 //
GEWICHT=SPHAR2 GOAL:aphrol=GEWICHT TDS=0.017
E=MG+2 Wyckoff=a y=0
E=(MG+2(1-p), FE+3(p)) p=0.25 Wyckoff=a y=0.33
E=FE+3(p) p=0.9 Wyckoff=a y=0.667
E=(AL+3(1-p), FE+2(p)) p=0.25 Wyckoff=b y=1/2
E=(AL+3(1-p), FE+2(p)) p=0.25 Wyckoff=b y=0.167
E=MG+2(p) p=0.75 Wyckoff=b y=0.833
E=(SI+4(1-p), AL+3(p)) p=0.7 Wyckoff=c x=0.226 y=1/2 z=0.193
E=(SI+4(1-p), AL+3(p)) p=0.2 Wyckoff=c x=0.226 y=0.167 z=0.193
E=O-2 Wyckoff=c x=0.19 y=0.17 z=0.072
E=O-2 Wyckoff=c x=0.19 y=1/2 z=0.072
E=O-2 Wyckoff=c x=0.017 y=0.068 z=0.235
E=O-2 Wyckoff=c x=0.517 y=0.117 z=0.235
E=O-2 Wyckoff=c x=0.192 y=0.328 z=-0.235
E=O-2 Wyckoff=c x=0.707 y=0.314 z=0.072
```

```
E=O-2 Wyckoff=c x=0.117 y=-0.025 z=0.435
E=O-2 Wyckoff=c x=0.157 y=0.333 z=0.435
E=O-2 Wyckoff=c x=0.117 y=0.683 z=-0.435
```

## Muscovite structure file *mus2m1n.str*

```
PHASE=Muskovit_2M1 SpacegroupNo=15 HermannMauguin=C12/c1 //
UniqueAxis=b //
PARAM=A=0.5184_0.51^0.53 PARAM=B=0.8993_0.89^0.91 //
PARAM=C=2.0069_2.0^2.1 PARAM=BETA=95.69_94.5^96.0 //
B1=ANISO PARAM=k1=0_0^1 k2=ANISO //
GEWICHT=SPHAR6 GOAL:mus2m1=GEWICHT
E=(AL+3(1-p),FE+3(p)) p=0.04 Wyckoff=f x=0.251 y=0.0838 z=0.0004 TDS=0.0074
E=K+1(p) PARAM=p=0.9_0.7^1 Wyckoff=e y=0.0986 TDS=0.0164
E=(SI+4(1-p),AL+3(p)) p=0.25 Wyckoff=f x=0.0345 y=0.4295 z=0.3646 TDS=0.0071
E=(SI+4(1-p),AL+3(p)) p=0.25 Wyckoff=f x=0.4514 y=0.2582 z=0.1355 TDS=0.0049
E=O-2 Wyckoff=f x=0.0429 y=0.0617 z=0.4501 TDS=0.0117
E=O-2 Wyckoff=f x=0.3836 y=0.2511 z=0.0536 TDS=0.0118
E=O-2 Wyckoff=f x=0.0380 y=0.4447 z=0.4463 TDS=0.0088
E=O-2 Wyckoff=f x=0.4128 y=0.0925 z=0.1682 TDS=0.008
E=O-2 Wyckoff=f x=0.2516 y=0.3726 z=0.1688 TDS=0.0088
E=O-2 Wyckoff=f x=0.2469 y=0.3083 z=0.3426 TDS=0.004
```

## Albite structure file *albtief1.str*

```
PHASE=Albit SpacegroupNo=2 HerrmannMauguin=C-1 BASIS=C //
PARAM=A=0.8144_0.812^0.817 PARAM=B=1.2787_1.27^1.29 //
PARAM=C=0.716_0.705^0.725 PARAM=ALPHA=94.26_93.0^96 //
PARAM=BETA=116.6_116^117 PARAM=GAMMA=87.67_87.0^89.0 //
RP=3 PARAM=B1=0_0^0.004 //
GEWICHT=SPHAR2 GOAL:albit=GEWICHT
E=(NA+1(p)) Wyckoff=i p=0.45 TDS=0.06 x=0.2675 y=0.9802 z=0.151
E=(NA+1(p)) Wyckoff=i p=0.55 TDS=0.06 x=0.2653 y=0 z=0.1385
E=(SI+4(1-p),AL+3(p)) Wyckoff=i p=0.91 x=0.0095 y=0.1680 z=0.2075
E=(SI+4(1-p),AL+3(p)) Wyckoff=i p=0.05 x=0.0053 y=0.8207 z=0.238
E=(SI+4(1-p),AL+3(p)) Wyckoff=i p=0.09 x=0.691 y=0.110 z=0.3105
E=(SI+4(1-p),AL+3(p)) Wyckoff=i p=0.04 x=0.6797 y=0.8818 z=0.3595
E=O-2 Wyckoff=i TDS=0.0015 x=0.0065 y=0.1283 z=0.9678
E=O-2 Wyckoff=i TDS=0.0015 x=0.5905 y=0.9962 z=0.2785
E=O-2 Wyckoff=i TDS=0.0035 x=0.8169 y=0.1070 z=0.1943
E=O-2 Wyckoff=i TDS=0.0035 x=0.8191 y=0.8525 z=0.2612
E=O-2 Wyckoff=i TDS=0.0035 x=0.0095 y=0.3011 z=0.268
E=O-2 Wyckoff=i TDS=0.0015 x=0.0247 y=0.6936 z=0.2295
E=O-2 Wyckoff=i TDS=0.0015 x=0.2085 y=0.1087 z=0.3885
E=O-2 Wyckoff=i TDS=0.0015 x=0.1844 y=0.8674 z=0.4345
```

## Microcline structure file *micmax.str*

```
PHASE=Micmax SpacegroupNo=2 HerrmannMauguin=C-1 BASIS=C //
PARAM=A=0.8581_0.845^0.875 PARAM=B=1.2961_1.285^1.31 //
PARAM=C=0.7223_0.715^0.735 PARAM=ALPHA=90.65_90.0^92 //
PARAM=BETA=115.94_115^117 PARAM=GAMMA=87.63_86.5^89.5 //
RP=3 PARAM=B1=0_0^0.005 //
PARAM=GEWICHT=0_0 GOAL:micmax=GEWICHT
E=K+1 Wyckoff=i x=0.283 y=-0.0067 z=0.1388
E=SI+4 Wyckoff=i x=0.7059 y=0.8856 z=0.3507
E=(SI+4(1-p),AL+3(p)) Wyckoff=i p=0.9 x=0.0104 y=0.1875 z=0.2169
E=(SI+4(1-p),AL+3(p)) Wyckoff=i p=0.03 x=0.0097 y=0.8198 z=0.2327
E=(SI+4(1-p),AL+3(p)) Wyckoff=i p=0.07 x=0.7110 y=0.1202 z=0.3399
E=O-2 Wyckoff=i x=0.6365 y=0.0058 z=0.2853
E=O-2 Wyckoff=i x=0.0007 y=0.1448 z=-0.0179
E=O-2 Wyckoff=i x=0.8202 y=0.1476 z=0.2205
E=O-2 Wyckoff=i x=0.8316 y=0.8570 z=0.2416
E=O-2 Wyckoff=i x=0.0352 y=0.3203 z=0.2514
E=O-2 Wyckoff=i x=0.0366 y=0.6953 z=0.2689
E=O-2 Wyckoff=i x=0.1911 y=0.1229 z=0.4053
E=O-2 Wyckoff=i x=0.1753 y=0.8742 z=0.4127
```

## Control file for refinement by BGMN

```
% Device Function XRD 3000TT, Transmission Geometry
VERZERR=tran0205.geq
% Mean particle size for Brindley correction
d=5
% Measuring values
VAL[1]=tbtr78.val
% Polarisation factor for secondary monochromator
pi=2*acos(0)
POL=sqr(cos(26.6*pi/180))
% Phases
STRUC[1]=quarz.str
STRUC[2]=aphro1.str
STRUC[3]=mus2m1n.str
STRUC[4]=albtief1.str
STRUC[5]=micmax.str
STRUC[6]=rutile.str
% Quantitative analysis
GOAL[1]=quarz/(quarz+aphro1+mus2m1+albit+micmax+rutile)
GOAL[2]=aphro1/(quarz+aphro1+mus2m1+albit+micmax+rutile)
GOAL[3]=mus2m1/(quarz+aphro1+mus2m1+albit+micmax+rutile)
GOAL[4]=albit/(quarz+aphro1+mus2m1+albit+micmax+rutile)
GOAL[5]=micmax/(quarz+aphro1+mus2m1+albit+micmax+rutile)
GOAL[6]=rutile/(quarz+aphro1+mus2m1+albit+micmax+rutile)
% Result files
OUTPUT=tbtr78.par
LIST=tbtr78.lst
DIAGRAMM=tbtr78.dia
% Angle correction parameters
PARAM[1]=EPS1=0
PARAM[2]=EPS2=0
% Minimum angle
WMIN=6
% Iteration protocol
PROTOKOLL=Y
```

## B.3 Files or learnt peak profiles

# Appendix C

## Additional data files

### C.1 Format of the *spacegrp.dat* spacegroup file

The user may enlarge the *spacegrp.dat* file according to the following rules: Each entry starts with a line that identifies the spacegroup. The lattice base is the only information necessary. However, it can be implicitly derived from the first letter of the Hermann-Mauguin symbol. Following entries are permitted:

SpacegroupNo= Number according to International Tables

HermannMauguin=  
abbreviated or full-length Hermann-Mauguin symbol

Lattice= One of  
{Triclinic | Monoclinic | Orthorhombic | Tetragonal |  
Trigonal | Hexagonal | Rhombohedral | Cubic}

UniqueAxis= {a | b | c} (Default: c)

CellChoice=

OriginChoice=

Setting=

The Wyckoff positions of the spacegroup are entered following. The first one is the general position, whereas the last one must be specified as *Wyckoff=a*. Each Wyckoff position contains the entries *Wyckoff=...* and *N=...* (for multiplicity). Entry of Wyckoff positions is followed by a count of lines with number *N* divided by the multiplicity of the base as retrieved from the first letter of the Hermann-Mauguin symbol. Every of those lines contains a coordinate triplet analogous to the International Tables. After changes, you should call the **SPACEGRP.EXE** program to test whether the file is correct. If the special positions coincide with general position, you only get some information about the spacegroup just being checked. For each error, there are displayed error message and remarks on possible reasons.

### C.2 Atomic form amplitudes

The *afaparm.dat* file contains atomic form amplitudes for neutral atoms and ions in parametric representation. Entry *e-1* was inserted to incorporate individual “localized” electrons into a structure

% Normal X-Ray scattering factors for Elements and Ions, cited from  
% different sources. This file afaparm.dat is copyrighted to  
% J. Bergmann Dresden 1991.

```

e-1 0 0 0 0 0 0 0 0 1
H 0.48992 20.6593 0.26200 7.74039 0.19677 49.5519 0.04988 2.20159 0.00130
HE 0.76844 10.9071 0.72694 4.30779 0.27631 1.33127 0.05172 25.6848 0.01249
LI 0.99279 4.33979 0.87402 1.26006 0.84240 98.7088 0.23101 212.088 0.05988
LI+1 6.08475 0.00498 0.86773 1.53730 0.80588 4.28524 0.17720 9.81413 -5.93560
BE 2.22744 0.04965 1.55249 42.9165 1.40060 1.66379 0.58290 100.361 -1.76339
BE+2 5.69034 -0.01336 1.19706 0.39000 1.10357 1.97441 0.20150 4.90642 -6.11950
B 2.03876 23.0888 1.41491 0.97848 1.11609 59.8985 0.73273 0.08538 -0.30409
C 1.93019 12.7188 1.87812 28.6498 1.57415 0.59645 0.37108 65.0337 0.24637
N 12.7913 0.02064 3.28546 10.7018 1.76483 30.7773 0.54709 1.48044 -11.3926
O 2.95648 13.8964 2.45240 5.91765 1.50510 0.34537 0.78135 34.0811 0.30413
O-1 3.22563 18.4991 3.01717 6.65680 1.42553 0.40589 0.90525 61.1889 0.42362
O-2 3.7504 16.5131 2.9429 6.5920 1.5430 0.3192 1.6209 43.3486 0.2421
F 3.30393 11.2651 3.01753 4.66504 1.35754 0.33760 0.83645 27.9898 0.48398
F-1 3.63220 5.27756 3.51057 14.7353 1.26064 0.44226 0.94071 47.3437 0.65340
NE 3.71272 3.91091 3.52631 9.63126 1.19237 0.40483 0.83080 23.9546 0.73728
NA 5.26400 4.02579 2.17549 10.4796 1.36690 0.84222 1.08859 133.617 1.09912
NA+1 3.99479 3.11047 3.37245 7.14318 1.13877 0.40692 0.65118 15.7319 0.84267
MG 5.59229 4.41142 2.68206 1.36549 1.72235 93.4885 0.73055 32.5281 1.26883
MG+2 4.30491 2.55961 3.14719 5.60660 1.12859 0.41574 0.49034 11.4840 0.92893
AL 5.35047 3.48665 2.92451 1.20535 2.27309 42.6051 1.16531 107.170 1.28489
AL+3 4.17448 1.93816 3.38760 4.14553 1.20296 0.22875 0.52814 8.28524 0.70679
SI 5.79411 2.57104 3.22390 34.1775 2.42795 0.86937 1.32149 85.3410 1.23139
SI+4 4.43918 1.64167 3.20345 3.43757 1.19453 0.21490 0.41653 6.65365 0.74630
P 6.92073 1.83778 4.14396 27.0198 2.01697 0.21318 1.53860 67.1086 0.37870
S 7.18742 1.43280 5.88671 0.02865 5.15858 22.1101 1.64403 55.4651 -3.87732
CL 9.83957 -0.00053 7.53181 1.11119 6.07100 18.0846 1.87128 45.3666 -8.31430
CL-1 18.0842 0.00129 7.47202 1.12976 6.46337 19.3079 2.43918 59.0633 -16.4654
AR 16.8752 -0.01456 8.32256 0.83310 6.91326 14.9177 2.18515 37.2256 -16.2972
K 8.11756 12.6684 7.48062 0.76409 1.07795 211.222 0.97218 37.2727 1.35009
K+1 9.70659 0.59947 7.37245 11.8765 5.67228 -0.08359 1.90688 26.7668 -6.65819
CA 8.60272 10.2636 7.50769 0.62794 1.75117 149.301 0.96216 60.2274 1.17430
CA+2 13.2063 0.39466 11.0586 -0.08204 7.73221 9.62976 1.72057 20.3341 -15.7176
SC 9.06482 8.77431 7.55526 0.53306 2.05017 123.880 1.28745 36.8890 1.03849
SC+3 13.4008 0.29854 8.02730 7.96290 1.65943 -0.28604 1.57936 16.0662 -6.66668
TI 9.54969 7.60057 7.60067 0.45899 2.17223 109.099 1.75438 27.5715 0.91762
TI+3 17.7344 0.22061 8.73816 7.04716 5.25691 -0.15762 1.92134 15.9768 -14.6519
TI+4 19.5114 0.17885 8.23473 6.67018 2.01341 -0.29263 1.52080 12.9464 -13.2803
V 10.0661 6.67721 7.61420 0.40322 2.23551 98.5954 2.23170 22.5720 0.84574
V+2 9.34513 6.49985 7.68833 0.39491 2.94531 15.9868 0.26998 41.0832 0.75143
V+3 9.43141 6.39535 7.74190 0.38339 2.15343 15.1908 0.01686 63.9690 0.65657
V+5 15.6887 0.67900 8.14208 5.40135 2.03081 9.97278 -9.57602 0.94046 1.71430
CR 10.4757 6.01658 7.51402 0.37426 3.50115 19.0654 1.54902 97.4599 0.95226
CR+2 9.54034 9.66078 7.75090 0.34426 3.58274 13.3075 0.50911 32.4224 0.61690
CR+3 9.68090 5.59463 7.81136 0.33439 2.87603 12.8288 0.11357 32.8761 0.51827
MN 11.2519 5.34818 7.36935 0.34373 3.04107 17.4089 2.27703 84.2139 1.05195
MN+2 9.78094 4.98303 7.79153 0.30421 4.18544 11.4399 0.72736 27.7750 0.51454
MN+3 9.84521 4.91797 7.87194 0.29439 3.56531 10.8171 0.32361 24.1281 0.39397
MN+4 9.96253 4.84850 7.97057 0.28330 2.76067 10.4852 0.05445 27.5730 0.25188
FE 11.9185 4.87394 7.04848 0.34023 3.34326 15.9330 2.27228 79.0339 1.40818
FE+2 10.1270 4.44133 7.78007 0.27418 4.71825 10.1451 0.89547 24.8302 0.47888
FE+3 10.0333 4.36001 7.90625 0.26250 4.20562 9.35847 0.55048 20.4105 0.30429
CO 12.6158 4.48994 6.62642 0.35459 3.57722 14.8402 2.25644 74.7352 1.91452
CO+2 10.5942 4.00858 7.67791 0.25410 5.15947 9.21931 1.01440 22.7516 0.55358
CO+3 10.3380 3.90969 7.88173 0.23867 4.76795 8.35583 0.72559 18.3491 0.28667
NI 13.3239 4.17742 6.18746 0.38682 3.74792 14.0123 2.23195 71.1195 2.49899
NI+2 11.1650 3.65944 7.45636 0.24397 5.51106 8.52596 1.09496 21.1647 0.77218
NI+3 10.7806 3.54770 7.75868 0.22314 5.22746 7.64468 0.84711 16.9673 0.38604
CU 13.9352 3.97779 5.84833 0.44555 4.64221 13.3971 1.44753 74.1605 3.11686
CU+1 12.4655 3.54270 6.63111 0.28920 5.76679 9.31140 1.34230 26.9799 1.79285
CU+2 11.8168 3.37484 7.11181 0.24408 5.78135 7.98760 1.14523 19.8970 1.14431
ZN 14.6744 3.71486 5.62816 0.50033 3.92540 12.8862 2.16398 65.4071 3.59838
ZN+2 12.5225 3.13961 6.68507 0.25431 5.98382 7.55544 1.17317 18.8453 1.63497
GA 15.3412 3.63868 5.74150 0.65640 3.10733 16.0719 2.52764 70.7609 4.26842
GA+3 12.6920 2.81262 6.69883 0.22789 6.06692 6.36441 1.00660 14.4122 1.53545
GE 15.4378 3.39715 6.00432 0.73097 3.05158 18.9533 2.93572 63.7969 4.56068
AS 15.4043 3.07517 6.13723 0.74113 3.74679 21.0014 3.01390 57.7446 4.69149
SE 15.5372 2.71530 5.98288 0.68962 4.83996 21.0079 2.93549 52.4308 4.70026
BR 15.9934 2.35651 6.02439 19.7393 5.51599 0.58143 2.88716 47.3323 4.57602
BR-1 15.4080 2.43532 6.78083 22.0832 6.00715 0.68621 2.99332 64.9193 4.80234
KR 16.8494 2.01856 7.19790 18.0409 4.92564 0.39741 2.91606 42.5054 4.10864
RB 11.4809 1.08140 9.46904 18.2800 9.16981 2.38825 1.42608 185.293 5.43921
RB+1 17.8943 1.71750 8.59341 0.09258 7.91428 15.4484 2.47499 32.5110 -0.87756
SR 11.6164 1.85574 9.73009 14.6109 8.68081 0.89852 2.60986 139.830 5.34841
SR+2 18.2430 1.51215 8.90811 13.6536 1.69192 27.8238 -32.1118 -0.01488 39.2691
Y 19.0567 1.24615 6.50783 9.68019 4.81524 18.8903 2.84786 121.353 5.76121
Y+3 18.4202 1.34457 9.75213 12.0631 1.05270 25.1684 -33.4755 -0.01023 40.2513
ZR 19.2273 1.15488 10.1378 10.7877 2.48177 120.126 2.42892 33.3722 5.71886
ZR+4 19.1301 1.16051 10.1098 10.4084 0.98896 20.7214 -0.00004 -3.20442 5.77164
NB 19.3496 1.06626 10.8737 10.5977 3.47687 32.6174 1.64516 120.397 5.65073
NB+3 19.1248 1.07235 18.2989 0.00315 11.0121 10.3385 2.04325 25.9292 -12.4799
NB+5 19.0175 1.06028 10.7591 9.36239 1.09900 0.03765 0.48469 20.9764 4.64045
MO 19.3885 0.97877 11.8308 10.0885 3.75919 31.9738 1.46772 117.932 5.55047
MO+3 19.6761 0.95118 18.0893 -0.00669 11.7086 9.61097 2.50624 24.0356 -12.9813
MO+5 19.6054 0.94029 17.9292 -0.00795 11.3451 8.76715 1.04247 19.3690 -12.9217
MO+6 19.4800 0.94043 17.6328 -0.00723 11.0940 8.29745 0.37154 18.9700 -12.5778
TC 19.3597 0.89356 12.8087 9.27497 3.41372 32.3513 1.99926 107.406 5.41556
RU 19.4316 0.82092 13.7309 8.97737 4.26537 28.2621 1.28720 111.501 5.28192
RU+3 20.8024 0.74711 13.2995 8.36626 3.27542 20.6179 2.21026 -0.14664 1.41087
RU+4 41.5821 0.61466 12.9936 7.99801 2.71276 18.1564 -24.2593 0.43857 6.97025
RH 19.4524 0.75019 14.6845 8.42622 4.50240 26.1564 1.24740 107.780 5.11007
RH+3 25.0958 0.61346 14.1510 7.80244 3.64428 19.0932 -12.5768 0.13532 11.6838
RH+4 41.5236 0.52905 13.8272 7.49419 3.07969 16.9498 -25.9694 0.32686 8.53824
PD 19.5123 0.68583 15.3800 7.95714 5.38330 23.1808 0.81015 65.9295 4.91427
PD+2 19.4652 0.68159 15.5805 7.80880 4.04748 20.9573 0.02216 110.020 4.88510
PD+4 51.1288 0.43734 14.6979 7.03139 3.41607 15.8623 -38.2678 0.26589 11.0241
AG 19.5284 0.62387 16.5811 7.39504 4.99150 22.2282 1.21404 100.226 4.68114
AG+1 19.5416 0.62273 16.4239 7.39663 5.12995 20.5530 0.24053 59.0604 4.66470
AG+2 19.5152 0.62050 16.4852 7.30347 4.32525 19.3673 0.02777 92.9184 4.64695

```

CD	19.5528	0.56604	17.5717	6.79630	4.47374	21.2907	1.98562	85.2777	4.41158
CD+2	19.5901	0.56389	17.3740	6.83082	4.62594	17.8856	0.03770	76.2909	4.37269
IN	19.5872	0.51510	18.7169	6.29430	4.02722	22.7308	2.51452	88.5675	4.14542
IN+3	19.6698	0.50926	18.1942	6.28098	4.09851	15.4189	0.00365	160.227	4.03396
SN	19.6527	0.46604	19.5108	5.76321	3.86895	24.0627	3.14764	78.1533	3.81227
SN+2	19.7166	0.46027	18.9265	5.66448	3.79775	17.7248	1.86248	42.8086	3.69648
SN+4	19.7914	0.45879	18.9162	5.76682	3.64761	13.3733	-0.0	-0.0	3.64494
SB	20.0759	5.24328	19.7766	0.41858	4.30389	26.0178	3.44952	70.1646	3.38881
SB+3	19.8617	0.41409	19.5199	5.18292	3.73465	16.8529	1.61027	35.1406	3.27356
SB+5	19.9613	0.41262	19.5889	5.30028	3.24333	11.7603	-0.0	-0.0	3.20701
TE	20.4608	4.74225	20.0336	0.37041	5.38664	27.3458	3.33079	65.0573	2.78462
I	20.7492	4.27091	20.5640	0.31960	6.86158	27.3186	2.97589	61.5375	1.84739
I-1	20.8307	4.29514	20.4454	0.32402	7.52618	29.8990	3.18616	81.4344	2.00513
XE	21.6679	0.26422	21.0085	3.83526	8.43382	26.2297	2.62265	58.4830	0.26635
CS	22.3163	0.23092	21.1792	3.49464	10.7382	25.1864	1.46163	232.829	-0.70709
CS+1	23.9649	0.20446	21.2204	3.43876	9.76727	23.4941	1.61550	49.7057	-2.56728
BA	27.7489	0.15152	21.3777	3.09817	11.0400	20.6774	2.68186	178.819	-6.85854
BA+2	29.2996	0.14047	21.4669	3.08785	10.9209	20.8818	0.80126	46.8842	-8.48753
LA	33.2109	0.11040	21.7181	2.83641	11.6222	19.3886	3.17239	144.438	-12.7404
LA+3	43.6346	0.07854	21.7192	2.78360	11.7264	18.4930	0.32945	49.2222	-23.4085
CE	29.4100	0.12335	22.2428	2.74837	11.9818	18.3794	3.19259	139.603	-8.84560
CE+3	49.1105	0.06535	22.3499	2.67229	11.8399	17.2040	0.67455	38.1904	-28.9739
CE+4	66.7693	0.04464	21.8563	2.53711	12.2486	16.4477	0.09617	64.4675	-46.9691
PR	22.9220	2.78604	22.2518	0.18015	12.2269	17.6663	2.72431	160.915	-1.13930
PR+3	49.4655	0.06197	22.9705	2.57634	11.8015	16.0371	1.12179	32.3673	-29.3586
PR+4	62.6752	0.04586	22.4952	2.45900	12.4946	15.5713	0.20294	46.5889	-42.8667
ND	23.4069	2.71587	19.7073	0.20950	12.5016	16.9122	2.72850	196.556	1.64038
ND+3	49.4292	0.05936	23.6116	2.48611	11.6190	14.9366	1.68986	28.4515	-29.3493
PM	23.8480	2.65746	17.5535	0.24780	12.7324	16.2463	2.72975	152.682	4.12018
PM+3	49.2699	0.05709	24.2700	2.40099	11.3481	13.9124	2.32869	25.6906	-29.2165
SM	24.2242	2.60993	15.9132	0.29475	12.9238	15.6554	2.72836	149.221	6.19355
SM+3	36.3271	0.07823	24.8502	2.33602	11.3426	13.1872	2.62300	24.3996	-16.1429
EU	24.9148	2.97255	14.8058	0.34930	13.0799	15.1280	2.72477	146.103	7.85731
EU+2	25.6516	2.36073	23.9387	0.13260	10.5738	12.6495	4.05853	25.0026	-3.22358
EU+3	33.2862	0.08350	29.5041	2.26275	11.1494	12.3883	3.13496	22.8351	-13.0748
GD	24.4004	2.47491	14.0308	0.40238	13.1754	14.4670	3.24472	119.738	9.12488
GD+3	29.0290	0.09521	26.1387	2.19696	11.0510	11.7141	3.52244	21.6929	-8.74150
TB	24.3736	2.46637	13.8649	0.47517	13.2510	14.0424	3.24435	117.446	10.2420
TB+3	26.7821	2.13333	25.9463	0.10597	10.9724	11.0974	3.88172	20.7042	-5.58307
DY	24.6193	2.52208	14.2735	0.54556	13.3567	13.8487	2.70316	138.385	11.0290
DY+3	27.3805	2.07832	22.2062	0.12643	10.9975	10.5960	4.10030	19.9671	-1.68516
HO	24.3162	2.52724	14.9012	0.61572	13.3895	13.5041	2.69309	136.246	11.6817
HO+3	27.9956	2.02324	19.9560	0.14275	11.0106	10.1165	4.33205	19.2589	0.70499
ER	23.8201	2.54419	15.8796	0.68445	13.3938	13.1932	2.68190	134.282	12.2062
ER+3	28.5315	1.97796	17.4316	0.17182	11.1113	9.73821	4.43156	18.7294	3.49325
TM	23.1386	2.57320	17.1707	0.74948	13.3703	12.9126	2.66981	132.468	12.6322
TM+3	29.0215	1.93707	15.6168	0.20467	11.2288	9.40342	4.49403	18.2607	5.63812
YB	22.3028	2.61393	18.7202	0.80868	13.3200	12.6590	2.65701	130.783	12.9818
YB+2	29.1313	1.99979	13.5855	0.32335	11.4132	9.59277	4.69659	20.3507	9.17182
YB+3	29.4761	1.89879	14.4357	0.23793	11.3446	9.09408	4.54681	17.8206	7.19600
LU	21.1866	0.88654	20.1760	2.68610	13.0532	12.2746	3.21190	107.128	13.3489
LU+3	29.8480	1.86596	13.6268	0.27623	11.4750	8.82479	4.56009	17.4364	8.48923
HF	24.6725	0.97400	17.2295	2.89038	12.8069	12.2897	3.55970	93.4381	13.7049
TA	28.1757	1.04034	14.4288	3.20784	12.6412	12.5054	3.74436	85.0183	13.9824
W	31.0935	1.07885	12.5273	12.8331	12.3769	3.63298	3.79138	79.7647	14.1842
RE	33.2961	1.09315	12.3497	13.2559	11.2819	4.16736	3.72367	76.6562	14.3239
OS	34.8667	1.08840	11.9524	13.8042	11.1851	4.79179	3.56436	75.1399	14.4097
IR	35.9454	1.06924	11.9980	5.43443	11.2501	14.4983	3.34312	74.7918	14.4449
PT	36.8102	1.04422	13.0747	6.07340	11.3323	15.7018	2.31421	73.8375	14.4526
AU	37.3027	1.00810	14.9306	6.52550	10.3425	16.5100	2.01229	76.9117	14.3992
HG	37.5186	0.96455	17.0353	6.65786	8.51121	16.8438	2.63340	76.7228	14.2911
TL	37.6947	0.92263	19.7195	6.78248	6.38290	19.2435	3.00960	85.9267	14.1800
PB	37.7383	0.87755	21.3394	6.58964	5.17527	21.2437	3.71604	78.8094	14.0203
BI	37.7143	0.83222	22.4542	6.27051	4.84549	24.4693	4.14816	72.1558	13.8301
PO	37.6297	0.78640	23.1323	5.86644	5.59203	27.8678	4.04218	68.1617	13.5991
AT	37.4971	0.74012	23.5635	5.42694	7.15953	29.8350	3.45924	66.3564	13.3183
RN	37.3308	0.69354	23.8933	4.98696	9.02222	30.0338	2.77349	65.5799	12.9796
FR	37.1902	0.65303	24.1306	4.61305	11.5026	29.2597	1.47980	257.965	12.6868
RA	36.9820	0.60394	24.2495	4.17857	11.8719	24.3782	2.72428	200.024	12.1642
AC	36.8705	0.56458	24.7131	3.88776	12.3889	23.1506	3.26501	161.726	11.7484
TH	36.7754	0.52510	25.2506	3.61658	13.0681	22.3410	3.63791	139.164	11.2497
PA	37.1457	0.52020	25.2998	3.66300	13.7846	20.6539	3.29611	150.973	11.4561
U	37.2808	0.90239	25.6563	3.58562	14.3501	19.6342	3.30732	146.633	11.3864
NP	37.3968	0.48676	26.0671	3.52325	14.8366	18.7419	3.31586	142.798	11.3632
PU	37.6407	0.47976	26.5603	3.57178	15.4492	17.9814	2.79814	165.232	11.5358
AM	37.6909	0.46617	27.1436	3.52195	15.7842	17.3069	2.79600	161.931	11.5685
CM	37.5543	0.44932	27.6657	3.38713	15.8858	16.6498	3.32758	133.547	11.5431
BK	37.5273	0.43930	28.3202	3.35014	16.1181	16.1000	3.32793	131.027	11.6823
CF	37.6111	0.43255	29.2465	3.39285	16.4566	15.6791	2.78216	153.766	11.8853
ES	37.4979	0.42353	30.0495	3.35234	16.5881	15.2381	2.77596	151.474	12.0698
FM	37.3380	0.41562	30.8936	3.31193	16.6818	14.8362	2.76929	149.344	12.2983
MD	37.1301	0.40883	31.7721	3.27132	16.7422	14.4683	2.76232	147.353	12.5741
NO	36.8731	0.40324	32.6784	3.23045	16.7732	14.1302	2.75513	145.481	12.9008
LW	36.3813	0.40165	33.1999	3.13608	16.6469	13.7255	3.31406	119.377	13.4313



# Bibliography

- [1] H. Berger. Study of the  $K\alpha$ -Emission Spectrum of Copper. *X-Ray Spectrometry*, 15:241–243, 1986.
- [2] J. Bergmann. *Beiträge zur Auswertung und Versuchsplanung in der Röntgenpulverdiffraktometrie*. PhD thesis, TU Dresden, 1984.
- [3] J. Bergmann and R. Kleeberg. Rietveld analysis of disordered layer silicates. *Materials Science Forum*, 278-281:300–305, 1998.
- [4] J. Bergmann, T. Monecke, and R. Kleeberg. Alternative algorithm for the correction of preferred orientation in rietveld analysis. *J. Appl. Cryst.*, 34:16–19, 2001.
- [5] E.F. Bertaut. Raies de Debye-Scherrer et Repartition des Dimensions de Bragg dans les Poudres Polycristallines. *Acta Cryst.*, 3:14–18, 1950.
- [6] D.L. Bish and J.E. Post. Reviews in Mineralogy. *Modern Powder Diffraction*, 20:73–99, 1989.
- [7] G. W. Brindley. The Effect of Grain or Particle Size on X-ray Reflections from Mixed Powders and Alloys, considered in relation to the Quantitative Determination of Crystalline Substances by X-ray Methods. *Phil. Mag.*, 36:347–369, 1945.
- [8] M.M. Burnett and C.K. Johnson. ORTEP-III: Oak Ridge Thermal Ellipsoid Plot Program for Crystal Structure Figures. Technical report, ORNL, 1996.
- [9] C. Giacovazzo and H.L. Monaco D. Viterbo and F. Scordari and G. Gilli and G. Zanotti and M. Catti. *Fundamentals of Crystallography*. Oxford University Press, 1992.
- [10] R.W. Cheary and A.A. Coelho. Axial Divergence in a Conventional X-ray Powder Diffractometer. II. Realization and Evaluation in a Fundamental-Parameter Profile Fitting Procedure. *J. Appl. Cryst.*, 31:862–868, 1998.
- [11] J.P. Cline, R.D. Deslattes, J.L. Staudemann, E.G. Kessler, L.T. Hudson, A. Henis, and R.W. Cheary. Nist certificate: standard reference material 660a. Technical report, NIST, 2000.
- [12] W.A. Dollase. Correction of Intensities for Preferred Orientation in Powder Diffractometry: Application of the March Model. *J. Appl. Cryst.*, 19:267–272, 1986.
- [13] R.J. Hill. Rietveld Round Robin: Part one. *J. Appl. Cryst.*, 25:589–610, 1992.
- [14] G. Hölzer, M. Fritsch, M. Deutsch, J. Härtwig, and E. Förster.  $K\alpha_{1,2}$  and  $K\beta_{1,3}$  x-ray emission lines of the 3d transition metals. *Phys. Rev. A*, 56(6):4554–4568, 1997.
- [15] E. Jansen, W. Schäfer, and G. Will.  $R$  Values in Analysis of Powder Diffraction Data using Rietveld Refinement. *J. Appl. Cryst.*, 27:492–496, 1994.

- [16] E.H. Kisi and C.J. Howard. *Applications of Neutron Powder Diffraction*. Oxford series on neutron scattering in condensed matter. Oxford University Press, Oxford, 2008.
- [17] H.P. Klug and L.E. Alexander. *X-ray Diffraction Procedures for Polycrystalline and Amorphous Materials*. Wiley & Sons, New York, 2<sup>nd</sup> edition, 1974.
- [18] W. Kraus and G. Nolze. *Handbuch für das Programm PowderCell*, 1996.
- [19] I.C. Madsen and R.J. Hill. Collection and Analysis of Powder Diffraction Data with Near Constant Counting Statistics. *J. Appl. Cryst.*, 27:385–392, 1994.
- [20] S. Matthies and K. Helming. General Consideration of the loss of information on . . . *phys. stat. sol. (b)*, 113:569–582, 1982.
- [21] D. Melcher. Beiträge zur Korn-/Subkorngrößenanalyse mittels Röntgenpulverdiffraktometrie. Master's thesis, TU Dresden, 1988.
- [22] S.F. Mughabghab. *Atlas of Neutron Resonances*. Elsevier, Amsterdam, 5<sup>th</sup> edition, 2006.
- [23] H.M. Rietveld. Line profiles of neutron powder-diffraction peaks for structure refinement. *Acta Cryst.*, 22:151–152, 1967.
- [24] H.M. Rietveld. A profile refinement method for nuclear and magnetic structures. *J. Appl. Cryst.*, 2:65–71, 1969.
- [25] H. Sadowski. Der RG-CD-Algorithmus für quadratische Optimierungsaufgaben. *Beiträge zur numerischen Mathematik*, 3:131–147, 1975.
- [26] R. Sayle. *RasMol Version 2.6 Manual, Molecular Visualization Program*, 1996.
- [27] H. Schwetlick. *Numerische Lösung nichtlinearer Gleichungssysteme*. Verlag Technik, Berlin, 1979.
- [28] R. Starke. Bestimmung der mineralischen Zusammensetzung des Tonschiefers TB durch quantitative Phasenanalyse. *Berichte deutsche Ges. geol. Wiss. B. Mineral. Lagerstättenforschung*, 14:73–77, 1969.
- [29] D.B. Wiles and R.A. Young. A new computer program for Rietveld analysis of X-ray powder diffraction patterns. *J. Appl. Cryst.*, 14:149–151, 1981.
- [30] A.J.C. Wilson. *Mathematical theory of x-ray powder diffractometry*. Philips technical library. Philips, 1963.

# Index

- Automatic divergence slits, 48
- BGMN, 86
  - Control file, 13, 86
  - DIAGRAMM, 15
  - Output protocol, 15
  - Protocol output, 89
  - Zero offset, 14
- Installation, 5
- Requirements, 5
- Structure file, 10, 91
  - Element/ion, 12
  - lattice, 11
  - Parameter GEWICHT (SCALE), 12
  - Phase identifier (PHASE), 11
  - real structure, 11
  - Temperature factor, 12, 94
  - Width parameters B1 and k1, 12
  - Width parameter k2, 12
- BGMN restrictions, 55
  - by software, 56
  - fault intensities due to bonded atoms, 55
  - No neutron data, 56
  - PO and grazing incidence, 55
  - Primary monochromator, 55
- Crystallite size, 32
  - vs. microscopic grain size, 34
- Diffraction control, 47
- Examples
  - Amorphous content, 62
  - Goethite/Quartz, 57
  - Metashale Böhlischeiben, 66
  - virgilite, 71
- Geometry function, 29
  - Interpolation, 30
  - Learning of, 79
  - Raytracing of, 30
- Goniometer function, 7
  - displaying, 10
  - Fundamental parameters, 8
  - interpolation, 9
  - Modelling, 7
- Measurement geometry, 51
  - Capillary, 51
  - Reflection, 51
  - Transmission, 51
- Microabsorption, 34, 44
- Optimization method, 23
- Preferred orientation, 25, 43
  - automatic reduction, 28
- Profile deformation
  - Due to X-rays penetrating into the sample, 9
- Profile function, 28
- Quality parameters, 38–40
- RasMol, 18, 89, 93
  - Graphic representation, 110
  - Installation, 5
- Result list
  - Global parameters, 16
  - Scale parameter, 17
  - Structure parameters, 16
  - Width parameter, 17
  - X-ray density, 16
- Rules for phase analysis, 69
- Sample function, 19, 28, 31, 93, 102
- Sample holder
  - Reflection, 44
- Sample illumination, 51
- Sample roughness, 44
- Sample statistics, 41
- Scale factor, 25
- ShelX
  - Result file, 111
- Structure factor, 35
- Temperature factor, 36
- Variable counting time, 47
- Wavelength distribution, 29

---

Dr. Jörg Bergmann, Ludwig-Renn-Allee 14, D-01217 Dresden, Germany

Fax: +49 941 5992 12660

email: [support@bgmn.de](mailto:support@bgmn.de)

---

Looking for technical improvements, we reserve the right for technical modifications without prior notice

Printed in Germany